Roles of Cold Shock Protein 1 from *Thermus thermophilus* HB8

Toshiko Miyazaki

Department of Biological Sciences
Graduate School of Science, Osaka University

Contents

page

ABBREVIATIONS

2-DE	two-dimensional electrophoresis
CD	circular dichroism
CSD	cold shock domain
Csp	cold shock protein
CT-box	the region rich in C and T bases
DTT	dithiothreitol
Δttcsp1	deletion mutant of *ttcsp1*
*ec*Csp	*Escherichia coli* Csp
h-RNA	hairpin RNA
MALDI-TOF MS	matrix-assisted laser desorption-ionization time-of-flight mass spectrometry
PMF	peptide mass fingerprinting
RNase	ribonuclease
ssDNA	single-stranded DNA
ssRNA	single-stranded RNA
TFA	trifluroacetic acid
*tt*Csp1	*T. thermophilus* cold shock protein 1 (TTHA0175)
*tt*Csp2	*T. thermophilus* cold shock protein 2 (TTHA0359)

INTRODUCTION

All living cells control their cellular condition for surviving many stresses. Among the systems to respond to stress conditions, cold shock response is well studied. The first study about cold stress was taken place using *Escherichia coli* as a model organism. The protein which was over-expressed under the cold conditions in *E. coli* was named cold shock protein (Csp) (Jones, P. G. *et al.*, 1987, Goldstin, J. *et al.*, 1990). Csp comprises a family of small proteins whose amino acid sequences are highly conserved and binds to single-stranded nucleic acids via the nucleotide-binding motifs, RNP1 and RNP2 (Newkirk, K. *et al.*, 1994, Feng, W. *et al.*, 1998). In *E. coli*, nine members of Csp family proteins have been identified. Among them, *ec*CspA, *ec*CspB, *ec*CspG and *ec*CspI are highly induced by the cold stress (Lee, S. J. *et al.*, 1994, Nakashima, K. *et al.*, 1996, Wang, N. *et al.*, 1999); *ec*CspD is induced by nutrient depletion (Yananaka, K *et al.*, 1997); and *ec*CspC and *ec*CspE are constitutively expressed at physiological temperature (Yamanaka, K. *et al.*, 1994). Some proteins belonging to CSP family, such as *ec*CspC and *ec*CspE, are considered to play not only in cold acclimation, but also in other cellular processes.

The most well-studied members of Csps are ecCspA and *ec*CspE. The *ec*CspA is known to have functions under the cold condition in transcriptional enhancement (Brandi, A. *et al.*, 1994), in post-transcriptional RNA defense from ribonucleases (RNases) (Ermolenko, D. N. *et al.*, 2002) and in translational enhancement. On the other hand, though the information about its functions is rather limited compared to *ec*CspA, *ec*CspE is known to unwind the RNA secondary structures and act as a transcriptional antiterminator (Phadtare, S.

et al., 2002). Therefore, *ec*CspE must work under normal conditions and there are more members of Csps which work under different conditions from cold shock.

Although a significant amount of research effort has been directed towards clarifying the cellular activities of Csps as cold-dependent or cold-independent functions, no clear results have been obtained. One reason for this difficulty is the presence of several Csps in a single species e.g. *E. coli* possesses nine Csps. The manipulation of multiple genes in various combinations is still technically difficult. Moreover, *E. coli* Csps are known to work redundantly, which makes the genetic analysis problematic. In addition, Csps are apparently involved in transcription as well as post-transcriptional and/or translational processes. Because many genes might be affected by an action of Csps, genome-wide analyses need to be performed in order to elucidate cellular functions of Csps.

The structure-function relationship of Csps have also been studied. The three-dimensional structures of some Csp family proteins have been solved. Twenty-two structures have been reported from six organisms, CspA from *E. coli*, CspB from *Bacillus caldolyticus*, CspB from *Bacillus subtilus*, CspA from *Thermotoga maritima*, Csp from *Neiseria meningitidis* and CspE from *Salmonella typhimurium*. Because these proteins have the same structural features (i.e., a five-stranded β-barrel), it is thought that Csps are also structurally conserved. However, all of these Csps with their structures determined are cold-inducible or uncharacterized Csps. It has not been revealed whether there is a structural difference between cold-inducible and none-cold-inducible Csps.

Unlike *E. coli*, *Thermus thermophilus* HB8 has only two Csps, TTHA0175 (73 residues) and TTHA0359 (68 residues). Sequence identity between them is 69%, suggesting

functional differentiation of these Csps. If this is the case, *T. thermophilus* is potentially an extremely useful organism for studying functions of different types of Csps, that is, it may make easy to analyze the function of Csps under the normal growth condition. In addidion, the proteins from *T. thermophilus* are known to be stable and suited for X-ray structural analysis. Together with the functional analysis, *T. thermophilus* Csps is also expected to contribute to study on the structure-function relationship of Csps.

Here, I studied the function and structure of *tt*Csp1, which is a non-cold-inducible protein. Specifically, I analyzed the effects of deleting *ttcsp1* on the transcriptome and proteome of *T. thermophilus*, determined the crystal structure of *tt*Csp1, compared surface charge distribution of *tt*Csp1 with those of other Csps, and analyzed its affinities for oligonucleotides. Finally, I evaluate my data and discuss the new findings in terms of the likely functions of non-cold-inducible Csps.

```
ttCsp1      MQ---KGRVKWFNAEKGYGFIEREGD-TDVFVHYTAINAK
ttCsp2      MN---KGIVKWFNAEKGYGFIQQEEG-PDVFVHFSAIEAD
ecCspD      ME---KGTVKWFNNAKGFGFICPEGGGEDIFAHYSTIQMD
ecCspA      MSGKMTGIVKWFNADKGFGFITPDDGSKDVFVHFSAIQND
ecCspB      MSNKMTGLVKWFNADKGFGFISPVDGSKDVFVHFSAIQND
ecCspG      MSNKMTGLVKWFNADKGFGFITPDDGSKDVFVHFTAIQSN
ecCspI      MSNKMTGLVKWFNPEKGFGFITPKDGSKDVFVHFSAIQSN
ecCspC      MA-KIKGQVKWFNESKGFGFITPADGSKDVFVHFSAIQGN
ecCspE      MS-KIKGNVKWFNESKGFGFITPEDGSKDVFVHFSAIQTN
ecCspF      MSRKMTGIVKTFDGKSGKGLITPSDGRIDVQLHVSALNLR
ecCspH      MSRKMTGIVKTFDRKSGKGFIIPSDGRKEVQVHISAFTPR
            *  .* ** *:  .* *:*  .  ::  * :::

                                    GFRTLNEGDIVTFDVEPGRNGKGPQAVNVTVVEPARR 73
                                    GFRTLSEGERVEFEVEPGRNGKGPQARRVRRL----- 68
                                    GYRTLKAGQSVQFDVHQGPKGNHASVIVPVEVEAAVA 74
                                    GYKSLDEGQKVSFTIESGAKG--PAAGNVTSL----- 70
                                    NYRTLFEGQKVTFSIESGAKG--PAAANVIITD---- 71
                                    EFRTLNENQKVEFSIEQGQRG--PAAANVVTL----- 70
                                    DFKTLTENQEVEFGIENGPKG--PAAVHVVAL----- 70
                                    GFKTLAEGQNVEFEIQDGQKG--PAAVNVTAI----- 69
                                    GFKTLAEGQRVEFEITNGAKG--PSAANVIAL----- 69
                                    DAEEITTGLRVEFCRINGLRG--PSAANVYLS----- 70
                                    DAEVLIPGLRVEFCRVNGLRG--PTAANVYLS----- 70
                                      . :  .  * *    * .*  . .
```

Figure S1. Sequence alignment of Csps from *T. thermophilus* and *E. coli*.

MATERIALS AND METHODS

1. Materials

All strains are derivatives of *T. thermophilus* HB8 (ATCC27634). DNA-modifying enzymes, including restriction enzymes, were from Takara Bio Inc. Yeast extract and polypeptone were from Nihonseiyaku. The DNA oligomers were synthesized by BEX Co. All other reagents used were of the highest grade commercially available.

2. Disruption of *ttcsp1* and *ttcsp2* genes

The gene null mutants of *T. thermophilus* were constructed by using a homologous recombination method (Hashimoto, Y. *et al.*, 2004). The plasmids for gene disruption were derivatives of pGEM-T (Promega) constructed by introducing a thermostable kanamycin nucleotidyltransferase gene (*HTK*) (Hoseki, J. *et al.*, 1999) flanked by approximately 500 base pairs of DNA upstream and downstream of the *ttcsp1* and *ttcsp2* genes, respectively. For the double gene knockout, a thermostable hygromycin-B kinase gene (*hygB*) (unpublished) was used for the disruption of the *ttcsp2* gene. The wild-type strain of *T. thermophilus* HB8 was cultured in TR medium (Hashimoto, Y. *et al.*, 2004) containing 0.4 mM $MgCl_2$ and 0.4 mM $CaCl_2$ (TT medium). When the OD_{600} value of the culture reached 0.5, 0.4 ml of the culture was incubated with 1 μg of the deletion constructs for 4 h, and transformants were isolated by positive selection on TR plates (TR medium containing 1.5 % Phytagel (Sigma-Aldrich Co.), 1.5 mM $MgCl_2$, and 1.5 mM $CaCl_2$) containing 50 μg/ml kanamycin or 20 μg/ml hygromycin-B. Deletion of the target gene in the chromosomal DNA was subsequently

verified by PCR analysis of genomic DNA from the mutant cells.

3. DNA microarray analysis

The cells of wild type and mutants were cultured to exponential phase (OD600 0.8) in TT medium and harvested. RNA isolation to the hybridization were performed as described previously (Shinkai, A. *et al.*, 2007). For biological replication, each strain was grown three times independently, and total RNA from each sample was hybridized to distinct array. The global expression level of genes from the strains was evaluated using DNA microarray system (Affymetrix GeneChip; Affymetrix inc). The probe array was scanned with a gene array scanner (Affymetrix). The expression intensities of the 2,242 ORFs were evaluated using image data and scaled by means of the on-step Tukey bi-weight algorithm using the GeneChip Operating Software version 1.0 (Affymetrix inc). Then, the three data were normalized through the following three normalization steps using the GeneSpring GX 7.3.1 program (Agilent Tech.): data transformation (set measurements of less than 0.01 to 0.01), per chip normalization (normalize as to median), and per gen normalization (the data before cold shock was used as a control). The microarray data discusssed in this study have been deposited in the NCBI gene Expression Omnibus (GEO; http://www.ncbi.nlm.nih.gov/geo/) and are accesible through GEO Series Accession No. GSE21195 and GSE21290.

4. Proteome analysis

4-1 Chemicals

The chemical for mass analysis were supplied by Bruker Daltonics, Applied

Biosystem and Fluka. Trypsin Gold was purchased at Promega Co. and the calibration standard, peptide standard for MALDI-TOF were provided by Bruker Daltonics.

4-2 Preparation of total cell extract of *T. thermophilus* HB8

T. thermophilus was cultured to prepare proteome sample for 2-DE analysis. The culture (200 mL) was harvested at 7,000 *g* for 10 min and the pellet was washed twice with ice-cold PBS buffer containing 1.0 mM PMSF and 2 mM EDTA to prevent proteolysis. After wash, the pellet was resuspended with 1.5 mL of lysis buffer (PBS containing 5 mM EDTA, and 1 mM PMSF, pH 8.0) and then disrupted six times by using ultrasonicator (TOMY). The crude extracts were centrifuged at 5,000 *g* for 10 min to remove cell debris and the supernatant was kept in -80°C for whole cell protein analysis until next experimental process. The same whole cell lysate was ultra centrifuged at 105,000 *g* for 1 h to separate soluble and insoluble proteins. The supernatant after ultracentrifugation was kept on -80°C as a soluble cytosolic protein sample. The pellet was washed a couple of times with cold PBS and then kept on -80°C as a insoluble membrane protein sample. The protein concentration was measured by Bradford method and 2-D Quant kit (GE Healthcare) using BSA as a standard.

4-3 Two-dimensional electrophoresis (2-DE)

One miligram of protein samples were precipitated with 3 volume of ice-cold acetone to minimize contamination by such as salts in lysis buffer, phospholipids and cell constituents in the cell lysate for analytical and preparative 2-DE gel, respectively. After mixing, the samples were incubated at –30°C for 2 h and precipitated at 10,000 *g* for 10 min. The

precipitate was further washed two times with 5 volume of cold acetone and dried at room temperature completely. After drying the sample, the protein pellet was suspended with 250 uL (for analytical gel) and 500 uL (for preparative gel) of activated rehydration buffer (8 M urea, 30% glycerol, 2% m/v CHAPS, 10 mM DTT, 0.5% IPG buffer and trace of bromophenol blue). Subsequently the sample was completely dissolved by vigorous vortexing and undissolved protein pellets were precipitated and eliminated by centrifugation at 14,000 *g* for 10 min at room temperature.

Total 250 uL and 500 uL of protein samples dissolved in rehydration buffer were applied into the 24 cm versatile strip holder (Amersham-Pharmacia) for analytical and preparative samples, respectively. Thirteen and twenty-four centimeter Immobiline DryStrip (linear pH 4-7 or non-linear pH 3-10, Amersham-Pharmacia) were employed for the first electro-focusing process with a IPGPhor II apparatus (Amersham-Pharmacia). Proteins were adsorbed onto the dry strip and strip gels were also rehydrated for 12 h at 20°C. For analytical 2-DE gel, the voltage set was 0.2 kV (6 h), 0.5 kV (1 h), 1.0 kV (1 h), until 8.0 kV (gradient 1 h) and 8.0 kV (upto 20 kVh); for preparative 2-DE gel, the voltage set was 0.2 kV (2 h), 0.5 kV (6 h), 1.0 kV (2 h), 3.0 kV (2 h), until 8.0 kV (gradient 1h) and 8.0 kV (upto 80 kVh). Prior to the second dimension SDS-PAGE, focused IPG strips were equilibrated for 15 min twice with 1% DTT and 2.5% iodoacetamide containing equilibration solution (7 M urea, 2% SDS, 30% glycerol and 50 mM Tris-HCl, pH 6.8), respectively. The second dimension PAGE was carried out on a 12.5% polyacrylamide linear gradient gels (13 cm x 15 cm x 1 mm for analytical gel and 25.5 cm x 20.5 cm x 1 mm for preparative gel) with constant voltage of 100 V and 2.5W/gel for 30 min then 100 W until the dye eluted from the

bottom of the gel. Protein spots on the both analytical and preparative gels were detected by a silver staining method (GE Healthcare) or highly sensitive blue silver staining method using colloidal coomassie brilliant blue G-250 (Candiano, G. *et al.*, 2004). 2-DE maps were obtained in triplicate for each analyzed sample for biological implication. Protein spots detected in all gels were analyzed for comparative expression study.

4-4 Comparative analysis of 2-DE map

The ImageMaster 2-D Platinum software package (GE Healthcare) and ImageScaner (GE Healthcare) were employed for the statistical data analysis with spot detection, pair matching and comparing analysis of up- and down-regulated proteins. 2-DE images were acquired with 300 dpi resolution as Melanie format and then background of each image was subtracted. Quantitative difference between each proteome map of *T. thermophilus* wild type and *Δttcsp1* mutant stains was evaluated by three independent analytical 2-DE PAGE gels. The significant differences ($p < 0.05$) of expression of each protein spots between data were tested by Student's *t*-test. The increasing and decreasing index (fold change) was calculated as ratio of averaged spot intensities (relative % volume) between the investigated and control 2-DE maps.

4-5 Protein in-gel digestion and MS analysis

The protein spots from 2-DE PAGE gel were excised and washed twice with 50 mM ammonium bicarbonate buffer, pH 8.0 and 100% acetonitrile alternatively. After wash with acetonitrile, shrank gel particle was completely dried in the speed-vacuum drier and then add

1.5 uL of 15 ng trypsin solution. After the gel particle was fully rehydrated under ice for more than 30 min, 6.5 uL of trypsin digestion buffer (40 mM ammonium carbonate, pH 8.0, and 10% acetonitrile) was added and incubated for overnight on the 37°C. One microliter of peptide mixtures extracted from 2-DE spot were mixed with equal volume of matrix solution that was prepared freshly by dissolving 0.2 mg α-cyano-4-hydroxycinnamic acid (CHCA) in 1 ml of 80% acetonitrile solution containing 0.1% trifluroacetic acid (TFA) and then, 0.5 uL of mixed solution were crystallized onto a 600 nm Anchor Chip (Bruker Daltonics). After dried and crystallized peptide/matrix mixtures on AnchorChip at the room temperature, it was washed with 0.1% TFA and re-dried at room temperature for analysis. The samples were analyzed with an Ultraflex TOF/TOF mass spectrometer (Bruker Daltonics) under reflector mode to collect peptide mass spectra for peptide mass fingerprinting (PMF) analysis. The mass spectra of tryptic digested peptides were acquired as the average of the ion signals which generated by the irradiation of the target with 100–150 times of laser pulses, in positive reflect mode with 20-25 kV voltage. For mass calibration (error tolerance < 10 ppm), peptide standard mixture mono (Bruker Daltonics) was engaged for external calibration. For MS/MS analysis, lift mode was employed with 25-30 kV voltage and post source decay fragments ion spectra were acquired after isolation of the appropriate parental ions. The mass spectra data produced in both reflect and lift mode were elaborated by using the FlexControl 2.2 (Bruker Daltonics). FlexAnalysis 2.2 (Bruker Daltonics) and Biotool 2.2 software (Bruker Daltonics) were used to process and collect PMF spectra obtained from each tryptic digested protein. Mascot (Matrix science) in-house version software was employed to identify the spots from *T. thermophilus* genome database in a local Mascot server by PMF

analysis. Database search parameter for PMF analysis allowed to methionine oxidation, cysteine carbamidomethylation and maximum missing cleavage, one for variable modification with 0.2 Da peptide error tolerance. A theoretical p*I* and Mw. were calculated by Biotools 2.2 program and functional classification was followed by KEGG classification (http://www. genome.jp /kegg/pathway.html).

5. X-ray crystallography

5-1 Protein overexpression and purification

Sequence data of the *ttha0175* gene coding for *tt*Csp1 was obtained from the *T. thermophilus* HB8 genome project (DDBJ/EMBL/GeneBank AP008226). The DNA fragment containing *ttcsp1* gene was amplified by PCR using the genomic DNA as a template with *Taq* DNA polymerase, forward (*5'*-ATATCATATGCAAAAGGGTCGGGTCAAGTGGTTCA-*3'*), and reverse (*5'*-ATATGGATCCTTATTAGCGCCGCGCGGGCTCCACCAC-*3'*) primers. To improve the gene expression, the second codon CAG was changed to CAA according to the effect of second codon variants on the expression of the *lacZ* gene in *E. coli* (Looman, A. C. *et al.*, 1987). The amplified fragment was digested with the restriction enzymes *Nde*I and *Bam*HI, and the ORF was ligated into the compatible sites of the expression vector pET-11a. Sequence analysis revealed that the construction was error free. *E. coli* Rosetta(DE3) cells transformed with the resultant pET-11a/*ttcsp1* plasmid were cultured at 37°C for 20 h in LB media containing 50 μg/ml ampicillin and were harvested by centrifugation.

Frozen cells (8.4 g) were thawed, suspended in 70 ml of buffer I (20 mM Tris-HCl and

50 mM NaCl, pH 8.0) and sonicated on ice for 10 min with an ultrasonic disrupter. Then, 70 ml of pre-warmed buffer I was added to the suspension. The cell extract was incubated at 70°C for 10 min and then centrifuged at 40,000 g for 60 min at 4°C. After this step, most of *E. coli* proteins were excluded as precipitates. The supernatant was loaded onto a TOYOPEARL SuperQ-650M column (Tosoh) equilibrated with buffer II (20 mM Tris-HCl, pH 8.0). The column was washed with 100 ml of buffer II and the fractions passed through the column were collected. The fractions containing *tt*Csp1 were desalted and loaded onto a Reource S column (GE Healthcare) equilibrated with buffer III (20 mM MES, pH 6.0). The column was washed with buffer III and the proteins were eluted with a linear gradient of 0–0.4 M NaCl in 120 ml of buffer III. The fractions containing *tt*Csp1 were concentrated and loaded onto HiLoadd 16/60 Superdex 75pg (GE Healthcare) equilibrated with 20 mM Tris-HCl and 150 mM NaCl, pH 8.0. The fraction containing *tt*Csp1 were concentrated and stored at –4°C. The purity of the protein was assessed by SDS-PAGE in eash step.

5-2 Crystallization and data collection

An initial attempt of *tt*Csp1 crystallization was performed with the sitting-drop vapor-diffusion method at 293 K and 480 conditions using 8 screening kits (Hampton Research and Emerald Biosystems). Drops were prepared by mixing 0.5 μl protein (17.0 mg/ml) solution with 0.5 μl reservoir solution and equilibrated against 200 μl of reservoir solution. Initial crystallization trials produced several crystal forms using solutions containing polyethylene glycol. The reservoir solution that gave best crystallization result contained 0.1 M Tris-HCl (pH 8.2) and 32% PEG1500.

X-ray diffraction data were collected at the RIKEN Structural Biology Beamline II (BL44B2) at SPring-8 (Hyogo, Japan) (Adachi, S *et al.*, 2001). The crystal was mounted on the goniometer at 100 K by and the crystal-to-detector distance was 150 mm. A total of 360° of data was collected with an oscillation angle of 1° and an exposure time of 10 sec per degree of oscillation. The collected data were processed with the HKL2000 suite (Otwinowski, Z. *et al.*, 1991) and the data collection statistics were summarized in Table 6-1.

5-3 Structure determination and analysis

The structure of *tt*Csp1 was determined by the molecular-replacement method using *MOLREP* (Vagin, A. *et al.*, 1997) from the CCP4 package (Collaborative Computational Project, Number 4, 1994). Among cold shock proteins whose structures are available, *Bacillus caldolyticus* cold shock protein (Bc-Csp) mutant V64T/L66E/67A showed the highest sequence homology to *tt*Csp1. Hence, the coordinate of Bc-Csp mutant (PDB code, 1HZA; Delbrück, H. *et al.*, 2001) was used as the search model. A solution was found with two molecules in the asymmetric unit with an R factor of 0.492. CNS (Brüger, A. T. *et al.*, 1998) was used to refine the atomic positions and thermal factors. 10% of the data was used for calculation of R_{free} during the refinement with CNS. After initial rigid body and simulated annealing refinement, the automatic-tracing procedure in ARP/wARP (Parrakis, A. *et al.*, 2001) was used to build a main-chain model for 124 of the 146 amino acid residues. The rest of the molecule was build into the electron density map using XtalView/X-fit (McRee, D. E., 2000) and model refinement was performed with CNS. The final model was validated using the program *PROCHECK* (Laskowski, R. A, *et al.*, 1997) in the CCP4

package. The refinement statistics are summarized in Table 5-1.

Least squares comparison of two structures and calculation of the root-mean-square (r.m.s) deviations of the main chain atoms were carried out using LAQKAB in CCP4 (Kabsh, W. 1976). The average structures were used in the case of the structures which were determined by NMR and calculated using CNS. Figures were drawn using the programs PyMOL (DeLano, W. L., 2002).

A model structure of *tt*Csp1 complexed with dT6 was constructed on the basis of bcCsp (2HAX) and dT6 (Max, K. E., 2007). Because two bcCsp molecules (A and B chains) form a domain-swapping dimer, the main-chain atoms were superimposed using LSQKAB as follows: residues 2–21 of *tt*Csp1, 2–21 of bcCsp A chain; 25–37 of *tt*Csp1, 25–37 of bcCsp A chain; 38–55 of *tt*Csp1, 38–55 of bcCsp B chain; and 58–68 of *tt*Csp1, 56–66 of bcCsp B chain.

5-4 Comparison of surface charges

The structural models of 15 Csps were obtained using the SWISS-MODEL (SIB) and ClustalW2 programs (EBI) using *ec*CspA as a template. The surface charges of the molecules were calculated using the APBS1.3 program.

6. Oligonucleotide-binding analysis

6-1 Nucleic Acid Binding Measured by Fluorescence Quenching

Fluorescence spectra were recorded with a Hitachi fluorescence spectrophotometer, model F4500. The protein solution contained 0.5–0.48 μM Csp1, 25 mM Tris-HCl, 100 mM

KCl, and 0.5 mM EDTA, at pH 7.5. This protein solution was successively titrated with ssDNA or ssRNA solution in a 5 x 5 mm cell at 25°C. The excitation and emission wavelengths were 295 and 350 nm, respectively. The nucleotide sequences of ssDNA and ssRNA used in this experiment are shown in Table 6-1. LoopdT7, loopdT7dA4, loopdT11, stem5dT7, stem3dT7, LoopU7, stem5U7 and stem3U7 were prepared by incubating at 95°C (ssDNA) or 80°C (ssRNA) for 2 min and 60°C for 10 min to form secondary structure as shown in Figure 6-1.

The K_d values for high-affinity oligonucleotides were determined by competition experiments with 10 μM dT4. The equilibrium dissociation constant, K_d, was determined as follows. The fluorescence quenching was analyzed assuming the following scheme for the interaction of *tt*Csp1 (P) with ssDNA or ssRNA ligand (S_2) (Fersht, A. R., 1999),

$$P + S_1 \overset{K_{PS1}}{\Longleftrightarrow} PS_1 \quad (1)$$

$$P + S_2 \overset{K_{PS2}}{\Longleftrightarrow} PS_2 \quad (2)$$

*tt*Csp1 (P) binds to a competitor dT4 (S_1) to form the complex PS_1 with dissociation constant KPS1 = $[P][S_1] / [PS_1]$. *tt*Csp1 competitively binds to a ligand (S_2) to form the complex PS2 with dissociation constant KPS2 = $[P][S_2] / [PS_2]$. Because the fluorescence intensity of oligonucleotide is nearly zero, the observed fluorescence intensity (F_{obs}) is expressed as follows:

$$F_{obs} = F_P[P] + F_{PS1}[PS_1] + F_{PS2}[PS_2] \quad (3)$$

where F_P, F_{PS1}, and F_{PS2} are the molar fluorescence intensities of P, PS_1, and PS_2, respectively.

The total concentrations of P, S_1, and S_2 are expressed by (4), (5), and (6), respectively.

$$[P]_t = [P] + [PS_1] + [PS_2] \quad (4)$$

$$[S_1]_t = [S_1] + [PS_1] \quad (5)$$

$$[S_2]_t = [S_2] + [PS_2] \quad (6)$$

From K_{PS1} and (5),

$$[S_1]_t = [S_1] + [PS_1] = \frac{K_{PS1}[PS_1]}{[P]} + [PS_1] = (\frac{K_{PS1}}{[P]} + 1)[PS_1] \quad (7)$$

Then,

$$[PS_1] = \frac{[P]}{[P]+K_{PS1}}[S_1]_t \quad (8)$$

From K_{PS2} and (6),

$$[PS_2] = \frac{[P]}{[P]+K_{PS2}}[S_2]_t \quad (9)$$

From (4), (8) and(9),

$$[P]_t = [P] + [PS_1] + [PS_2]$$

$$= [P] + [S_1]_t(\frac{[P]}{[P]+K_{PS1}}) + [S_2]_t(\frac{[P]}{[P]+K_{PS2}}) \quad (10)$$

Therefore,

$$-([P] + K_{PS1})([P] + K_{PS2})[P]_t + ([P] + K_{PS1})([P] + K_{PS2})[P]$$

$$+[S_1]_t[P]([P] + K_{PS2}) + [S_2]_t[P]([P] + K_{PS1}) = 0 \quad (11)$$

By using this [P] value obtained from (11), $[PS_1]$ and $[PS_2]$ were obtained from (8) and (9), respectively. For the competition experiments, (3) was fitted to the observed data by fixing F_P, F_{PS1}, and K_{PS1}, using Igor Pro software (WaveMetrics). The constructed theoretical curves are shown in Figure 6-3.

6-2 Analytical Size-exclusion Chromatography

(1) The oligomeric structure of *tt*Csp1 in the presence or absence of nucleic acid

ligand and (2) the number of nucleotide molecule bound to *tt*Csp1 were analyzed by size-exclusion chromatography.

The Superdex 75 10/300 GL column (GE healthcare) was pre-equilibrated with 20 mM Tris-HCl and 200 mM NaCl at pH 8.0. In the presence of oligonucleotide, the reaction mixture contained Csp1 (47 μM) and dT7 (47 μM) or dT31 (8 μM) in the same buffer, and was incubated for 5 min before applying to the column. The eluent from the column was monitored by the UV-absorption at 280 and 260 nm. The apparent molecular mass was estimated by comparing its retention time with those of molecular mass markers (Sigma).

7. RNase assay

A 50-mer hairpin RNA (h-RNA, 5'-CCCCCCGGGGGGGGGGAUUCCGUUUA UUCAACCUCCCCCCCCCCCCCCCC-3') was chemically synthesized and was radiolabelled at the 3'-end with [γ-^{32}P]ATP using T4 RNA ligase. h-RNA forms a hairpin structure shown in Figure 7-1. *tt*Csp1 was incubated with 0.1 μM h-RNA at 37°C for 20 min. After incubation, 0.3 μM TTHA0252, a single-strand-specific 5' to 3' exonuclease, was added. Aliquots of the reaction mixture was removed at various times to stop the reaction by adding the denaturing dye (5 mM EDTA, 80% deionized formamide, 10 mM NaOH, 0.1% bromophenol blue and 0.1% xylene cyanol) and heat-treatment at 95°C for 5 min. The reaction mixtures were loaded onto 25% acrylamide gels (8M urea and x 1 TBE buffer (89 mM Tris-borate, 2 mM EDTA)) and electrophoresed with x 1 TBE buffer. The gel was dried and placed in contact with an imaging plate. The bands were visualized and analyzed using a BAS2500 image analyzer (Fuji film).

RESULTS AND DISCUSSION

1. Cell viability of *csp* deletion mutants

1.1 Both *tt*Csp1 and *tt*Csp2 were not essential for the growth at 70°C.

When plasmids for producing the *ttcsp1* and/or *ttcsp2* deletion mutants described in Materials and Methods transformed the wild type cells, the transformants formed colonies on the TT plates (rich media) containing selection markers at 70°C. As shown in Figure 1-A, no obvious growth defect was observed in the mutants at 70°C. It indicates that both *tt*Csps are not essential for the growth at 70°C.

1.2 *tt*Csp1 and *tt*Csp2 seemed to function redundantly under cold condition.

Then I investigated whether the *ttcsp1* and/or *ttcsp2* deletion mutants are viable under cold condition. The temperature of each culture was shifted from 70°C to 45℃ immediately by addition of the ice-cold medium. Such sudden cooling (or such a sharp temperature drop) is termed as "cold shock." Despite the disruption of the *ttcsp1* gene, the cells were viable under cold condition. As shown in Figure 1-1, the growth of the wild type and Δ*ttcsp1* cells were paused for 120 min, and then resumed slowly. Such a transient growth arrest has been known as a typical cold shock response in many bacteria (Horn, G. *et al.*, 2007). The Δ*ttcsp1* mutant could adapt to the cold condition and re-grow in the same manner as the wild type. No growth defect was observed in the Δ*ttcsp1* mutant under the cold condition. On the other hand, the growth of the Δ*ttcsp2* cells exhibited very shorter

growth arrest compared to the wild type and Δ*ttcsp1* cells. The double deletion mutant could not grow at 45℃ after the temperature downshift and a substantial portion of the cells appeared to die. Cells grown after the cold shock may be revertants. The observation that the *ttcsp1*/*ttcsp2* double deletion strain was lethal indicates that at least one Csp homologue is essential for the survival of *T. thermphilus* HB8 at low temperatures. Since the Δ*ttcsp2* cells did not exhibit a typical cold shock response, *tt*Csp2 was considered to be more important in cold adaptation of the organism.

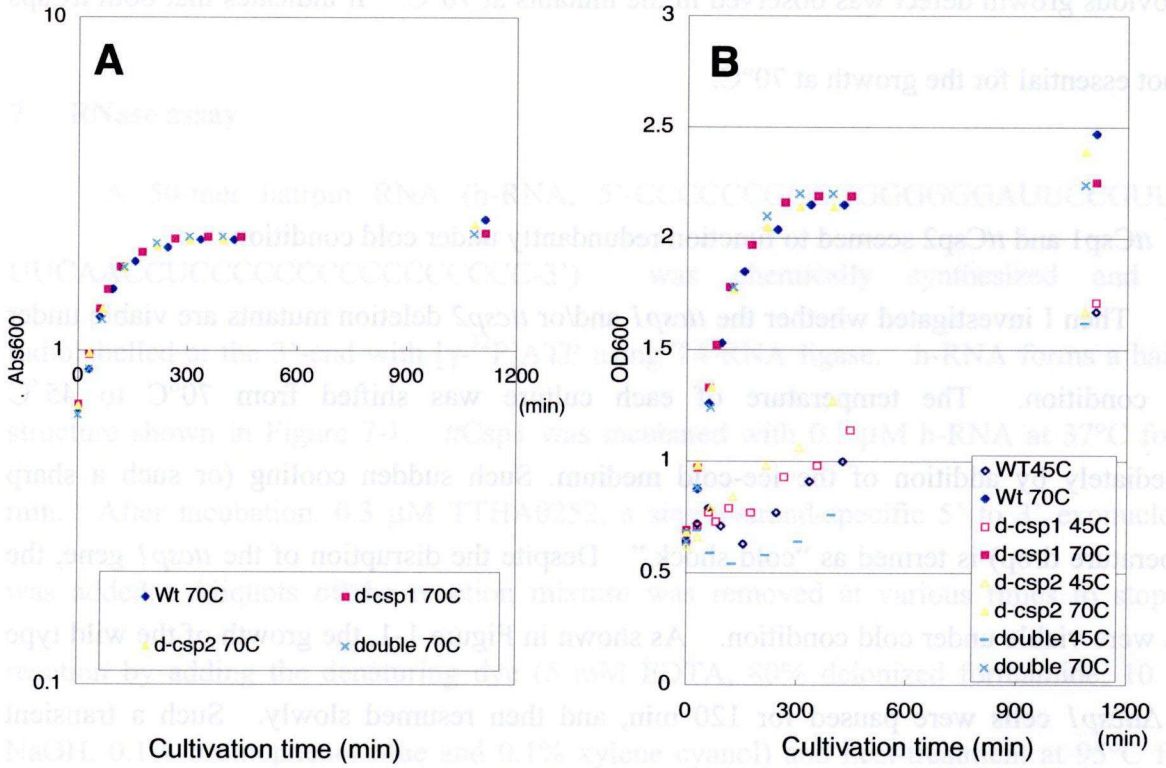

Figure 1-1. Growth curves of the wild type and the *ttcsp* deletion mutant strains.
The values of the absorbance at 600 nm were measured at the time points indicated.
(A) WT (◆), the Δ*ttcsp1* mutant (■), the Δ*ttcsp2* mutant (▲) and the Δ*ttcsp1*Δ*ttcsp2* double mutant (×) were grown at 70°C
(B) WT (◆/◇), the Δ*ttcsp1* mutant (■/□), the Δ*ttcsp2* mutant (▲/△) and the Δ*ttcsp1*Δ*ttcsp2* double mutant (×/−) were grown at (70°C /45°C).

2. DNA microarray analysis

2.1 *tt*Csp1 was constitutively expressed even under the cold condition.

Since the viability of the *ttcsp1* deletion mutant provided no functional information, I examined the change in the transcriptional level of *tt*Csp1 in the wild type cells upon temperature downshift. DNA microarray analysis was performed using Affymetrix GeneChip system and GeneSpring software. The array signals were normalized to the value of 50 percentile per Chip. I selected the genes whose normalized signals were changed more than 2-fold. I prepared three independent samples sets, and the significant changes ($p < 0.05$) were tested by Student's *t*-test to eliminate false positive and false negative results. The samples were collected 0, 30 and 120 min after the temperature downshift to 45°C. The microarray results, shown in Figure 2-1, indicated that the *ttcsp1* gene was constantly transcribed: its transcription level did not change depending on either the growth phase or the temperature in the wild type cells. The constant expression of *ttcsp1* seemed similar to that of housekeeping gene, although *ttcsp1* is not essential for cell viability.

It should be noted here that cell cultures were centrifuged for 5 min at 4°C when I harvested the cells for the microarray analysis. This means that the cells were subjected to temporary cold shock during the centrifugation. To check the effects of this short cold shock to the microarray data, I prepared two samples of cell culturers: one was prepared as described above, whereas the other was fixed by adding cold ethanol (final 50%) before the centrifugation. The results of these two samples shown in Figure 2-2 indicated that the temporary cold shock treatment did not affect the transcriptional transient levels of all genes

except two genes, *ttha0359* and *ttha0948*. *ttha0359* and *ttha0948* code for *tt*Csp2 and fatty acid desaturase, respectively. Therefore, it was validated that the transcription of *ttcsp1* was not affect by temporal cold shock upon harvesting the cells. It should also be mentioned here that the transcription of mRNA for *tt*Csp2 and fatty acid desaturase initially responded to the cold stress.

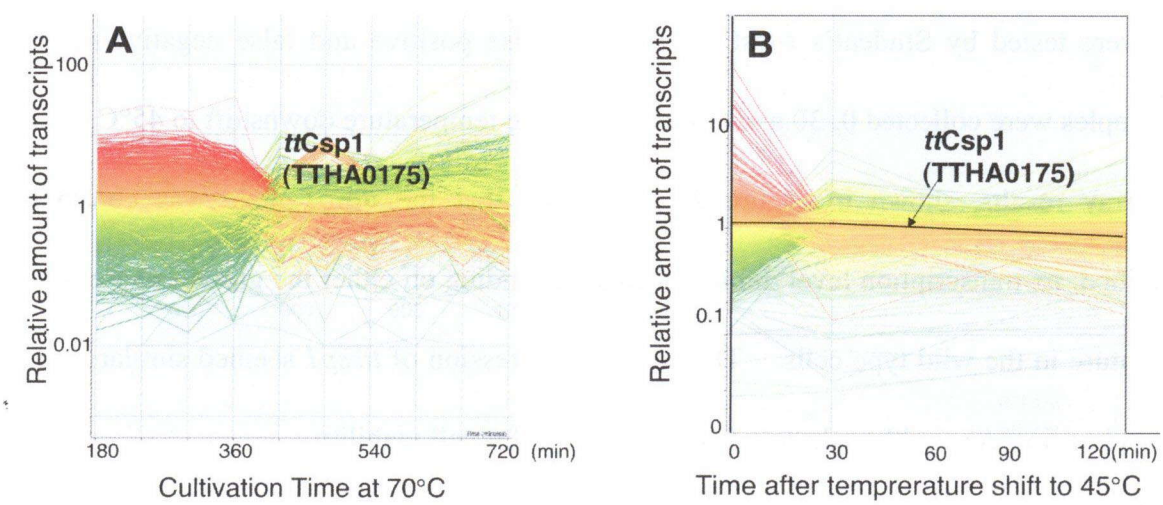

Figure 2-1. Expression profile of *ttcsp1* gene.

(A) Expression profile of the wild type during the growth at 70°C.

(B) Expression profile of the wild type after temperature downshift to 45°C.

The profile for the *ttcsp1* gene is indicated as black lines. Green, yellow, and red lines represent increased expression, no change, and decreased expression during culture, respectively.

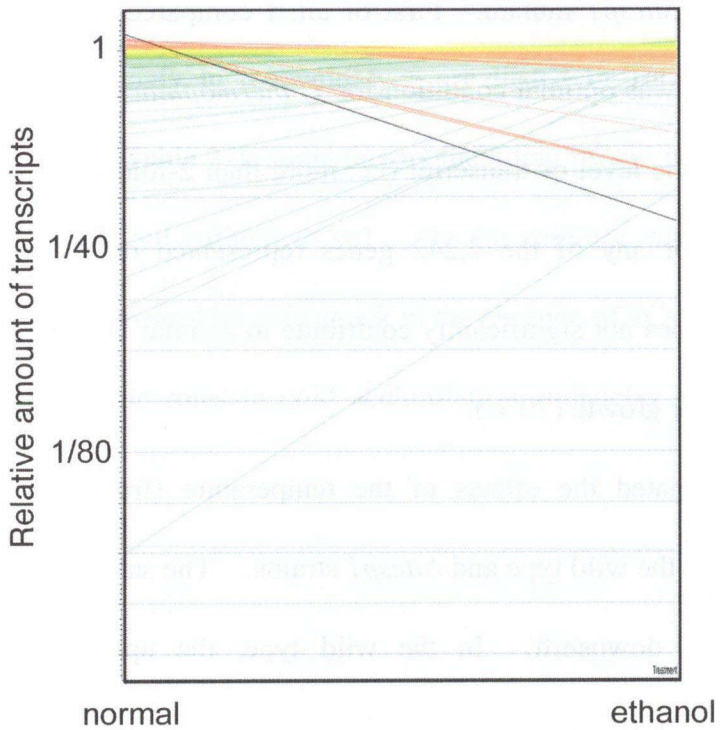

Figure 2-2. Effect of the temporary cold shock treatment on the microarray signals. The array signals from the samples prepared by different ways was compared. The signals of those prepared by normal way, centrifugation at 4°C for 5 min, are shown on the left axis, whereas those prepared by fixation with ethanol before centrifugation are shown on the right axis. The signals of *tt*Csp2 and fatty acid desaturase are represented as thick black line and thick red line, respectively.

2.3 *tt*Csp1 might controll the transcription of some genes required for survival.

To obtains some clues to the *tt*Csp1 function, I investigated the transcriptional profiles of the wild type and Δ*ttcsp1* mutant. First of all, I compared the profiles from the cells grown at 70°C, which was optimal condition for *T. thermophilus* HB8. To my surprise, no significant change in the level of transcript (i.e. more than 2-fold in the Δ*ttcsp1* mutant, $q < 0.05$) was detected for any of the 2,242 genes represented on the array. This finding suggests that *tt*Csp1 does not significantly contribute to cellular transcriptional control at the optimal temperature for growth (70°C).

Next I investigated the effects of the temperature (from 70°C to 45℃) on the transcriptional level in the wild type and Δ*ttcsp1* strains. The samples were prepared 30 min after the temperature downshift. In the wild type, the up-regulated (75 genes) and down-regulated (76 genes) genes were identified as listed in Tables 2-1 and 2-2. Similar transcriptional changes are reported for other bacteria under the cold stress condition. These results suggest that cold adaptation mechanisms of *T. themophlus* HB8 is not so different from those of other bacteria.

Then I analyzed the microarray data of the Δ*ttcsp1* mutant under the same conditions (from 70°C to 45℃). Tables 2-5 and 2-6 are the lists of up- and down-regulated genes at 45°C in the Δ*ttcsp1* mutant. The numbers of the up- and dowon-regulated genes are 136 and 139, respectively, which were larger than those in the wild-type. The decrease in the expression level in the Δ*ttcsp1* mutant implies that *tt*Csp1 is involved in alteration of transcription upon the cold shock. *tt*Csp1 might support initiation or continuation of transcription of the genes listed in Table 2-6. Inversely, *tt*Csp1 might inhibit the

transcription initiation and elongation, or support the mRNA degradation of the genes listed in Table 2-5.

Next I compared the results of the wild type with those of Δ*ttcsp1*. Cold-inducible and cold-repressible genes only in the wild type are lilsted in Table 2-3 and Table 2-4, respectively. As shown in Table 2-3, some factors including *tt*Csp2 needed to adjust to cold condition could not be induced without *tt*Csp1. On the contrary, many factors function in metabolism could not be repressed by cold shock in the absence of *tt*Csp1 (see Table 2-4). It implies that *tt*Csp1 has some roles in cold acclimilation and delay of cell division in the transcriptional level.

Table 2-1. The genes increased under the cold condition in the wild type.

Function	Gene Name	fold	Description
Genetic Information Processing	TTHA1002	3.9	response regulator
	TTHA1003	3	sensor histidine kinase
	TTHA1502	2.8	response regulator
	TTHA1036	2.7	signal recognition particle protein
	TTHB016	2.7	oxidoreductase, short-chain dehydrogenase/reductase family
	TTHA0008	2.4	phage shock protein A
Chaperones	TTHB117	3.4	putative type IV pilin
	TTHB119	2.6	prepilin-like protein
Csp2	TTHA0359	2.7	cold shock protein
detox	TTHB118	3.1	probable secretion system protein
DNA repair/ recombination/ replication	TTHA1440	2.4	excinuclease ABC subunit A (UvrA)
	TTHB201	2.4	transposase-like protein
	TTHA0112	2.2	endonuclease III
	TTHA1539	2.2	putative phage integrase/recombinase
RNA helicase	TTHA0109	2.4	ATP-dependent RNA helicase
transcription	TTHA0622	3.5	transcription elongation factor GreA
	TTHB023	4.7	transcriptional regulator, TetR family
translation/ ribosomal protein	TTHA1138	2.1	30S ribosomal protein S15
Metabolism of nucleotide	TTHA1442	4.1	glucose inhibited division protein
	TTHA0135	2.8	MutT/nudix family protein
	TTHA1920	2.3	thioredoxin reductase
Membrane/ Transporter/ Lipoprotein	TTHA1004	4.5	conserved hypothetical membrane protein
	TTHA1008	4.4	ABC transporter, permease protein
	TTHA1007	3.6	ABC transporter, ATP-binding protein
	TTHA0377	3.3	sugar ABC transporter, permease protein
	TTHA1391	2.9	GTP-binding protein
	TTHA0725	2.6	membrane-bound protein LytR
	TTHA0194	2.4	probable tripartite transporter, small subunit
Metabolism of ammino acid	TTHA1914	2.6	homocitrate synthase
	TTHA1743	2.5	orotidine 5'-phosphate decarboxylase
	TTHA1320	2.4	periplasmic serine protease
	TTHA0957	2.2	dihydrodipicolinate synthase
	TTHA0958	2.1	2-hydroxyhepta-2,4-diene-1,7-dioate isomerase/ 5-carboxymethyl-2-oxo-hex-3-ene-1,7-dioate decarboxylase
	TTHA0760	2	O-acetyl-L-homoserine sulfhydrylase
Metabolism of Carbohydrate	TTHA1066	3.6	proabable transaldolase
	TTHB019	2.5	MaoC-related acyl dehydratase
	TTHA0022	2.4	glucose-1-phosphate adenylyltransferase
	TTHB017	2.3	medium-chain acyl-CoA ligase-related protein
	TTHA1261	2.2	4-alpha-glucanotransferase (amylomaltase) (disproportionating enzyme) (D-enzyme)
Metabolism of energy	TTHA0021	2.1	putative NADPH oxidoreductase
Metabolism of fatty acid	TTHB022	5.1	putative acyl-CoA dehydrogenase
	TTHA0750	4	3-oxoacyl-[acyl carrier protein] reductase
	TTHB015	3.4	putative acyl-CoA dehydrogenase
	TTHB020	3.4	3-oxoacyl-[acyl carrier protein] reductase
	TTHA0948	2.2	fatty acid desaturase

Others /Unknown	TTHA0838	2.5	glutaredoxin-like protein
	TTHA0840	2.5	probable thiol:disulfide interchange protein
	TTHA0929	2.1	phosphopantetheine adenylyltransferase
	TTHA1162	2.4	excisionase domain protein
	TTHA1217	2.2	prepilin-like protein
	TTHA1369	2	phospholipase domain protein
	TTHA1511	2.9	putative catechol 1,2-dioxygenase
	TTHA1512	2.8	putative nucleotidyltransferase
	TTHB012	4.1	phosphoglycerate mutase family protein
	TTHB014	3.7	probable phosphotransferase
hypothetical protein	TTHA0025	2.3	hypothetical protein
	TTHA0105	2.2	hypothetical protein
	TTHA0163	2.9	hypothetical protein
	TTHA0592	2.4	hypothetical protein
	TTHA0613	2	hypothetical protein
	TTHA0777	2.1	hypothetical protein
	TTHA0808	2.1	hypothetical protein
	TTHA0828	2.6	hypothetical protein
	TTHA1001	8	hypothetical protein
	TTHA1005	4.1	hypothetical protein
	TTHA1006	3.9	hypothetical protein
	TTHA1469	2	hypothetical protein
	TTHA1510	2.1	hypothetical protein
	TTHA1540	2.1	hypothetical protein
	TTHA1581	2.7	hypothetical protein
	TTHA1734	2	hypothetical protein
	TTHB003	3	hypothetical protein
	TTHB013	4.2	hypothetical protein
	TTHB021	3.6	hypothetical protein
	TTHB120	2.1	hypothetical protein

Table 2-2. The genes decreased under the cold condition in the wild type.

Function	Gene Name	fold	Discription
Genetic Information Processing	TTHA0829	3.1	putative acetoin utilization protein, acetoin dehydrogenase
transcription	TTHB186	2.9	putative transcriptional regulator
transcription	TTHB073	2.9	transcriptional regulator
transcription	TTHA0058	2.2	transcriptional repressor of class I heat-shock genes
translation	TTHA1498	3.4	elongation factor G (EF-G-2)
LytR/CspA/Psr family	TTHA1778	2.4	LytR/CspA/Psr family protein
Metabolism of nucleotide	TTHA0735	2.2	cytidine deaminase
Membrane/ Transporter/ Lipoprotein	TTHA1141	6	cation-transporting ATPase
	TTHA1408	4.8	ABC transporter, ATP-binding protein
	TTHA1407	3.9	cytochrome c-type biogenesis protein, heme exporter protein B
	TTHB076	3.4	putative C4-dicarboxylate transporter, large permease protein
	TTHA1137	3	major facilitator superfamily transporter
	TTHA0452	2.5	branched-chain amino acid ABC transporter, ATP-binding protein
	TTHB218	2.2	ABC transporter, ATP-binding protein
	TTHA0451	2.2	probable branched-chain amino acid ABC transporter, amno acid binding protein
	TTHA1337	2.1	peptide ABC transporter, permease protein
	TTHA1338	2	ABC transporter permease protein
Metabolism of ammino acid	TTHA0606	2	aspartate 1-decarboxylase
Metabolism of Carbohydrate	TTHA1836	15	isocitrate lyase
	TTHA0506	3.1	malate synthase
	TTHA0097	2.3	NADH-quinone oxidoreductase chain 14
Metabolism of Cofactors and Vitamins	TTHA1506	3.8	glutamyl-tRNA reductase
	TTHA0190	2.1	dihydroneopterin aldolase
	TTHA1775	2	pantoate--beta-alanine ligase
Metabolism of energy	TTHA1133	20	ba3-type cytochrome c oxidase polypeptide IIA
	TTHA1134	14	ba3-type cytochrome c oxidase polypeptide II
	TTHA1942	13	putative cytochrome c oxidase assembly protein
	TTHA1447	12	alanine dehydrogenase
	TTHA1135	9.6	ba3-type cytochrome c oxidase polypeptide I
	TTHA0663	3.4	pyruvate orthophosphate dikinase
	TTHA1117	2.9	iron-sulfur protein
	TTHA1505	2.7	cytochrome c assembly protein-related protein
	TTHA0310	2.6	cytochrome c oxidase assembly factor (CtaA) protoheme IX farnesyltransferase (CtaB)
	TTHA1276	2.2	V-type ATP synthase subunit E
	TTHA1272	2.1	V-type ATP synthase subunit B
	TTHA1271	2	V-type ATP synthase subunit D
	TTHA1273	2	V-type ATP synthase subunit A
Metabolism of fatty acid	TTHB116	2.2	acyl-CoA dehydrogenase, short-chain specific (probable AidB protein)
	TTHA0604	2	medium-chain-fatty-acid--CoA ligase
Others /Unknown	TTHA0982	2.7	bacterioferritin
	TTHA0642	2.4	putative glycosyltransferase
	TTHA1448	4.2	4-hydroxybutyrate CoA-transferase
	TTHB010	2.6	transposase-related protein
	TTHA1335	2.2	branched-chain amino acid ABC transporter, ATP-binding protein

hypothetical protein	TTHA0236	2.3	hypothetical protein
	TTHA0268	2.1	hypothetical protein
	TTHA0316	16	hypothetical protein
	TTHA0467	3.2	hypothetical protein
	TTHA0487	2	hypothetical protein
	TTHA0646	2.3	hypothetical protein
	TTHA0681	2.5	hypothetical protein
	TTHA0682	2.1	hypothetical protein
	TTHA0727	5.3	hypothetical protein
	TTHA0757	16	hypothetical protein
	TTHA1136	4.9	hypothetical protein
	TTHA1160	4.2	hypothetical protein
	TTHA1626	30	hypothetical protein
	TTHA1725	2	hypothetical protein
	TTHA1759	2.9	hypothetical protein
	TTHA1848	2	hypothetical protein
	TTHA1869	2	hypothetical protein
	TTHA1870	2.1	hypothetical protein
	TTHA1895	4.3	hypothetical protein
	TTHA1943	16	hypothetical protein
	TTHA1948	2.5	hypothetical protein
	TTHA1954	2.7	hypothetical protein
	TTHB006	3.6	hypothetical protein
	TTHB007	2.9	hypothetical protein
	TTHB008	4.3	hypothetical protein
	TTHB009	4.8	hypothetical protein
	TTHB147	2.4	hypothetical protein
	TTHB150	2	hypothetical protein
	TTHB156	4.4	hypothetical protein
	TTHB157	8.9	hypothetical protein
	TTHB158	3.6	hypothetical protein
	TTHB203	2.9	hypothetical protein

Table 2-3. Cold-inducible genes only in the wild type.

Function	Gene Name	Discription
Genetic Information Processing	TTHA0008	phage shock protein A
Csp2	TTHA0359	cold shock protein
Metabolism of Carbohydrate	TTHA0022	glucose-1-phosphate adenylyltransferase
	TTHA1261	4-alpha-glucanotransferase (amylomaltase) (disproportionating enzyme) (D-enzyme)
Metabolism of energy	TTHA0021	putative NADPH oxidoreductase
Metabolism of fatty acid	TTHA0750	3-oxoacyl-[acyl carrier protein] reductase
hypothetical protein	TTHA0613	hypothetical protein
	TTHA0777	hypothetical protein
	TTHA0808	hypothetical protein
	TTHA1581	hypothetical protein
	TTHB003	hypothetical protein
	TTHC006	hypothetical protein

Table 2-4. Cold-repressible genes only in the wild type.

Function	Gene Name	Discription
transcription	TTHB186	putative transcriptional regulator
transcription	TTHB073	transcriptional regulator
LytR/CspA/Psr family	TTHA1778	LytR/CspA/Psr family protein
Membrane/ Transporter/ Lipoprotein	TTHB076	putative C4-dicarboxylate transporter, large permease protein
	TTHA0452	branched-chain amino acid ABC transporter, ATP-binding protein
	TTHB218	ABC transporter, ATP-binding protein
	TTHA0451	probable branched-chain amino acid ABC transporter, amno acid binding protein
Membrane/ Transporter/ Lipoprotein	TTHA1337	peptide ABC transporter, permease protein
	TTHA1338	ABC transporter permease protein
Metabolism of ammino acid	TTHA0606	aspartate 1-decarboxylase
Metabolism of Carbohydrate	TTHA0506	malate synthase
	TTHA0097	NADH-quinone oxidoreductase chain 14
Metabolism of Cofactors and Vitamins	TTHA0190	dihydroneopterin aldolase
Metabolism of energy	TTHA0663	pyruvate orthophosphate dikinase
	TTHA1276	V-type ATP synthase subunit E
	TTHA1272	V-type ATP synthase subunit B
	TTHA1271	V-type ATP synthase subunit D
	TTHA1273	V-type ATP synthase subunit A
Others /Unknown	TTHA0982	bacterioferritin
	TTHA1335	branched-chain amino acid ABC transporter, ATP-binding protein
hypothetical protein	TTHA0467	hypothetical protein
	TTHA0487	hypothetical protein
	TTHA0646	hypothetical protein
	TTHA0681	hypothetical protein
	TTHA0682	hypothetical protein
	TTHA1160	hypothetical protein
	TTHA1725	hypothetical protein
	TTHA1869	hypothetical protein

Table 2-5. The genes increased under the cold conditions in Δ*ttcsp1* mutant.

Function	Gene Name	fold	Discription
Genetic Information Processing	TTHA0841	3.8	stage V sporulation protein R (SpoVR) related protein
	TTHB016	3.6	oxidoreductase, short-chain dehydrogenase/reductase family
	TTHA1036	3.4	signal recognition particle protein
	TTHA1502	3.4	response regulator
	TTHA1190	2.7	rod shape-determining protein MreD
	TTHA0249	2.6	preprotein translocase SecE subunit
	TTHA1002	2.3	response regulator
	TTHA1189	2.3	rod shape-determining protein MreC
	TTHA1003	2	sensor histidine kinase
Chaperones	TTHA0630	2.8	heat shock protein HslU
detoxification	TTHC012	2.7	anti-toxin-like protein
	TTHA0554	2.9	small multidrug export protein
transcription	TTHB023	9.3	transcriptional regulator, TetR family
	TTHA0622	6.6	transcription elongation factor GreA
	TTHA0248	4.4	transcription antitermination protein NusG
	TTHA1065	3.4	transcription termination factor Rho
translation	TTHA1679	5.1	30S ribosomal protein S14
	TTHA1570	2.7	deoxyhypusine synthase
translation/ ribosome	TTHA1465	2.5	50S ribosomal protein L13
	TTHA1138	2.1	30S ribosomal protein S15
RNA ligase	TTHA1819	2.2	2'-5' RNA ligase
RNA helicase	TTHA0109	3.1	ATP-dependent RNA helicase
DNA repair/ recombination/ replication	TTHA1162	3.7	excisionase domain protein
	TTHA1539	3.4	putative phage integrase/recombinase
	TTHA1440	3.1	excinuclease ABC subunit A (UvrA)
	TTHA0112	3.1	endonuclease III
Metabolism of nucleotide	TTHA0135	7.1	MutT/nudix family protein
	TTHA1743	4	orotidine 5'-phosphate decarboxylase
	TTHA1795	2.4	MutT/nudix family protein
	TTHA0361	2.3	survival protein SurE
	TTHA1920	3.8	thioredoxin reductase
Membrane/ Transporter/ Lipoprotein	TTHA1004	6.8	conserved hypothetical membrane protein
	TTHA0377	6.1	sugar ABC transporter, permease protein
	TTHA1391	6	GTP-binding protein
	TTHA1007	5.6	ABC transporter, ATP-binding protein
	TTHA1008	5.5	ABC transporter, permease protein
	TTHA0255	5.1	ferric uptake regulation protein
	TTHA0725	4.8	membrane-bound protein LytR
	TTHA1896	3.4	glucosamine--fructose-6-phosphate aminotransferase [isomerizing]
	TTHB251	3.4	ABC transporter, periplasmic solute-binding protein-related protein
	TTHA0194	3.3	probable tripartite transporter, small subunit
	TTHA0627	3.3	large-conductance mechanosensitive channel
	TTHA1170	3	amino acid ABC transporter, permease protein
	TTHA1185	2.8	GTP-binding protein
	TTHA0045	2.5	probable potassium uptake protein TrkA
	TTHA0629	2.5	putative O-linked GlcNAc transferase (TPR repeat)
	TTHA1060	2.4	Mg2+ transporter MgtE
	TTHA1171	2.4	amino acid ABC transporter, periplasmic amino acid-binding protein
	TTHA1173	2.2	Trk system potassium uptake protein (TrkG)
	TTHA0120	2.1	GTP-binding protein Era
	TTHA0717	2	molybdenum ABC transporter molybdate-binding protein

Metabolism of amino acid	TTHA1208	2.4	probable citramalate synthase
	TTHA1457	2.2	S-adenosylmethionine decarboxylase proenzyme
	TTHA1914	4.9	homocitrate synthase
	TTHA1844	3.3	anthranilate synthase component I (TrpE)
	TTHA0760	3.2	O-acetyl-L-homoserine sulfhydrylase
	TTHA1320	3.1	periplasmic serine protease
	TTHA0759	2.6	homoserine O-acetyltransferase
	TTHA1911	2.6	probable homoaconitase large subunit (homoaconitate hydratase)
	TTHA1378	2.5	homoisocitrate dehydrogenase
	TTHA1642	2.5	S-adenosylmethionine synthetase
	TTHA0824	2.3	spermidine synthase
	TTHA0825	2.3	S-adenosylmethionine decarboxylase proenzyme
	TTHA1910	2.3	probable homoaconitase small subunit (homoaconitate hydratase)
	TTHA0957	2.2	dihydrodipicolinate synthase
	TTHA1843	2.2	anthranilate synthase component II (TrpG)
	TTHA1041	2.1	lysyl-tRNA synthetase (lysine--tRNA ligase) (LysRS)
	TTHA1842	2	anthranilate phosphoribosyltransferase (TrpD)
Metabolism of Carbohydrate	TTHA1066	9	proabable transaldolase
	TTHB017	3.5	medium-chain acyl-CoA ligase-related protein
	TTHA1707	2.7	sugar fermentation stimulation protein family protein
	TTHA0947	2.4	triosephosphate isomerase
Metabolism of Cofactors and Vitamins	TTHA0011	2.5	molybdenum cofactor biosynthesis protein A (MoaA)
	TTHA0929	2.2	phosphopantetheine adenylyltransferase
	TTHA1796	2	probable thiamine biosynthesis protein ThiI
Metabolism of energy	TTHA1326	5	cytochrome c-552 like protein
	TTHA1325	4.7	putaitve sulfite oxidase
	TTHA1422	2.3	thioredoxin
Metabolism of fatty acid	TTHB022	9.8	putative acyl-CoA dehydrogenase
	TTHB020	5.9	3-oxoacyl-[acyl carrier protein] reductase
	TTHB015	5.7	putative acyl-CoA dehydrogenase
	TTHA0948	2.8	fatty acid desaturase
Others /Unknown	TTHA0962	6.8	homoprotocatechuate 2,3-dioxygenase
	TTHA0840	3.3	probable thiol:disulfide interchange protein
	TTHA0838	2.9	glutaredoxin-like protein
	TTHA1140	2.4	metallo-beta-lactamase superfamily protein
	TTHA0737	2	putative dihidrodipicolinate synthase
	TTHB014	15	probable phosphotransferase
	TTHB012	9.3	phosphoglycerate mutase family protein
	TTHB117	5.4	putative type IV pilin
	TTHA1511	4	putative catechol 1,2-dioxygenase
	TTHB119	4	prepilin-like protein
	TTHA1209	3.2	probable acetyltransferase
	TTHA1619	2.5	probable methyltransferase
	TTHA1512	2.4	putative nucleotidyltransferase
	TTHA1897	2.4	GidA-related protein
	TTHA1217	2.2	prepilin-like protein
	TTHB201	2.2	transposase-like protein
	TTHA0241	3.1	oxidoreductase, short-chain dehydrogenase/reductase family
	TTHA0013	2.2	geranylgeranyl diphosphate synthetase

hypothetical protein	TTHA0025	2.2	hypothetical protein
	TTHA0079	2.9	hypothetical protein
	TTHA0105	2.4	hypothetical protein
	TTHA0111	3.6	hypothetical protein
	TTHA0163	5.5	hypothetical protein
	TTHA0212	5	hypothetical protein
	TTHA0228	2	hypothetical protein
	TTHA0253	2.5	hypothetical protein
	TTHA0362	2.2	hypothetical protein
	TTHA0396	2.7	hypothetical protein
	TTHA0419	2.1	hypothetical protein
	TTHA0539	2.3	hypothetical protein
	TTHA0560	2	hypothetical protein
	TTHA0568	4.4	hypothetical protein
	TTHA0592	2.8	hypothetical protein
	TTHA0702	3.1	hypothetical protein
	TTHA0728	2.9	hypothetical protein
	TTHA0802	2	hypothetical protein
	TTHA0828	2.8	hypothetical protein
	TTHA0942	2.3	hypothetical protein
	TTHA0961	3.5	hypothetical protein
	TTHA1001	4.7	hypothetical protein
	TTHA1005	6	hypothetical protein
	TTHA1006	6.6	hypothetical protein
	TTHA1075	2.1	hypothetical protein
	TTHA1102	2.4	hypothetical protein
	TTHA1108	2.2	hypothetical protein
	TTHA1118	2.5	hypothetical protein
	TTHA1158	3.3	hypothetical protein
	TTHA1175	2.9	hypothetical protein
	TTHA1187	2.1	hypothetical protein
	TTHA1268	2.3	hypothetical protein
	TTHA1327	4.4	hypothetical protein
	TTHA1467	2	hypothetical protein
	TTHA1510	3	hypothetical protein
	TTHA1708	2.4	hypothetical protein

Table 2-6. The genes decreased under the cold conditions in Δ*ttcsp1* mutant.

Function	Gene Name	fold	Discription
Genetic Information Processing	TTHA0829	5.2	putative acetoin utilization protein, acetoin dehydrogenase
	TTHA1774	2.6	pili retraction protein PilT
	TTHA1352	2.1	response regulator
	TTHA1625	2.1	osmotically inducible protein OsmC
Chaperones	TTHA1499	6.8	MoxR-related protein
	TTHA1487	2.1	ATP-dependent Clp protease, ATP-binding subunit ClpB
transcription	TTHA0058	2.52	transcriptional repressor of class I heat-shock genes
	TTHB248	2.3	transcriptional regulator, IclR family
	TTHA0508	2	transcriptional regulator, MerR family
translation	TTHA1498	9.5	elongation factor G (EF-G-2)
DNA repair/ recombination/ replication	TTHA1806	2.1	MutM protein (formamidopyrimidine-DNA glycosylase) (Fpg)
Metabolism of nucleotide	TTHA0735	3.1	cytidine deaminase
Membrane/ Transporter/ Lipoprotein	TTHA1141	6.5	cation-transporting ATPase
	TTHA1137	4.5	major facilitator superfamily transporter
	TTHA1407	4.1	cytochrome c-type biogenesis protein, heme exporter protein B
	TTHA1408	3.9	ABC transporter, ATP-binding protein
	TTHA1651	3	maltose ABC transporter, permease protein
	TTHA1652	2.6	maltose ABC transporter, periplasmic maltose-binding protein
	TTHA0566	2.4	GTP-binding protein HflX
	TTHA1807	2.4	ABC transporter, permease protein
	TTHA0766	2.3	ABC transporter, solute-binding protein
	TTHA0767	2.3	putative small integral membrane tranport protein
	TTHA0977	2.2	sugar ABC transporter, permease protein
	TTHA0356	2	ABC transporter, periplasmic substrate-binding protein
Metabolism of amino acid	TTHA0237	2	3-hydroxyisobutyrate dehydrogenase
	TTHA1246	2.5	methylmalonyl-CoA mutase
	TTHA0489	2.3	homoserine dehydrogenase
	TTHA0500	2.3	glycerate dehydrogenase/hydroxypyruvate reductase
	TTHA0534	2.2	aspartokinase (aspartate kinase)
			[contains: aspartokinase alpha subunit; aspartokinase beta subunit]
	TTHA0525	2	glycine dehydrogenase (decarboxylating) subunit 1
Metabolism of Carbohydrate	TTHA1836	27	isocitrate lyase
	TTHA0233	3.2	pyruvate dehydrogenase complex, dihydrolipoamide dehydrogenase E3 component
	TTHA0278	3.2	ATP-dependent phosphoenolpyruvate carboxykinase
	TTHA0232	3	pyruvate dehydrogenase complex, dihydrolipoamide acetyltranferase E2 component
	TTHA0595	2.4	galactokinase
	TTHA0726	2.4	aconitate hydratase (aconitase)
	TTHA1809	2.4	proline iminopeptidase-related protein
	TTHA1113	2.1	L-lactate dehydrogenase
Metabolism of Cofactors and Vitamins	TTHA1506	3.3	glutamyl-tRNA reductase
	TTHA1775	2.6	pantoate--beta-alanine ligase
	TTHA0206	2.4	nicotinamide nucleotide transhydrogenase, alpha subunit 1

Metabolism of energy	TTHA1134	32	ba3-type cytochrome c oxidase polypeptide II
	TTHA1135	23	ba3-type cytochrome c oxidase polypeptide I
	TTHA1133	22	ba3-type cytochrome c oxidase polypeptide IIA
	TTHA1447	11	alanine dehydrogenase
	TTHA1942	11	putative cytochrome c oxidase assembly protein
	TTHA1500	7.7	phosphoenolpyruvate synthase
	TTHA1505	3.4	cytochrome c assembly protein-related protein
	TTHA0486	2.8	probable iron-sulfur protein
	TTHA1117	2.7	iron-sulfur protein
	TTHA1930	2.7	quinol-cytochrome c reductase, cytochrome b subunit
	TTHA0310	2.5	cytochrome c oxidase assembly factor (CtaA) + protoheme IX farnesyltransferase (CtaB)
	TTHA0089	2.33	NADH-quinone oxidoreductase chain 1
	TTHA0152	2.02	tungsten-containing aldehyde:ferredoxin oxidoreductase
	TTHA0153	2.01	NADPH:quinone reductase
	TTHA1933	2	probable c-type cytochrome
Metabolism of fatty acid	TTHA1463	10	long-chain-fatty-acid--CoA ligase
	TTHB116	2.5	acyl-CoA dehydrogenase, short-chain specific (probable AidB protein)
	TTHA0604	2.1	medium-chain-fatty-acid--CoA ligase
Others /Unknown	TTHA0642	3.2	putative glycosyltransferase
	TTHA0632	2	predicted nucleotidyltransferase
	TTHA1448	8.5	4-hydroxybutyrate CoA-transferase
	TTHB010	3.6	transposase-related protein
	TTHB074	3.1	putative C4-dicarboxylate transporter, periplasmic C4-dicarboxylate-binding protein
	TTHA1317	2.8	immunogenic protein related protein
	TTHA1259	2.3	adenylate cyclase related protein
	TTHA1612	2.1	putative hydrolase
	TTHA0488	2.5	antitoxin of toxin-antitoxin stability system
hypothetical protein	TTHA1626	34	hypothetical protein
	TTHA0757	17	hypothetical protein
	TTHA1943	15	hypothetical protein
	TTHB009	13	hypothetical protein
	TTHA0316	11	hypothetical protein
	TTHB203	8.6	hypothetical protein
	TTHB008	8.1	hypothetical protein
	TTHA0727	6.6	hypothetical protein
	TTHB156	6.4	hypothetical protein
	TTHB006	5.4	hypothetical protein
	TTHA1759	5.4	hypothetical protein
	TTHB158	5	hypothetical protein
	TTHB204	4.6	hypothetical protein
	TTHB157	4.3	hypothetical protein
	TTHA1895	4.2	hypothetical protein
	TTHA1954	3.9	hypothetical protein
	TTHA1837	3.9	hypothetical protein
	TTHA1752	3.7	hypothetical protein
	TTHA1136	3.7	hypothetical protein
	TTHB007	3.6	hypothetical protein
	TTHA0463	3.3	hypothetical protein
	TTHB147	3.2	hypothetical protein

TTHA0641	3.2	hypothetical protein
TTHB150	3.1	hypothetical protein
TTHA0332	3.1	hypothetical protein
TTHA0980	2.9	hypothetical protein
TTHB185	2.6	hypothetical protein
TTHB149	2.6	hypothetical protein
TTHB151	2.6	hypothetical protein
TTHA1301	2.6	hypothetical protein
TTHA0168	2.53	hypothetical protein
TTHB148	2.5	hypothetical protein
TTHA1247	2.5	hypothetical protein
TTHA0603	2.5	hypothetical protein
TTHA1870	2.4	hypothetical protein
TTHA0640	2.3	hypothetical protein
TTHA0501	2.3	hypothetical protein
TTHA0780	2.3	hypothetical protein
TTHA1610	2.3	hypothetical protein
TTHB152	2.2	hypothetical protein
TTHA1020	2.2	hypothetical protein
TTHA1848	2.1	hypothetical protein
TTHB165	2.1	hypothetical protein
TTHA0268	2.1	hypothetical protein
TTHA0236	2.1	hypothetical protein
TTHA1948	2.1	hypothetical protein
TTHA1258	2	hypothetical protein
TTHA0464	2	hypothetical protein
TTHB126	2	hypothetical protein
TTHA1045	2	hypothetical protein
TTHA1646	2	hypothetical protein

3. Proteome analysis

To know more substantive effects of the transcriptional changes on the cells under cold stress condition, I performed proteome analysis of the extracts from the wild type and Δ*ttcsp1* mutant, using 2D-PAGE and MALDI-TOF-MS. For the proteome analysis of the wild type under cold stress condition, the cells were grown until the absorbance of culture at 600 nm reached 0.8 before transferring the culture from 70°C to 45°C. As a first step, the whole cell lysates of each cell grown at 70°C and 45°C were separated by using pH 3 to 10 broad range strip followed by the second dimension on 12.5% linear SDS-PAGE gel. However, I could not distinguish up- and down-regulated proteins under cold stress condition due to abundant proteins in whole cell lysates (data not shown). Therefore, I carried out fractionation of the whole cell lysate into soluble fraction (cytosolic proteins) and insoluble fraction (membrane and cell wall proteins) using ultracentrifugation at 105,000 *g* for 1 h before 2-DE separation. After ultracentrigation, the soluble and insoluble proteins were resolved onto pH 4 to 7 strip in the first dimension and 12.5% SDS-PAGE 2-DE gel in the second dimension. This procedure enabled us to detect changes in protein spots on gels. According to this procedure, the samples of the wild type and Δ*ttcsp1* mutant strains were prepared after transfer of the cultures from 70°C to 45°C and further incubation at 45°C for 30 min. This cold shock treatment was likely to confer acclimating period before cold adaptation to cells. Totally, eight sets of 2-DE gel, cytosolic and membrane proteins for the wild type and Δ*ttcsp1* mutant grown under optimal and cold stress conditions, respectively, were prepared. The analysis of 2-DE gels by ImageMaster Premium 5.0 allowed spot

detection, pairing and matching of each group of 2-DE gel. The 2-DE map for cytosolic proteins was completely different from that of membrane proteins, indicating successful separation of soluble cytosolic proteins and insoluble membrane proteins by ultracentrifugation. This improved procedure is a simple and valuable approach method for 2-DE based proteome study in *T. thermophilus* HB8.

Table 3-1 represents respectively detected spot numbers on the 2-DE gel of the eight samples, which was named G-III to G-X as a group. More than 740 and 240 protein spots were detected at cytosolic and membrane protein samples on 2-DE gel, respectively. Tables 3-2 and 3-3 represent the percentage of gel-to-gel matching of spots in cytosolic and membrane proteins of each group by ImageMaster, respectively. Spot matching across the obtained sets of gel images showed more than 50%. These spots could be used to compare expression level between respective groups. The quantitative change of concerned spots was carefully evaluated using triple different gels for each group sample. Significant changes ($p < 0.05$) of up- or down-regulated protein spots between 2-DE data were tested by Student's *t*-test to eliminate false positive and false negative results.

Table 3-1. Detected spot number on the 2-DE gel of each group.

Group name	Sample name	Spots*
G-III	wild type, 70°C, 30 min, cytosolic protein	983.3 ± 97
G-IV	Δ*ttcspl*, 70°C, 30 min, cytosolic protein	1034.3 ± 31
G-V	wild type, 45°C, 30 min, cytosolic protein	896.0 ± 66
G-VI	Δ*ttcspl*, 45°C, 30 min, cytosolic protein	742.0 ± 14
G-VII	wild type, 70°C, 30 min, membrane protein	253.3 ± 18
G-VIII	Δ*ttcspl*, 70°C, 30 min, membrane protein	240.0 ± 53
G-IX	wild type, 45°C, 30 min, membrane protein	290.3 ± 52
G-X	Δ*ttcspl*, 45°C, 30 min, membrane protein	248.6 ± 8

*The results represent detected spot number from different triple 2-DE gels with standard deviation.

Table 3-2. Spot matching across gel images for cytosolic proteins of each group.

	Pair matches result of cytosolic proteins (%)*			
	G-III	G-IV	G-V	G-VI
G-III	67.3 ± 4.2[†]	67.6 ± 5.1	69.4 ± 1.4	ND[#]
G-IV		79.6 ± 1.1	ND[#]	67.4 ± 2.7
G-V			84.7 ± 0.8	74.5 ± 1.2
G-VI				84.6 ± 1.2

*The results represent percentage of spot matching of each group with cognate group.

[†] The matching results were derived from different triple 2-DE gels with standard deviation.

[#] ND, not determined.

Table 3-3. Spot matching across gel images for membrane proteins of each group.

	Pair match result of membrane proteins (%)*			
	G-VII	G-VIII	G-IX	G-X
G-VII	78.9 ± 1.6[†]	74.1 ± 1.9	51.8 ± 3.3	ND[#]
G-VIII		82.3 ± 1.2	ND[#]	60.0 ± 3.8
G-IX			73.5 ± 4.7	62.0 ± 19
G-X				78.1 ± 0.4

*The results represent percentage of spot matching of each group with cognate group.

[†] The matching results were derived from different triple 2-DE gels with standard deviation.

[#] ND, not determined.

3-1 Difference of proteome results between the wild type and Δ*ttcsp1* mutant under optimal growth condition.

To investigate the functional role of *tt*Csp1, I first focused on proteins that showed different expression pattern between the wild type and Δ*ttcsp1* mutant strains under optimal growth condition (at 70°C). Figure 3-1 showed 2-DE maps of cytosolic and membrane proteins of the wild type (A and C) and Δ*ttcsp1* mutant (B and D) on the pH 4 to 7 and 12.5% SDS-PAGE 2-DE gel. The gel-to-gel matching of spots (wild type vs. the Δ*ttcsp1* mutant) showed 67.6% (G-III vs. G-IV) and 74.1% (G-VII vs. G-VIII) for cytosolic and membrane protein fractions, respectively (Tables 3-2 and 3-3). By comparing these spots between two strains, I identified up- and down-regulated proteins in the Δ*ttcsp1* mutant grown at 70°C against the wild type grown at the same temperature. In cytosolic protein fraction, 63 up-regulated (Table 3-4) and 23 down-regulated (Table 3-5) proteins showed more than 1.5 times expression change and $p < 0.05$. In membrane protein fraction, 8 up-regulated (Table 3-6) and 9 down-regulated (Table 3-7) proteins were identified on the same criteria.

In the cytosolic protien fraction, some translational controlers including translation elongation factor EF-Tu (both TTHA0251 and TTHA1694), translation initiation factor IF-2 (TTHA0699) and elongation factor EF-G (TTHA1695) were down-regulated at 70°C in the Δ*ttcsp1* mutant against the wild type (Table 3-5). It implies that *tt*Csp1 has influences on translational control. On the other hand, as shown in Table3-4, many essential factors for cell growth are down-regulated by *tt*Csp1. *tt*Csp1 may ready to stall cell growth in case of some stresses.

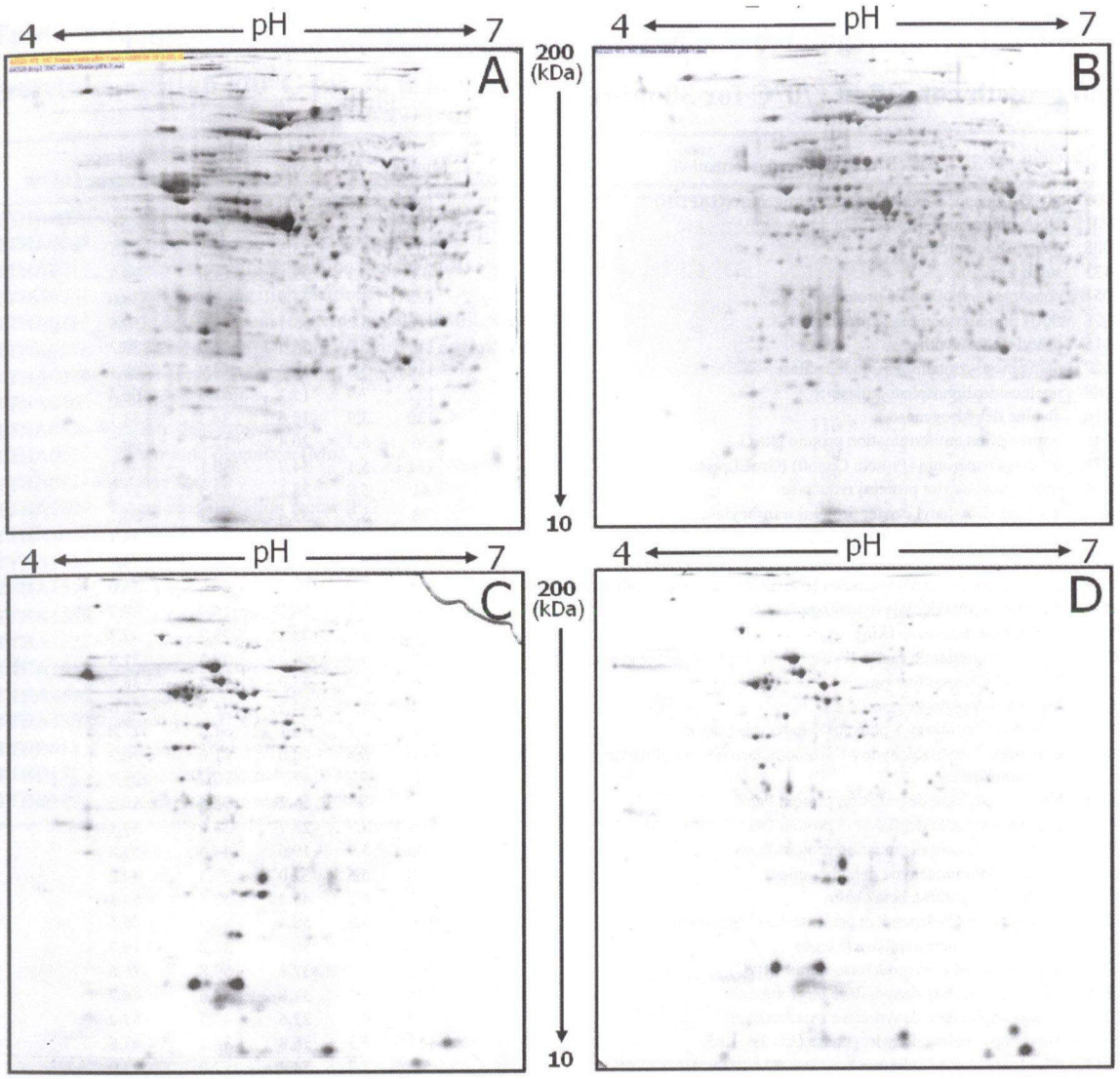

Figure 3-1. 2-DE proteome profiling of the wild type and Δ*ttcsp1* mutant under 70°C after 30 min from transient state.

The cytosolic and membrane proteins were extracted from wild type and Δ*ttcsp1* mutant after transfer to 70°C for 30 min. Each protein sample was separated onto the pH 4 to 7, and 12.5% SDS-PAGE gel (13 cm x 15 cm x 1 mm) and followed CBB G-250 staining with aluminium sulfate. **A**, The cytosolic proteins of the wild type. **B**, The cytosolic proteins of Δ*ttcsp1* mutant. **C**, The membrane proteins of the wild type. **D**, The membrane proteins of Δ*ttcsp1* mutant.

Table 3-4. The up-regulated cytosolic proteins in Δ*ttcsp1* mutant under optimal growth condition (70°C for 30 min).

orf I.D	Annotated information	Mowse	pI	Mw.	Intensity coverage	Sequence coverage
TTHA0905	glyceraldehyde 3-phosphate dehydrogenase(GAPDH)	74	7.8	35.9	30.5	31.7
TTHA0001	DNA polymerase III beta subunit	167	4.9	40.5	34.6	60.5
TTHA0008	phage shock protein A	103	5.3	25.5	30.5	54.1
TTHA0431	sugar kinase	53	5.3	32.1	19.0	29.7
TTHA0051	conserved hypothetical protein	125	4.9	31.5	42.7	38.0
TTHA0098	SufB protein (membrane protein)	173	5.2	53.1	41.8	50.9
TTHA0115	prolyl-tRNA synthetase	117	5.9	54.5	44.0	38.2
TTHA0122	manganese-containing pseudocatalase	112	5.3	33.3	44.9	40.1
TTHA0188	nucleoside diphosphate kinase	122	7.9	15.3	61.6	66.4
TTHA0216	alanine dehydrogenase	130	5.9	38.6	34.3	53.1
TTHA0248	transcription antitermination protein NusG	86	5.3	20.4	17.3	46.7
TTHA0271	60 kDa chaperonin (Protein Cpn60) (GroELprotein)	171	5.1	54.7	50.1	44.1
TTHA0304	enoyl-[acyl carrier protein] reductase	51	5.8	28.1	23.3	21.8
TTHA0416	malonyl CoA-[acyl carrier protein] transacylase	78	5.9	33.4	34.1	35.1
TTHA0432	IMP dehydrogenase/GMP reductase	96	6.5	53.1	40.6	33.1
TTHA0506	malate synthase	69	6.1	58.7	20.6	19.1
TTHA0534	aspartokinase (aspartate kinase) [contains:aspartokinase alpha subun	134	5.7	43.3	44.0	36.0
TTHA0545	aspartate-semialdehyde dehydrogenase	86	6.1	36.1	16.0	38.7
TTHA0557	superoxide dismutase [Mn]	71	6.4	23.2	38.2	37.3
TTHA0699	translation initiation factor IF-2	88	5.3	56.4	39.5	31.8
TTHA0712	histidyl-tRNA synthetase	76	6.0	47.0	18.2	35.4
TTHA0722	histidinol dehydrogenase	230	4.9	44.1	51.5	65.5
TTHA0856	1-deoxy-D-xylulose-5-phosphate reductoisomerase	81	6.2	40.1	41.5	27.8
TTHA0934	glutamate-1-semialdehyde 21-aminomutase (GSA)(glutamate-1-semialdeh	140	6.4	46.0	81.0	30.2
TTHA0940	aminotransferase	52	5.8	42.2	10.2	25.7
TTHA0968	phenylacetic acid degradation protein PaaZ	158	6.4	55.2	48.4	28.5
TTHA0970	phenylacetic acid degradation protein PaaC	106	4.7	28.7	38.9	37.1
TTHA0971	phenylacetic acid degradation protein PaaB	106	5.9	19.6	44.6	53.8
TTHA0996	succinate-semialdehyde dehydrogenase	139	5.5	52.0	52.3	44.2
TTHA1095	tryptophan synthase beta chain	182	6.2	45.3	52.8	54.1
TTHA1111,	alternative ATP-dependent protease La (Lonprotease)	157	5.2	58.4	42.9	46.5
TTHA1210	2-isopropylmalate synthase (LeuA)	60	5.7	56.5	32.2	19.7
TTHA1211,	probable ketol-acid reductoisomerase (IlvC)	242	6.2	37.1	59.8	76.6
TTHA1228,	3-isopropylmalate dehydratase large subunit	148	6.4	51.8	54.6	48.7
TTHA1229	3-isopropylmalate dehydratase small subunit	152	4.7	22.6	47.3	57.2
TTHA1230	3-isopropylmalate dehydrogenase (EC 1.1.1.85)	141	5.3	36.8	38.1	47.8
TTHA1234	dihydroxyacid dehydratase	52	5.7	54.4	17.0	23.0
TTHA1243	septum site-determining protein MinD	172	5.3	28.9	58.2	55.4
TTHA1248	acetyl-coenzyme A synthetase	158	6.0	58.4	38.9	38.1
TTHA1329	glutamine synthetase	99	6.2	50.5	46.3	39.7
TTHA1355,	DNA gyrase subunit A	79	6.0	57.0	38.7	20.1
TTHA1392	Sir2 family protein	60	5.7	27.8	9.7	22.4
TTHA1435	purine nucleoside phosphorylase	118	6.1	25.4	47.4	51.9
TTHA1498	elongation factor G (EF-G-2)	87	5.1	56.7	24.2	29.5
TTHA1519	phosphoribosylformylglycinamidine synthase II	154	5.5	55.7	26.5	45.5
TTHA1535	isocitrate dehydrogenase	91	6.3	54.4	35.0	24.4
TTHA1557	propionyl-CoA carboxylase beta subunit	78	5.8	55.9	38.2	26.6
TTHA1625	osmotically inducible protein OsmC	115	5.4	15.3	63.1	66.9
TTHA1649	nucleotidyltransferase	52	7.8	10.6	25.6	47.4
TTHA1659	tetratricopeptide repeat family protein	184	6.1	48.9	56.4	38.6
TTHA1664	DNA-directed RNA polymerase alpha chain	214	4.8	35.0	58.7	57.8
TTHA1695	elongation factor G (EF-G)	120	5.2	57.2	22.9	43.9
TTHA1698	carboxypeptidase G2	72	5.8	40.0	17.2	23.0
TTHA1797,	probable amidase	73	5.9	46.5	15.1	27.4
TTHA1814	SufD protein (membrane protein)	75	6.1	47.9	15.3	30.9
TTHA1816	rod shape-determining protein MreB	106	5.4	36.8	54.3	29.0
TTHA1836	isocitrate lyase	55	5.6	49.1	12.2	22.1
TTHA1840	SufD protein (membrane protein)	214	6.1	47.9	44.6	62.9
TTHA1914	homocitrate synthase	216	5.8	42.1	58.2	62.2
TTHA0987	beta-ketoadipyl CoA thiolase	89	6.0	42.7	44.7	31.2
TTHB125	chromosome partitioning ATPase ParA family	111	6.6	35.9	55.8	32.6
TTHB152	conserved hypothetical protein	185	6.8	51.1	60.9	42.2
TTHB190	conserved hypothetical protein	290	5.6	40.8	80.8	66.8

Table 3-5. The down-regulated cytosolic proteins in Δ*ttcsp1* mutant under optimal growth condition (70°C for 30 min).

orf I.D	Annotated information	Mowse	p*I*	Mw.	Intensity coverage	Sequence coverage
TTHA0090	NADH-quinone oxidoreductase chain 3	109	5.6	57.1	40.9	21.1
TTHA0098	arginyl-tRNA synthetase	177	6.6	57.5	65.5	43.6
TTHA0248,	transcription antitermination protein NusG	51	5.3	20.4	21.7	32.6
TTHA0251	translation elongation factor EF-Tu.B	50	5.3	44.8	14.4	32.5
TTHA0271	60 kDa chaperonin (Protein Cpn60) (GroELprotein)	197	5.1	54.7	49.9	42.6
TTHA0278	ATP-dependent phosphoenolpyruvate carboxykinase	172	6.4	57.6	45.4	47.5
TTHA0304	enoyl-[acyl carrier protein] reductase	54	5.8	28.1	31.0	25.3
TTHA0465	thioredoxin reductase	65	6.5	36.2	15.3	39.1
TTHA0536	malate dehydrogenase	116	5.7	35.4	35.6	52.3
TTHA0557	superoxide dismutase [Mn]	150	6.4	23.2	54.6	54.4
TTHA0614	trigger factor	198	4.9	46.3	55.4	43.1
TTHA0699	translation initiation factor IF-2	48	5.3	56.4	18.4	31.4
TTHA1066	proabable transaldolase	113	5.5	24.0	68.7	45.7
TTHA1123	acetyl-CoA carboxylase biotin carboxylasesubunit	208	6.1	49.3	57.5	51.2
TTHA1355	DNA gyrase subunit A	114	6.0	57.0	33.4	35.0
TTHA1589	50S ribosomal protein L25 (TL5)	142	5.1	23.2	70.3	42.7
TTHA1637	ribose-phosphate pyrophosphokinase	106	5.9	33.5	60.5	46.1
TTHA1694	elongation factor Tu (EF-Tu)	257	5.3	44.8	56.4	67.2
TTHA1695	elongation factor G (EF-G)	90	5.2	57.2	27.1	25.4
TTHA1852	oligoendopeptidase F	132	5.5	58.0	46.8	32.0
TTHB052	cobalamin biosynthesis precorrin-8X isomerase	147	7.8	23.2	44.5	52.8
TTHB152	conserved hypothetical protein	60	6.8	51.1	13.9	24.1
TTHB179	conserved hypothetical protein	59	9.8	23.9	9.4	37.6

Table 3-6. The up-regulated membrane proteins in *Δttcsp1* mutant under optimal growth condition (70°C for 30 min).

orf I.D	Annotated information	Mowse	pI	Mw.	Intensity coverage	Sequence coverage
TTHA0075	ribonucleoside-diphosphate reductase	95	6.0	57.2	26.3	29.5
TTHA0271	60 kDa chaperonin (Protein Cpn60) (GroELprotein)	233	5.1	54.7		
TTHA0359	cold shock protein					
TTHA0509	N-acyl-L-amino acid amidohydrolase		5.5	47.9		
TTHA0525	glycine dehydrogenase (decarboxylating) subunit 1					
TTHA1210	2-isopropylmalate synthase (LeuA)	56	5.7	56.5		
TTHA1689	50S ribosomal protein L2	201	11.7	30.4		
TTHA1813	DNA-directed RNA polymerase beta chain (RpoB)	147	6.3	57.8		

Table 3-7. The down-regulated membrane proteins in *Δttcsp1* mutant under optimal growth condition (70°C for 30 min).

orf I.D	Annotated information	Mowse	pI	Mw.	Intensity coverage	Sequence coverage
TTHA0206	nicotinamide nucleotide transhydrogenase, alpha subunit 1					
TTHA0229	2-oxoisovalerate dehydrogenase E1 componentalpha subunit	141	5.3	41.1		
TTHA0246	50S ribosomal protein L1					
TTHA1272	V-type ATP synthase subunit B					
TTHA1483	conserved putative protein	123	5.9	25.7		
TTHA1487	ATP-dependent Clp protease, ATP-binding subunit ClpB					
TTHA1570	deoxyhypusine synthase					
TTHA1642	S-adenosylmethionine synthetase					
TTHA1818	RecA protein	189	5.5	35.4		

3-2 Cold stress response of the wild type under 45°C

Next, I investigated the response of the wild-type to cold stress condition. Figure 3-2 shows 2-DE proteome profiling of the wild type under 70°C and 45°C. In the cytosolic protein fraction, PMF analysis using MALDI-TOF MS identified 34 up-regulated (Table 3-8) and 24 down-regulated protein (Table 3-9) spots at 45°C which showed more than 1.5 times expression change by comparing G-III to G-V data. In addition, 43 up-regulated protein spots (Table 3-10) and 19 down-regulated proteins (Table 3-11) at 45°C were also identified in membrane protein samples. In the following, I describe the observed changes by classifying proteins into their functional categories.

(i) Translation process. A lot of up-regulated and highly expressed proteins under cold stress condition are involved in translation process: TTHA0162, 30S ribosomal proteins S1; TTHA0251, translation elongation factor EF-Tu; TTHA0271, 60 kDa chaperonin; TTHA0272, 10 kDa chaperonin; TTHA0699, tranlation initiation factor IF-2; TTHA0614, trigger factor TTHA0098, arginyl-tRNA synthetase; and TTHA0573, glutamyl-tRNA amidotransferase subunit A. These results suggest that the up-regulation of these proteins rescues impaired translation process significantly under cold stress condition. mRNA-stabilizing proteins and translation related proteins have been defined as up-regulated proteins under cold shock condition for various bacteria. It was reported that various bacteria overexpressed the following proteins as a cold shock response protein: 60kDa chaperonin, 10 kDa chaperonin, cold shock protein (TTHA0359), EF-Tu, NusA, 30S ribosomal protein S1, S-adenosyl methionine synthetase (TTHA1642), trigger factor, RNA polymerase α chain (TTHA1664), and RNA polymerase β chain (TTHA1813).

(ii) Amino acid metabolism. Several proteins involved in amino acid metabolism were up-regulated under cold stress condition: TTHA1577, putative NAD-dependent glutamate dehydrogenase; TTHA0124, branched-chain amino acid aminotransferase; TTHA1329, glutamine synthetase; and with TTHA0525, glycine dehydrogenase.

(iii) Proteases. I also found up-regulation of peptidase family proteins at 45°C: TTHA0770, ATP-dependent protease La; TTHA1111, alternative ATP-dependent protease La; TTHA1487, ATP-dependent Clp protease ATP-binding subunit ClpB; and TTHA0256, leucine aminopeptidase.

(vi) Cold shock proteins. *tt*Csp2 (TTHA0359) was dramatically up-regulated in the wild type cells under 45°C, demonstrating that *tt*Csp2 plays important role under cold stress condition. The difference of *tt*Csp1 (TTHA0175) expression under between cold stress condition and optimal growth condition was not detected onto pH 3-10 broad range strip and 16.5% SDS-PAGE-Tricine gels. However, the *tt*Csp1 was constitutively expressed under both 70°C and 45°C using 15% Tris–Tricine SDS–PAGE gel and western blotting (data not shown). This result was in agreement with the result of transcriptome analysis.

(v) Energy production. Several subunits of V-type ATP synthase were severly down-regulated for 30 min under cold stress condition: TTHA1272, ATP synthase subunit B; TTHA1273, ATP synthase subunit A; TTHA1276, ATP synthase subunit E; and TTHA1279, ATP synthase subunit V. This result suggests that energy production is reduced during acclimation period under cold stress condition.

(vi) Fatty acid synthesis. The wild type cells increased expression of several proteins associated with acetyl-CoA metabolism under cold stress condition: TTHA0229,

2-oxoisovalerate dehydrogenase E1 component α subunit; TTHA0232, pyruvate dehydrogenase complex dihydrolipoamide acetyltransferase E2 component; TTHA0287, 2-oxoglutarate dehydrogenase E3 component; and TTHA0288, 2-oxoglutarate dehydrogenase E2 component (dihydrolipoamide succinyltransferase). Acetyl-CoA plays an important role as a building block in production of fatty acids through malonyl-CoA. I also found the up-regulation of malonyl CoA-[acyl carrier protein] transacylase (TTHA0416) and citrate synthase (TTHA1343) in cytosolic protein fraction, and acetyl-CoA carboxylase biotin carboxylase subunit (TTHA1123), propionyl-CoA carboxylase α subunit (TTHA1148), and 2-siopropylmalate synthase (TTHA1210) in membrane protein fraction. These proteins are involved in fatty acid biosynthesis pathway. In contrast, I found the down-regulation of proteins which are able to degrade acetyl-CoA and malonyl CoA: acetyl-CoA synthetase (TTHA1248), malate synthase (TTHA0506), 3-isopropylmalate dehydratase large subunit (TTHA1228) and small subunit (TTHA1229). These proteome results support the notion that fatty acid production is effectively activated to maintain and stabilize lipid bilayer under cold stress condition.

As indicated above (i) to (vi), components of the cell are drastically changed. Some of these alteration may result from the function of *tt*Csp1 and others may not. To investigate which changes were caused by *tt*Csp1, the influences of deletion of *ttcsp1* on the transcriptome analysis were determined in the following section.

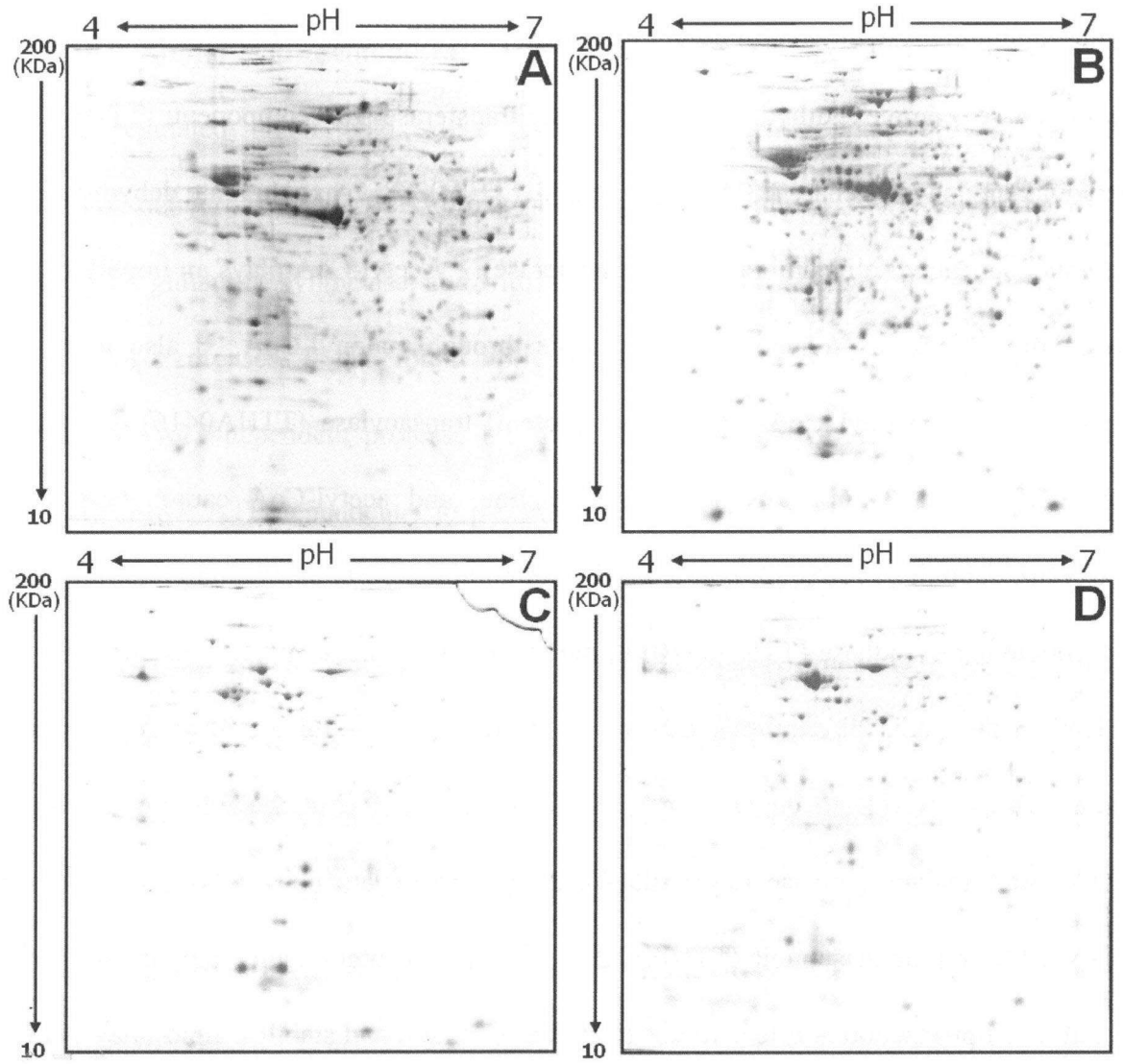

Figure 3-2. 2-DE proteome profiling of the wild type under 45°C and 70°C after 30 min from transient state.

The cytosolic and membrane protein were extracted from wild type after transfer to 45°C and 70°C for 30 min, respectively. Each protein sample was separated onto the pH 4 to 7, and 12.5% SDS-PAGE gel (13 cm x 15 cm x 1 mm) and followed CBB G-250 staining with aluminium sulfate. **A**, The cytosolic proteins under 70°C. **B**, The cytosolic proteins under 45°C. **C**, The membrane proteins under 70°C. **D**, The membrane proteins under 45°C.

Table 3-8. The up-regulated cytosolic proteins in the wild type under cold stress condition (45°C for 30 min).

orf I.D	Annotated information	Mowse	p*I*	Mw.	Intensity coverage	Sequence coverage
TTHA0001	DNA polymerase III beta subunit		4.9	40.5	20.2	25.9
TTHA0008	phage shock protein A	112	5.3	25.5	51.0	34.1
TTHA0090	NADH-quinone oxidoreductase chain 3	60	5.6	57.1	24.4	15.2
TTHA0098	arginyl-tRNA synthetase	246	6.6	57.5	55.2	53.5
TTHA0108	transketolase	183	6.1	56.7	47.0	38.5
TTHA0120	GTP-binding protein Era	89	5.9	33.8	57.3	33.6
TTHA0124	branched-chain amino acid aminotransferase(IlvE)	76	5.9	34	41.2	24.4
TTHA0162	30S ribosomal protein S1	50	6.3	57.4	23.9	16.6
TTHA0188	nucleoside diphosphate kinase	59	7.9	15.3	29.3	40.1
TTHA0209	50S ribosomal protein L10	64	?	18.6	66.1	20.2
TTHA0210	50S ribosomal protein L12	100	4.9	13.1	34.7	61.6
TTHA0251	translation elongation factor EF-Tu.B	63	5.3	44.8	14.5	32.5
TTHA0256	leucine aminopeptidase	102	8.7	54.6	37.9	36.1
TTHA0271	60 kDa chaperonin (Protein Cpn60) (GroELprotein)	181	5.1	54.7	71.9	38.1
TTHA0288	2-oxoglutarate dehydrogenase E2 component(dihydrolipoamide succinylt		5.7	44.5	35.8	42.1
TTHA0328	probable isochorismatase	49	5.4	22	72.4	31.6
TTHA0365	type IV pilus assembly protein pilus retractionprotein PilT	71	7.8	39.9	25.6	31.9
TTHA0416	malonyl CoA-[acyl carrier protein] transacylase	205	5.9	33.4	78.2	39.7
TTHA0557	superoxide dismutase [Mn]	107	6.4	23.2	48.6	45.6
TTHA0573	glutamyl-tRNA(Gln) amidotransferase subunit A	172	5.4	50.2	64.9	42.9
TTHA0699	translation initiation factor IF-2	145	5.3	56.4	52.4	45.7
TTHA0701	N utilization substance protein A (NusA)	248	5.7	43.9	50.0	62.8
TTHA1111	alternative ATP-dependent protease La (Lonprotease)	65	5.2	58.4	32.6	20.9
TTHA1276	V-type ATP synthase subunit E	262	5.3	20.6	77.2	63.8
TTHA1343	citrate synthase		6.2	42.3	38.8	41.6
TTHA1482	bacterioferritin	47	4.7	16.2	49.8	36.8
TTHA1577	putative NAD-dependent glutamate dehydrogenase		4.9	44.7	66.5	25.1
TTHA1578	1-pyrroline-5-carboxylate dehydrogenase	97	5.4	56.5	45.0	28.3
TTHA1750	putative mannose-1-phosphate guanylyltransferase (GDP)/mannose-6-	94	5.2	37.4	34.5	30.9
TTHA1769	conserved hypothetical protein	53	6.21	13.1	31.4	51.2
TTHA1779	metal dependent phosphohydrolase (HD domainprotein)	73	5.7	17.8	33.9	38.4
TTHB057	cobalamin biosynthesis protein CbiG	124	6.5	38.7	71.3	46.8
TTHB152	conserved hypothetical protein	186	6.8	51.1	72.2	36.0
TTHB189	conserved hypothetical protein	60	9.6	19.4	14.9	52.7

Table 3-9. The down-regulated cytosolic proteins in the wild type under cold stress condition (45°C for 30 min).

orf I.D	Annotated information	Mowse	p*I*	Mw.	Intensity coverage	Sequence coverage
TTHA0027	probable potassium channel beta subunit(oxidoreductase)	120	5.4	35.9	54.9	42.4
TTHA0122	manganese-containing pseudocatalase	132	5.3	33.3	59.2	40.1
TTHA0407	3-methyl-2-oxobutanoatehydroxymethyltransferase	126	6	28.2	83.4	42.5
TTHA0465	thioredoxin reductase	144	6.5	36.2	53.0	46.6
TTHA0481	oligo-16-glucosidase	119	5.6	59.5	49.5	30.9
TTHA0506	malate synthase	139	6.1	58.7	79.3	23.0
TTHA0562	purine nucleoside phosphorylase	69	5.9	30.3	44.2	33.5
TTHA0614	trigger factor		4.9	46.3	70.4	52.2
TTHA0654	ATP-binding protein Mrp/Nbp35 family	72	5.9	37.2	36.0	24.9
TTHA1131	probable gliding protein (MglB)	77	4.8	17.8	32.3	40.5
TTHA1228	3-isopropylmalate dehydratase large subunit	134	6.4	51.8	62.4	30.1
TTHA1229	3-isopropylmalate dehydratase small subunit	168	4.7	22.6	89.2	54.7
TTHA1248	acetyl-coenzyme A synthetase	83	6	58.4	18.0	34.8
TTHA1373	conserved hypothetical protein	68	6.7	15.7	24.7	40.4
TTHA1427	UvrD protein	51	6.8	57.4	14.8	21.3
TTHA1435	purine nucleoside phosphorylase	138	6.1	25.4	77.4	58.3
TTHA1480	small heat shock protein HSP20 family	69	5.5	15.8	39.8	32.8
TTHA1487	ATP-dependent Clp protease ATP-binding subunitClpB	107	5.5	57.5	40.9	37.1
TTHA1545	hypothetical protein	65	5	19.3	31.3	31.8
TTHA1695	elongation factor G (EF-G)	78	5.2	57.2	43.6	22.3
TTHA1775	pantoate--beta-alanine ligase	49	6.3	30.7	10.4	30.1
TTHA1778	LytR/CspA/Psr family protein	55	6.8	39.7	21.1	19.5
TTHA1809	proline iminopeptidase-related protein	108	4.5	31.5	89.1	24.1
TTHB088	Zn-dependent hydrolase	51	6	30.3	17.3	36.1

Table 3-10. The up-regulated membrane proteins in the wild type under cold stress condition (45°C for 30 min)

orf I.D	Annotated information	Mowse	pI	Mw.	Intensity coverage	Sequence coverage
TTHA0075	ribonucleoside-diphosphate reductase	95	6	57.2	26.3	29.5
TTHA0098	arginyl-tRNA synthetase	147	6.6	57.5	81.2	22.5
TTHA0109	ATP-dependent RNA helicase	144	9.6	56.2	76.9	28.5
TTHA0120	GTP-binding protein Era	119	5.9	33.8	79.5	30.5
TTHA0122	manganese-containing pseudocatalase	121	5.3	33.3	59.2	41.4
TTHA0162	30S ribosomal protein S1	59	6.3	57.4	12	35.9
TTHA0229	2-oxoisovalerate dehydrogenase E1 componentalpha subunit	141	5.3	41.1	81.1	22.9
TTHA0232	pyruvate dehydrogenase complex dihydrolipoamideacetyltranferase E2	213	5.6	50.1	65.7	51.7
TTHA0251	translation elongation factor EF-Tu.B	205	5.3	44.8	63.8	51.7
TTHA0271	60 kDa chaperonin (Protein Cpn60) (GroELprotein)	233	5.1	54.7	61	50.2
TTHA0272	10 kDa chaperonin (Protein Cpn10) (groESprotein)	129	5.1	11	37.4	53.5
TTHA0287	2-oxoglutarate dehydrogenase E3 component(dihydrolipoamide dehydr	198	6.8	49	56.9	36.9
TTHA0359	cold shock protein	49	7.6	7.8	31.4	70.6
TTHA0364	type IV pilus assembly protein PilF	123	4.9	56.6	45.5	32.2
TTHA0525	glycine dehydrogenase (decarboxylating) subunit1	59	5.3	47	29.2	16
TTHA0538	succinyl-CoA synthetase beta chain					
TTHA0553	50S ribosomal protein L20	80	12.1	13.7	24.1	40.7
TTHA0614	trigger factor	183	4.9	46.3	86.5	47.8
TTHA0701	N utilization substance protein A (NusA)	209	5.7	43.9	71.9	39
TTHA0770	ATP-dependent protease La (Lon protease)	57	6.1	58.5	37.8	20.7
TTHA0861	30S ribosomal protein S2	154	5.3	29.3	77.1	41.8
TTHA1088	cell division protein FtsA	92	5.7	43.7	38.2	26.5
TTHA1111	alternative ATP-dependent protease La (Lonprotease)	48	5.2	58.4	35.3	11.5
TTHA1123	acetyl-CoA carboxylase biotin carboxylasesubunit	277	6.1	49.3	79.7	58.8
TTHA1148	propionyl-CoA carboxylase alpha subunit	112	5.8	56.3	56.8	25.6
TTHA1210	2-isopropylmalate synthase (LeuA)	56	5.7	56.5	36.7	16
TTHA1211	probable ketol-acid reductoisomerase (IlvC)	114	6.2	37.1	91.1	24.6
TTHA1251	preprotein translocase SecA subunit	135	6.3	58.3	22.3	31.4
TTHA1294	ribosomal subunit interface protein	136	6.4	21.6	49.3	58.1
TTHA1329	glutamine synthetase	53	6.2	50.5	43.6	16.6
TTHA1459	ABC transporter ATP-binding protein	219	6.5	33.9	75.1	68.4
TTHA1483	conserved putative protein	123	5.9	25.7	61.9	56.6
TTHA1487	ATP-dependent Clp protease ATP-binding subunitClpB	64	5.5	57.5	59.2	18.9
TTHA1642	S-adenosylmethionine synthetase		5.5	43.2	63.4	55.7
TTHA1664	DNA-directed RNA polymerase alpha chain	74	4.8	35	27.2	22.2
TTHA1665	30S ribosomal protein S4	110	11.3	24.3	71	27.8
TTHA1689	50S ribosomal protein L2	201	11.7	30.4	65	58
TTHA1696	30S ribosomal protein S7	84	11	18	41.5	32.7
TTHA1783	50S ribosomal protein L21	89	10.5	11	57.4	31.7
TTHA1813	DNA-directed RNA polymerase beta chain (RpoB)	147	6.3	57.8	39.2	41.6
TTHA1818	RecA protein	189	5.5	35.4	72.4	58.5
TTHA1840	SufD protein (membrane protein)	205	61	47.9	46.3	43.6
TTHB190	conserved hypothetical protein	122	5.6	40.8	57.9	30.2

Table 3-11. The down-regulated membrane proteins in the wild type under cold stress condition (45°C for 30 min).

orf I.D	Annotated information	Mowse	p*I*	Mw.	Intensity coverage	Sequence coverage
TTHA0027	probable potassium channel beta subunit(oxidoreductase)	246	5.4	35.9	56.7	76.9
TTHA0122	manganese-containing pseudocatalase	147	5.3	33.3	62.5	42.1
TTHA0210	50S ribosomal protein L12	100	4.9	13.1	31.4	66.4
TTHA0229	2-oxoisovalerate dehydrogenase E1 componentalpha subunit	131	5.3	41.1	71.2	23.2
TTHA0245	30S ribosomal protein S6 (TS9)	89	7.2	12	52.9	31.7
TTHA0246	50S ribosomal protein L1	179	10	24.8	65.4	58.5
TTHA0286	serine protease subtilase family					
TTHA0561	outer membrane protein	294	4.9	56.2	60.2	55.9
TTHA0602	peptidyl-prolyl cis-trans isomerase	204	5.4	37.4	53.3	58.2
TTHA1272	V-type ATP synthase subunit B	157	5.1	53.1	50.7	38.1
TTHA1273	V-type ATP synthase subunit A	340	5	56.1	73.1	64.8
TTHA1276	V-type ATP synthase subunit E	221	5.3	20.6	60.4	71.8
TTHA1279	V-type ATP synthase subunit (VAPC-THERM)	69	7.3	13.1	40.7	31.7
TTHA1480	small heat shock protein HSP20 family	95	5.5	15.8	68	30
TTHA1570	deoxyhypusine synthase	127	5.7	38.3	68.9	27.5
TTHA1689	50S ribosomal protein L2	72	11.7	30.4	26	32.6
TTHA1695	elongation factor G (EF-G)	86	5.2	57.2	29.3	30.3
TTHA1773	fructose-16-bisphosphate aldolase	59	6	33	48.9	20.3
TTHB182	conserved hypothetical protein	99	5.2	56.2	40.7	28.3

3-3 Cold stress response of Δ*ttcsp1* under 45℃

Next, 2-DE-based proteome analysis was performed for the Δ*ttcsp1* mutant. The 2-DE map of Δ*ttcsp1* mutant strain was constructed using the same procedures and compared with that of the wild type. Figure 3-3 shows 2-DE maps of cytosolic and membrane proteins of Δ*ttcsp1* mutant under 45°C and 70°C, respectively. The detected spot number on 2-DE gel of each group and matching of spots in cytosolic and membrane proteins are represented in Tables 3-1, 3-2 and 3-3, respectively.

3.3.1 Overall trend of proteome change in Δ*ttcsp1* mutant

The identification results of up- and down-regulated proteins in cytosolic and membrane protein fractions under 45°C are summarized in Tables 3-12 to 3-15. The proteome change in Δ*ttcsp1* mutant under cold stress condition showed that 21 and 37 proteins were up- and down-regulated in cytosolic protein fraction, respectively (Tables 3-12 and 3-13), whereas 41 and 17 proteins were up- and down-regulated in membrane protein fraction, respectively (Tables 3-14 and 3-15). As a whole, the trend of the proteome change in Δ*ttcsp1* mutant as cold stress response seems similar to that of the wild type. It should be noted, however, that the the number of up-regulated proteins in cytosolic proteome of Δ*ttcsp1* mutant was smaller than that of down-regulated ones.

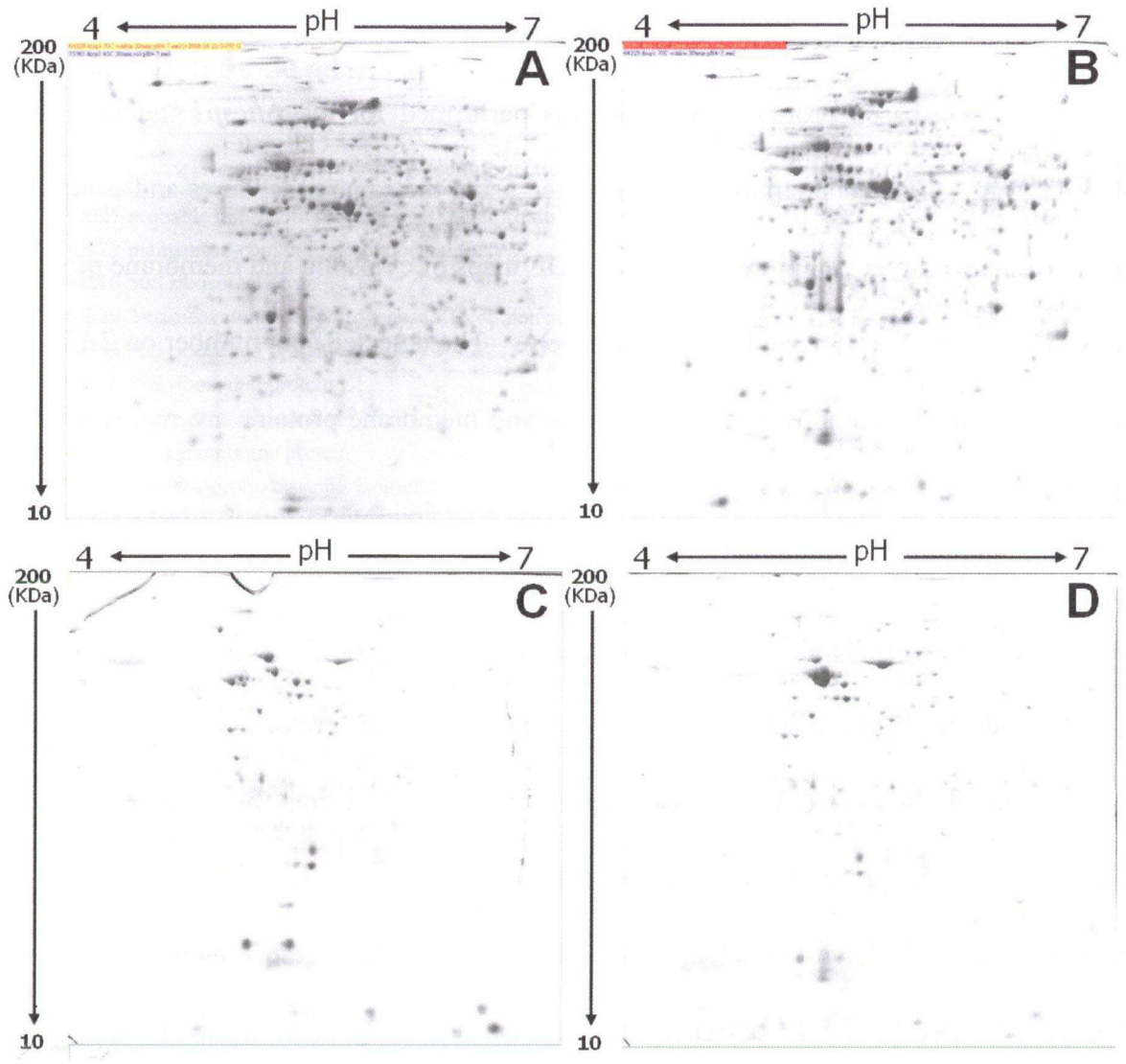

Figure 3-3. 2-DE proteome profiling of Δ*ttcsp1* mutant under 45°C and 70°C after 30 min from transient state.

The cytosolic and membrane proteins were extracted from Δ*ttcsp1* mutant after transfer to 45°C and 70°C for 30 min, respectively. Each protein sample was separated onto the pH 4 to 7, and 12.5% SDS-PAGE gel (13 cm x 15 cm x 1 mm) and followed CBB G-250 staining with aluminium sulfate. **A**, The cytosolic proteins under 70°C. **B**, The cytosolic proteins under 45°C. **C**, The membrane proteins of under 70°C. **D**, The membrane proteins under 45°C.

3.3.2 *tt*Csp1 also involves the expression of 30S ribosomal protein S1 under cold stress condition.

Significant fraction of the up-regulated proteins in the wild type under cold shock condition was down-regulated in the Δ*ttcsp1* mutant under 45°C. These includes proteins involved in mRNA stabilizing and translational process (TTHA0162, 30S ribosomal protein S1; TTHA0739, L-serine dehydratase beta subunit; TTHA1586, DNA gyrase B; TTHA0115, prolyl-tRNA synthetase; TTHA0161, leucyl-tRNA synthetase; TTHA1875, threonyl-tRNA synthetase; and TTHA1958, phenylalanyl-tRNA synthetase alpha chain) and amino acid metabolism (TTHA1605, probable acylamino-acid-releasing enzyme; and TTHA1755, acetylornithine/acetyl-lysine aminotransferase) (Table 3-13). These results demonstrate that *tt*Csp1 is involved in the translational process, especially synthesis of aminoacyl-tRNAs, under cold stress condition. Especially, the 30S ribosomal protein S1 was strongly up-regulated in the wild type strains, but down-regulated in Δ*ttcsp1* mutant under cold stress condition. These results imply that the *tt*Csp1 is involved in the expression of 30S ribosomal protein S1 under cold stress condition.

3.3.3 Regulation of the energy production and the fatty acid biosynthesis pathway were not influenced by deletion of *ttcsp1*.

Likewise the wild type, Δ*ttcsp1* mutant showed down-regulation of several proteins involved in the energy production under cold stress condition. The ATP synthase subunits, TTHA1272, TTHA1273, and TTHA1276, were strongly down-regulated in Δ*ttcsp1* mutant under 45°C (Table 3-15). The core enzymes related to fatty acid biosynthesis pathway,

including TTHA0229, TTHA0232, TTHA0287, and TTHA0288, were up-regulated in Δ*ttcsp1* mutant (Table 3-14) as in the wild type. These results indicate that regulation of the energy production and the fatty acid biosynthesis pathway were not influenced by deletion of *ttcsp1* under the cold condition.

Table 3-12. The up-regulated cytosolic proteins in Δ*ttcsp1* mutant under cold stress condition (45°C for 30 min).

orf I.D	Annotated information	Mowse	p*I*	Mw.	Intensity coverage	Sequence coverage
TTHA0214	probable kinase	147	4.9	54.8	42.8	40.6
TTHA0256	leucine aminopeptidase	133	8.7	54.6	61.4	36.7
TTHA0321	polypeptide deformylase	71	5.0	22.1	21.7	35.4
TTHA0537	succinyl-CoA synthetase alpha chain	83	5.5	29.8	80.6	29.9
TTHA0812	phosphoribosylamine--glycine ligase	57	5.3	44.4	14.7	25.9
TTHA1028	thiosulfate sulfurtransferase	72	5.2	32.9	36.1	27.0
TTHA1111	alternative ATP-dependent protease La (Lonprotease)	84	5.2	58.4	39.5	24.4
TTHA1276	V-type ATP synthase subunit E	110	5.3	20.6	35.7	43.1
TTHA1434	3-hydroxybutyryl-CoA dehydratase	79	4.6	29.2	87.3	25.8
TTHA1473	conserved hypothetical protein	101	4.9	16.8	71.3	50.0
TTHA1479	conserved hypothetical protein	80	5.0	16.8	43.3	37.2
TTHA1482	bacterioferritin	104	4.7	16.2	48.6	60.4
TTHA1527	NADPH-quinone reductase	122	8.8	33.8	74.8	44.3
TTHA1615	conserved hypothetical protein	66	5.1	15.4	14.8	57.7
TTHA1624	conserved hypothetical protein	155	5.0	27.4	75.6	60.3
TTHA1714	conserved hypothetical protein	55	5.7	28.9	23.6	34.1
TTHA1914	homocitrate synthase	177	5.8	42.1	48.6	50.3
TTHB023	transcriptional regulator TetR family	51				
TTHB057	cobalamin biosynthesis protein CbiG	159	6.5	38.7	68.8	48.5
TTHB125	chromosome partitioning ATPase ParA family	183	6.6	35.9	84.1	34.2
TTHB179	conserved hypothetical protein	114	9.8	23.9	46.2	48.6

Table 3-13. The down-regulated cytosolic proteins in Δ*ttcsp1* mutant under cold stress condition (45°C for 30 min).

orf I.D	Annotated information	Mowse	p*I*	Mw.	Intensity coverage	Sequence coverage
TTHA0001	DNA polymerase III beta subunit	72	4.9	40.5	22.4	32.3
TTHA0115	prolyl-tRNA synthetase	139	5.9	54.5	52.8	43.4
TTHA0122	manganese-containing pseudocatalase	130	5.3	33.3	61.1	38.7
TTHA0136	LAO/AO transport system kinase	180	6.4	33.5	54.2	53.0
TTHA0161	leucyl-tRNA synthetase	110	6.0	59.2	62.2	32.6
TTHA0162	30S ribosomal protein S1	216	6.3	57.4	54.7	50.0
TTHA0232	pyruvate dehydrogenase complex dihydrolipoamideacetyltranferase E2 compo	109	5.6	50.1	36.3	32.2
TTHA0256	leucine aminopeptidase	115	8.7	54.6	48.0	37.3
TTHA0271	60 kDa chaperonin (Protein Cpn60) (GroELprotein)	89	5.1	54.7	63.3	28.1
TTHA0380	aldehyde:ferredoxin oxidoreductase	54	6.7	54.7	41.4	21.5
TTHA0512	conserved hypothetical protein	93	6.3	39.2	46.4	29.6
TTHA0520	NAD-dependent malic enzyme (malatedehydrogenase)	106	6.2	57.4	20.7	41.0
TTHA0558	fumarate hydratase class II (EC 4.2.1.2)	169	6.3	50.9	86.9	33.9
TTHA0591	UDP-glucose 4-epimerase	139	6.2	33.8	62.3	46.9
TTHA0599	protoporphyrinogen oxidase (HemG	63	10.5	49.2	13.9	34.6
TTHA0634	magnesium chelatase related protein	245	5.7	51.4	77.4	57.1
TTHA0704	pyridoxine biosynthesis protein	61	5.4	32.4	17.3	20.2
TTHA0739	L-serine dehydratase beta subunit	48	6.4	23.6	54.6	26.8
TTHA0968	phenylacetic acid degradation protein PaaZ	102	6.4	55.2	56.8	21.3
TTHA1097	DNA ligase [NAD+]	107	7.8	58.9	30.5	36.1
TTHA1124	acetyl-CoA carboxylase biotin carboxyl carrierprotein	57	4.5	17.7	47.5	38.2
TTHA1429	metallo-beta-lactamase family protein	113	6.2	35.4	68.3	41.0
TTHA1527	NADPH-quinone reductase	137	8.8	33.8	75.8	55.7
TTHA1569	hypothetical protein	203	5.3	57.5	44.9	43.0
TTHA1576	NAD-dependent glutamate dehydrogenase	138	6.8	43.4	9.8	24.1
TTHA1586	DNA gyrase subunit B	89	6.1	55.8	31.4	31.1
TTHA1605	probable acylamino-acid-releasing enzyme	94	5.4	56.9	43.3	20.5
TTHA1637	ribose-phosphate pyrophosphokinase	76	5.9	33.5	86.3	32.6
TTHA1659	tetratricopeptide repeat family protein	186	6.1	48.9	49.4	45.0
TTHA1735	iron-sulfur cluster biosynthesis protein IscS(cysteine desulfurase)	198	6.3	44.7	58.6	48.3
TTHA1755	acetylornithine/acetyl-lysine aminotransferase	137	6.8	43.4	48.5	58.5
TTHA1774	pili retraction protein PilT	62	6.2	41.1	42.2	17.1
TTHA1813	DNA-directed RNA polymerase beta chain (RpoB)	146				
TTHA1875	threonyl-tRNA synthetase	138	5.6	58.8	56.8	30.1
TTHA1958	phenylalanyl-tRNA synthetase alpha chain	219	5.7	39.2	92.1	46.3
TTHB125	chromosome partitioning ATPase ParA family	89	6.6	35.9	28.6	29.5
TTHB163	conserved hypothetical protein	210	5.6	30.7	50.6	59.8

Table 3-14. The up-regulated membrane proteins in Δ*ttcsp1* mutant under cold stress condition (45°C for 30 min).

orf I.D	Annotated information	Mowse	p*I*	Mw.	Intensity coverage	Sequence coverage
TTHA0090	NADH-quinone oxidoreductase chain 3	74	5.6	57.1	32.3	13.9
TTHA0098	arginyl-tRNA synthetase	147	6.6	57.5		
TTHA0120	GTP-binding protein Era	119	5.9	33.8		
TTHA0122	manganese-containing pseudocatalase	121	5.3	33.3		
TTHA0158	alpha-dextran endo-16-alpha-glucosidase((amylo)pullulanase)	109	6.0	58.9	28.6	21.3
TTHA0206	nicotinamide nucleotide transhydrogenase alphasubunit 1	103	6.9	39.9	51.6	17.1
TTHA0229	2-oxoisovalerate dehydrogenase E1 componentalpha subunit	141	5.3	41.1		
TTHA0230	2-oxoisovalerate dehydrogenase E1 componentbeta subunit		5.8	35.1	29.4	24.7
TTHA0232	pyruvate dehydrogenase complex dihydrolipoamideacetyltranferase E2 compor	213	5.6	50.1		
TTHA0251	translation elongation factor EF-Tu.B					
TTHA0271	60 kDa chaperonin (Protein Cpn60) (GroELprotein)	233	5.1	54.7		
TTHA0272	10 kDa chaperonin (Protein Cpn10) (groESprotein)		5.1	11.0	8.4	68.3
TTHA0287	2-oxoglutarate dehydrogenase E3 component(dihydrolipoamide dehydroge	198	6.8	49.0		
TTHA0288	2-oxoglutarate dehydrogenase E2 component(dihydrolipoamide succinylt	135	5.7	44.5		
TTHA0304	enoyl-[acyl carrier protein] reductase		5.8	28.1	9.4	25.7
TTHA0364	type IV pilus assembly protein PilF	123	4.9	56.6		
TTHA0442	probable DNA/RNA-binding protein (Jag-relatedprotein)		6.1	21.0	8.7	25.9
TTHA0525	glycine dehydrogenase (decarboxylating) subunit1	59	5.3	47.0		
TTHA0614	trigger factor	183	4.9	46.3		
TTHA0701	N utilization substance protein A (NusA)	209	5.7	43.9		
TTHA0702	conserved hypothetical protein	136	4.9	17.8	82.8	58.0
TTHA0770	ATP-dependent protease La (Lon protease)	57	6.1	58.5		
TTHA0861	30S ribosomal protein S2	154	5.3	29.3		
TTHA1111	alternative ATP-dependent protease La (Lonprotease)	48	5.2	58.4		
TTHA1123	acetyl-CoA carboxylase biotin carboxylasesubunit	277	6.1	49.3		
TTHA1210	2-isopropylmalate synthase (LeuA)		5.7	56.5	38.9	27.0
TTHA1211	probable ketol-acid reductoisomerase (IlvC)	114	6.2	37.1		
TTHA1243	septum site-determining protein MinD	52	5.3	28.9	28.4	19.1
TTHA1251	preprotein translocase SecA subunit	135	6.3	58.3		
TTHA1294	ribosomal subunit interface protein	134	6.4	21.6	54.6	43.5
TTHA1459	ABC transporter ATP-binding protein	219	6.5	33.9		
TTHA1483	conserved putative protein	123	5.9	25.7		
TTHA1484	small heat shock protein HSP20 family	91	5.8	15.7	64.5	46.7
TTHA1487	ATP-dependent Clp protease ATP-binding subunitClpB	64	5.5	57.5		
TTHA1642	S-adenosylmethionine synthetase		5.5	43.2		
TTHA1665	30S ribosomal protein S4	134	11.3	24.3	74.3	48.3
TTHA1689	50S ribosomal protein L2	201	11.7	30.4		
TTHA1696	30S ribosomal protein S7	84	11.0	18.0		
TTHA1813	DNA-directed RNA polymerase beta chain (RpoB)	147	6.3	57.8		
TTHA1818	RecA protein	189	5.5	35.4		
TTHA1840	SufD protein (membrane protein)	205	61.0	47.9		

Table 3-15. The down-regulated membrane proteins in *Δttcsp1* mutant under cold stress condition (45°C for 30 min).

orf I.D	Annotated information	Mowse	p*I*	Mw.	Intensity coverage	Sequence coverage
TTHA0122	manganese-containing pseudocatalase	98	5.3	33.3	55.7	27.2
TTHA0210	50S ribosomal protein L12	54	4.9	13.1	23.0	32.0
TTHA0229	2-oxoisovalerate dehydrogenase E1 componentalpha subunit	149	5.3	41.4	67.6	23.2
TTHA0245	30S ribosomal protein S6 (TS9)	142	7.2	12.0	35.7	62.4
TTHA0251	translation elongation factor EF-Tu.B	116	5.3	44.8	54.0	26.6
TTHA0271	60 kDa chaperonin (Protein Cpn60) (GroELprotein)	260	5.1	54.7	59.0	50.0
TTHA0561	outer membrane protein	209	4.9	56.2	72.0	35.5
TTHA0602	peptidyl-prolyl cis-trans isomerase	204	5.4	37.4	53.3	58.2
TTHA0906	phosphoglycerate kinase	151	5.5	41.8	43.0	40.0
TTHA1210	2-isopropylmalate synthase (LeuA)	107	5.7	56.5	61.4	21.1
TTHA1272	V-type ATP synthase subunit B	64	5.1	53.1	68.4	20.7
TTHA1273	V-type ATP synthase subunit A	340	5.0	56.1	73.1	64.8
TTHA1276	V-type ATP synthase subunit E	221	5.3	20.6	60.4	71.8
TTHA1484	small heat shock protein HSP20 family	71	5.8	15.7	52.6	34.3
TTHA1570	deoxyhypusine synthase	101	5.7	38.3	83.3	16.2
TTHA1694	elongation factor Tu (EF-Tu)	133	5.3	44.8	65.6	31.0
TTHA1839	SufB protein (membrane protein)	106	5.2	53.1	39.1	26.7

3-4 Difference of proteome results between wild type and the *Δttcsp1* mutant under cold stress condition.

I focused on proteins that showed different expression pattern between the wild type and *Δttcsp1* mutant strains under cold stress condition (at 45°C). The gel-to-gel matching of spots (wild type vs. the *Δttcsp1* mutant) showed 74.5% (G-V vs. G-VI) and 62.0% (G-IX vs. G-X) for cytosolic and membrane protein fractions, respectively (Tables 3-2 and 3-3). Then I identified up- and down-regulated proteins (with more than 1.5-fold change, $p < 0.05$) in the *Δttcsp1* mutant grown at 45°C against the wild type grown at the same temperature. 20 up-regulated proteins (Table 3-16) and 28 down-regulated proteins (Table 3-17) were identified in cytosolic protein fraction, and 7 up-regulated (Table 3-18) and 11 down-regulated proteins (Table 3-19) were identified in membrane protein fraction.

Under cold stress condition, EF-Tu (TTHA0251 and TTHA1694), NusA (TTHA0701), and *tt*Csp2 (TTHA0359) were identified as cold stress response proteins in the wild type strain (Tables 3-8 and 3-10), but were down-regulated in the Δ*ttcsp1* mutant (Tables 3-17 and 3-19). These proteins were also down-regulated in the Δ*ttcsp1* mutant even at 70°C. These results indicate that the *ttcsp1* deletion resulted in the down-regulation of cold shock responsible proteins under both optimal and cold stress conditions (70°C and 45°C).

I also identified 13 candidates for proteins of which expression may be affected by *tt*Csp1. By comparative proteome analysis, I extracted the proteins which were commonly found both in up-regulated protein list of the wild type at 45°C (G-III vs. G-V (Table 3-8) and G-VII vs. G-IX (Table 3-10)) and down-regulated protein list of the Δ*ttcsp1* mutant at optimal growth temperature (G-III vs. G-IV (Table 3-5) and G-VII vs. G-VIII (Table 3-7)). These are TTHA0090 (NADH-quinone oxidoreductase chain 3), TTHA0098 (arginyl-tRNA synthetase), TTHA0229 (2-oxoisovalerate dehydrogenase, E1 component α subunit), TTHA0271 (60 kDa chaperonin), TTHA 0557 (superoxide dismutase), TTHA 0614 (trigger factor), TTHA0699 (IF2), TTHA1123 (acetyl-CoA carboxylase biotin carboxylase subunit), TTHA1483 (conserved hypothetical protein), TTHA1487 (ClpB), TTHA1642 (S-adenosylmethionine synthetase), TTHA1818 (RecA), and TTHB152 (CRISPR-associated protein).

Table 3-16. The up-regulated cytosolic proteins in Δ*ttcspI* mutant under cold stress condition (45°C for 30 min).

orf I.D	Annotated information	Mowse	pI	Mw.	Intensity coverage	Sequence coverage
TTHA0141	hypothetical protein	148	4.9	16.7	57.5	72.8
TTHA0271	60 kDa chaperonin (Protein Cpn60) (GroELprotein		5.1	54.7	21.4	11.3
TTHA0614	trigger factor	124	4.9	46.3	38.8	31.9
TTHA0699	translation initiation factor IF		5.3	56.4	51.3	24.0
TTHA0860	elongation factor Ts (EF-Ts)	80	6.2	22.4	44.2	37.8
TTHA0924	conserved hypothetical protein	198	5.3	36.0	74.5	46.9
TTHA0970	phenylacetic acid degradation protein PaaC	150	4.7	28.7	61.5	39.5
TTHA1169	valyl-tRNA synthetase (valine--tRNA ligase)(ValRS)	84	6.0	59.1	44.1	18.0
TTHA1243	septum site-determining protein MinD	248	5.3	28.9	73.7	58.4
TTHA1479	conserved hypothetical protein	107	5.0	16.8	43.7	45.3
TTHA1498	elongation factor G (EF-G-2)	134	5.1	56.7	31.0	28.5
TTHA1519	phosphoribosylformylglycinamidine synthase II	137	5.5	55.7	55.7	32.8
TTHA1602	conserved hypothetical protein	67	5.3	11.9	12.5	44.2
TTHA1610	conserved hypothetical protein	110	5.5	8.7	57.4	75.3
TTHA1625	osmotically inducible protein OsmC		5.4	15.3	30.5	44.4
TTHA1670	methionine aminopeptidase		5.4	27.8	61.5	53.3
TTHA1695	elongation factor G (EF-G)		5.2	57.2	42.1	35.7
TTHA1519	phosphoribosylformylglycinamidine synthase II					
TTHA1938	acyl-CoA dehydrogenase	181	5.5	41.5	70.4	35.7
TTHA1958	phenylalanyl-tRNA synthetase alpha chain	114	5.7	39.2	75.3	24.0

Table 3-17. The down-regulated cytosolic proteins in Δ*ttcspl* mutant under cold stress condition (45°C for 30 min).

orf I.D	Annotated information	Mowse	pI	Mw.	Intensity coverage	Sequence coverage
TTHA0090	NADH-quinone oxidoreductase chain 3	165	5.6	57.1	62.6	26.4
TTHA0108	transketolase	101	6.1	56.7	18.1	35.9
TTHA0116	phosphonopyruvate decarboxylase	97	6.1	44.4	39.7	32.8
TTHA0245	30S ribosomal protein S6 (TS9)	60				
TTHA0278	ATP-dependent phosphoenolpyruvate carboxykinase	203	6.4	57.6	71.5	41.0
TTHA0359	cold shock protein, Csp2	69	7.6	7.8	40.4	82.4
TTHA0512	conserved hypothetical protein	123	6.3	39.2	62.6	31.3
TTHA0520	NAD-dependent malic enzyme (malatedehydrogenase)	93	6.2	57.4	23.0	21.9
TTHA0525	glycine dehydrogenase (decarboxylating) subunit1	148	5.3	47.1	83.2	24.4
TTHA0614	trigger factor	206	4.9	46.3	58.6	50.0
TTHA0630	heat shock protein HslU	220	5.6	46.5	59.7	51.2
TTHA0634	magnesium chelatase related protein	153	5.7	51.4	71.0	40.1
TTHA0704	pyridoxine biosynthesis protein	158	5.4	32.4	43.9	32.7
TTHA0989	conserved hypothetical protein	137	5.6	40.3	32.8	40.2
TTHA1124	acetyl-CoA carboxylase biotin carboxyl carrierprotein	55	4.5	17.7	25.8	29.7
TTHA1197	N-acetyl-gamma-glutamyl-phosphate reductase	115	6.0	37.6	24.2	30.7
TTHA1274	V-type ATP synthase subunit F	46	4.5	11.3	6.0	67.3
TTHA1447	alanine dehydrogenase	85	5.9	36.4	45.1	28.7
TTHA1577	putative NAD-dependent glutamate dehydrogenase	142	4.9	44.7	74.0	27.2
TTHA1589	50S ribosomal protein L25 (TL5)	134	5.1	23.2	55.0	35.0
TTHA1637	ribose-phosphate pyrophosphokinase	102	5.9	33.5	67.9	43.9
TTHA1694	elongation factor Tu (EF-Tu)	231	5.3	44.8	60.7	56.2
TTHA1779	metal dependent phosphohydrolase (HD domainprotein)	210	5.7	17.8	60.8	64.2
TTHA1839	SufB protein (membrane protein)	131	5.2	53.1	38.1	32.7
TTHA1875	threonyl-tRNA synthetase	115	5.6	58.8	34.6	33.0
TTHA1958	phenylalanyl-tRNA synthetase alpha chain	58	5.7	39.2	13.7	20.6
TTHB057	cobalamin biosynthesis protein CbiG	168	6.5	38.7	49.4	51.3
TTHB179	conserved hypothetical protein	59				

Table 3-18. The up-regulated membrane proteins in Δ*ttcspl* mutant under cold stress condition (45°C for 30 min).

orf I.D	Annotated information	Mowse	pI	Mw.	Intensity coverage	Sequence coverage
TTHA0233	pyruvate dehydrogenase complex dihydrolipoamidedehydrogenase E3 component	94	6.4	49.1	49.8	17.7
TTHA0288	2-oxoglutarate dehydrogenase E2 component(dihydrolipoamide succinylt	78	5.7	44.5	42.9	22.7
TTHA0561	outer membrane protein	184	4.9	56.2	33.7	38.1
TTHA0602	peptidyl-prolyl cis-trans isomerase	231	5.4	37.4	66.7	65.9
TTHA0770	ATP-dependent protease La (Lon protease)	53	6.1	58.5	43.0	18.8
TTHA0861	30S ribosomal protein S2	126	5.3	29.0	46.1	53.9
TTHA1383	general secretion pathway protein (PilQ)	236	6.5	56.0	72.4	43.9

Table 3-19. The down-regulated membrane proteins in Δ*ttcsp1* mutant under cold stress condition (45°C for 30 min).

orf I.D	Annotated information	Mowse	pI	Mw.	Intensity coverage	Sequence coverage
TTHA0122	manganese-containing pseudocatalase	67	5.3	33.3	59.3	28.3
TTHA0229	2-oxoisovalerate dehydrogenase E1 componentalpha subunit	138	5.3	41.1	67.3	21.5
TTHA0251	translation elongation factor EF-Tu.B	124	5.3	44.8	86.7	32.5
TTHA0701	N utilization substance protein A (NusA)	67	5.7	43.0	38.9	31.0
TTHA1210	2-isopropylmalate synthase (LeuA)	228	5.7	56.5	57.4	50.0
TTHA1294	ribosomal subunit interface protein	140	6.4	21.6	72.6	55.9
TTHA1642	S-adenosylmethionine synthetase	257	5.5	43.2	59.4	60.0
TTHA1665	30S ribosomal protein S4	151	11.3	24.0	79.6	53.1
TTHA1689	50S ribosomal protein L2	236	11.7	30.4	86.2	66.3
TTHA1695	elongation factor G (EF-G)	122	5.2	57.2	59.3	28.9
TTHA1813	DNA-directed RNA polymerase beta chain (RpoB)	66	6.3	57.0	33.6	15.8

At least part of the proteins whose expression level was caused by *ttcsp1* deletion is considered to be controlled by the cold shock response pathway involving *tt*Csp1. It should be mentioned, however, that the Δ*ttcsp1* mutant showed similar growth rate to the wild type strain under both optimal and cold stress conditions (Figure 1-1B). The Δ*ttcsp1* mutant led to significant down-regulation of *tt*Csp2, the other cold shock-induced protein. Nevertheless, this mutant strain was rapidly adapted to cold stress condition. Such fast adaptation to cold stress condition without *tt*Csp1 and *tt*Csp2 in Δ*ttcsp1* mutant raises the possibility that an alternative cold-adaptation mechanism exists in *T. thermophilus* HB8.

As up-regulated proteins under cold stress condition without *tt*Csp1 and *tt*Csp2 in the Δ*ttcsp1* mutant (Tables 3-16 and 3-18), elongation factor Ts (EF-Ts, TTHA0860), elongation factor G2 (TTHA1498), osmotically inducible protein OsmC (TTHA1625) and elongation factor G (TTHA1695) in cytosolic protein fraction, and 30S ribosomal protein S2 (TTHA0861), outer membrane protein (TTHA0561), general secretion pathway protein (TTHA1383) in membrane protein fraction were newly identified. Although most of them

belong to proteins involved in translation process, it is uncertain at present whether these proteins are related to alternative cold-adaptation mechanism. In addition, it was also noted that six hypothetical proteins (TTHA0141, TTHA0924, TTHA1479, TTHA1498, TTHA1602 and TTHA1610) were also up-regulated. Also among the up-regulated proteins (45°C vs. 70°C) in the *Δttcsp1* mutant under cold stress condition, seven hypothetical proteins (TTHA1473, TTHA1479, TTHA1482, TTHA1615, TTHA1624, TTHA1714 and TTHB179) were identified. The study to elucidate functional role of these hypothetical proteins will be needed to verify the relationship to stress response mechanism.

4. Comparison of transcriptome and protepme results

I obtained two types of data sets from transcriptome and proteome analyses. Making use of these data, I could obtain more information about the functions of *tt*Csp1. Although I have not finished identification of all protein spots on the gels under each condition (some spots remained to be identified, because their amounts were too small to be detected or their pIs were out of range), I could compare the result from proteome with that from microarray.

Here I classify the genes identified by the proteome analysis into three groups (A to C) according to the relationship to the transcriptome data. Group A contains the proteins whose expression changes were detected also in the transcriptome samples under the same condition, and 24 proteins can be classified into Group A (Table 4-1). As shown in Table 4-1, up-regulated protein under certain condition (for example, TTHA1498) were also up-regulated on the (*ttha1498*) transcription level, and down-regulated proteins (for example, TTHA1695) were also down-regulated on the (*ttha1695*) transcription level. Because the expression changes were correlated with the changes of the mRNA, it means the expression patterns of proteins might be directly influenced by the amount of mRNAs in these cases.

In regard to some proteins, the changing ratio calculated from microarray analysis was not identical to the ratio from proteome analysis. It is likely that *tt*Csp1 helped the degradation of the proteins or decreased the translation efficiency. On the other hand, mRNAs of *tt*Csp2 (Group A) were increased only 2.7-fold under the cold shock condition in the wild type, its protein spot intensity of the *tt*Csp2 was increased more than 50-fold. This raises the possibility that *tt*Csp1 functions not only as a transcriptional regulator but also as a

translational regulator. This hypothesis might be supported by existence of Group B proteins whose expression changes were detected only from proteome analysis.

More than 50% of proteins are classified into Group B, whose expression changes were detected only by proteome analysis. For example, the expression pattern of TTHA0699 (translation initiation factor IF-2) was decreased even though the amounts of mRNAs were not affected by deletion of *ttcsp1* gene. Futhermore, some proteins belonging to Group B were increased at protein level in the Δ*ttcsp1* mutant, even though the mRNA transcripts were not changed. Therefor, it is infered that *tt*Csp1 can both suppress and enhance translation independent of transcription. It was already reported that *ec*CspA and *ec*CspE are involved in mRNA stabilization to increase life time of mRNA through a protection from cellular RNases (Feng, Y. *et al.*, 2001). However, up-regulation of Group B proteins could not be explained only by stabilization of the mRNAs because their mRNA levels were not changed. Some cold-inducible Csps from other organisms are thought to promote translational repression by destabilizing mRNA structures (Phadtare, S. and Inouye, M. 1999). However, this is the first report to indicate that a Csp family protein facilitates translation without altering mRNA levels under optimal growth conditions. The results suggest that *tt*Csp1 can suppress aspects of cellular metabolism and alter the properties of protein production machinery. These results also imply that *tt*Csp1 can sense minor fluctuations in the growth conditions and prepare for the stress response. There might be a regulation system controlling the initiation or elongation of translation.

Some proteins belonging to Group C made a protein spot at the unexpected position, or made several spots on the same gel. TTHA0271 (GroEL), TTHA0614 (trigger factor) and

some ribosomal proteins are the members of Group C. Such phenomena might reflect the changes of protein maturation states, folding states and modification patterns after translation event. The proteins identified from membrane protein fraction are classified into Group C at higher frequency than cyosolic proteins. I have not been able to identify the resons of spots shift completely yet, however, with regard to GroEL, phospholylation and acethylation were detected. Although the functions of these modifications have not been clear, the ratio of modification forms of chaperonin and translational regulators were changed in the abcense of *tt*Csp1. Deletion of *ttcsp1* may cause the alteration of the frequency of protein synthesis.

Table 4-1. Genes classified into Group A.

Group A contains the genes which showed similar expression changes both in the transcriptome and proteome samples under the same conditions.

Functional category	orf I.D	Annotated information
Δ ttcspl > WT (at 70℃)		
translation	TTHA1498	elongation factor G (EF-G-2)
Δ ttcspl < WT (at 70℃)		
transcription	TTHA0248	transcription antitermination protein NusG
translation	TTHA1695	elongation factor G (EF-G)
Metabolism of Carbohydrate	TTHA1066	proabable transaldolase
45℃ > 70℃ (in WT)		
Csp2	TTHA0359	cold shock protein
RNA helicase	TTHA0109	ATP-dependent RNA helicase
Genetic Information Processing	TTHA0008	phage shock protein A
45℃ < 70℃ (in WT)		
LytR/CspA/Psr family	TTHA1778	LytR/CspA/Psr family protein
Metabolism of carbohydrate	TTHA0506	malate synthase
Metabolism of Cofactors and Vitamins	TTHA1775	pantoate--beta-alanine ligase
Metabolism of energy	TTHA1272	V-type ATP synthase subunit B
Metabolism of energy	TTHA1273	V-type ATP synthase subunit A
Metabolism of energy	TTHA1276	V-type ATP synthase subunit E
45℃ > 70℃ (in *Δ ttcspl*)		
transcription	TTHB023	transcriptional regulator, TetR family
translation	TTHA1570	deoxyhypusine synthase
Metabolism of ammino acid	TTHA1642	S-adenosylmethionine synthetase
Membrane/ Transporter/ Lipoprotein	TTHA0120	GTP-binding protein Era
Metabolism of ammino acid	TTHA1914	homocitrate synthase
hypothetical protein	TTHA0702	hypothetical protein
45℃ < 70℃ (in *Δ ttcspl*)		
Chaperones	TTHA1487	ATP-dependent Clp protease, ATP-binding subunit ClpB
Metabolism of amino acid	TTHA0525	glycine dehydrogenase (decarboxylating) subunit 1
Metabolism of Carbohydrate	TTHA0232	pyruvate dehydrogenase complex, dihydrolipoamide acetyltranferase E2 component
Metabolism of Cofactors and Vitamins	TTHA0206	nicotinamide nucleotide transhydrogenase, alpha subunit 1
Genetic Information Processing	TTHA1774	pili retraction protein PilT

5. Crystal structure of *tt*Csp1

5-1 Overall structure

The crystal structure of *tt*Csp1 was determined at 1.65 Å resolution by molecular-replacement method (Table 5-1). The asymmetric unit contains two molecules (A and B). With the exception of loop4, the structure of these structures are almost the same. Therefore, the molecule A was used for the following analyses.

The overall structure of *tt*Csp1 is shown in Figure 5-1B, C. *tt*Csp1 is composed entirely of an antiparallel five-stranded β-sheet (β1–β5) with connecting a turn and loops (trun1 and loop2–loop4). The five-stranded antiparallel β-barrel of *tt*Csp1 is characteristic of the defined oligonucleotide/oligosaccharide-binding fold (OB-fold, Murzin, A. G., 1993) as shown in Figure 5-1C. Strands β1 to β4 of the barrel form the Greek key motif which is common to many known proteins with beta-barrels and almost all proteins with beta-sandwich structures (Zhang, C. *et al.*, 2000).

5-2 Structural comparison with cold shock proteins and the Y-box binding protein

Cold shock proteins exist in almost bacteria and the cold shock domain (CSD) is a nucleic acid-binding domain of the eukaryotic gene-regulatory Y-box factors which are involved in transcriptional and translational regulation for messenger RNA (mRNA) and for a wide rage of genes containing the Y-box sequence (5'-CTGATTGGCCAA-3') (Ladomery, M., 1997). In addition to the structure of *tt*Csp1, the structures of cold shock proteins from six species of bacteria and a structure of the CSD of human Y-box binding protein 1 (*hs*YB1;

PDB code, 1H95; Kolks, C. P. A. M. *et al.*, 2002) have been determined so far. A sequence alignment of *tt*Csp1, *tt*Csp2, cold shock proteins from six bacteria and CSD of *hs*YB1 is shown in Figure 5-1A. The sequence identities of the *tt*Csp1 with *tt*Csp2, *bc*Csp, *bs*CspB, *tm*Csp, *ec*CspA, *nm*Csp, *st*CspE and *hs*YB1 are 72%, 63%, 59%, 54%, 55%, 55%, 55% and 50%, respectively, showing that the amino acid sequences are conserved among not only bacterial cold shock proteins but also the eukaryotic CSDs.

The three dimensional structures of cold shock proteins have been determined not only by using wild type proteins, mutant proteins and complex with single stranded DNA (ssDNA), and but also by using crystallographic and NMR methods. Therefore, the structural analyses were carried out using the following structures, cold shock protein from *B. caldolyticus* (*bc*Csp), A chain in 1C9O (Mueller, U. *et al.*, 2000); CspB from *Bacillus subtilis* (*bs*CspB), A chain in 1CSP (Schindelin, H., *et al.*, 1993); CspA from *E. coli* (*ec*CspA), A chain in 1MJC (Schindelin, H., *et al.*, 1994); cold shock protein from *Thermotoga martima* (*tm*Csp), A chaind in 1G6P (Kremer, W. *et al.*, 2001); cold shock protein from *Neisseria meningitides* (*nm*Csp), 1–38 residues of A chain and 39–67 of B chain in 3CAM (Kremer, W. *et al.*, 2001); CspE from *Salmonella typhimurium* (*st*CspE), A chain in 3I2Z (Morgan, HP. *et al.*, 2009) and the CSD of *hs*YB1, A chain in 1H95 (Kolks, C. P. A. M. *et al.*, 2002).

To analysis the structural similarity, least-squares fitting of main-chain atoms were carried out using the residues 2–21, 25–51, 62–68 of *tt*Csp1 (216 atoms) and the corresponding atoms of six cold shock proteins and CSD of YB1. *nm*Csp forms a dimmer by exchange of two β-strands, β4 and β5 in the crystal structure, although *nm*Csp behaved as a monomer in solution. Therefore, the residues 2–38 in A chain and residues 39–67 in B

chain of *nm*Csp were used to calculate the r.m.s. deviation. The r.m.s. deviations from the structure of *tt*Csp1 are 0.96 in the structure of *bc*Csp, 1.13 of *bs*CspB, 1.06 of *ec*CspA, 1.53 of *nm*Csp, 1.90 of *tm*Csp, 1.27 of *st*CspE and 3.16 of CSD of *hs*YB1, respectively. As shown in Figure 5-1F, the secondary structures of β-barrel are almost same and there are local differences in loop 3 and especially in loop 4. The r.m.s. deviation of CSD of *hs*YB1 from *tt*Csp1 is higher than those of other cold shock proteins. The five-stranded antiparallel β-barrel consists of the front β sheet containing strands β1–β3 and the back β sheet containing β4 and β5. As shown in Figure 5-1A, four residues are inserted in loop 3 of CSD of *hs*YB1, forming lager loop 3 than that of *tt*Csp1 between the front and back β sheets (Figure 5-1G). Since the r.m.s. deviations from the front β sheet of *tt*Csp1 (117 atoms) are 1.04 in the front β sheet of *bc*Csp and 1.39 of CSD of *hs*YB1, the structures of the front β sheet are conserved in not only the cold shock proteins but also CSD of *hs*YB1, suggesting the lager loop3 of CSD of *hs*YB1 changes the orientation of the front and back β sheets in the structure of CSD. These structural similarities and differences could emphasize again that the front β sheet containing RNP1 and RNP2 motifs is highly conserved in not only bacterial cold shock protein, but also in eukaryotic CSDs and that RNP1 and RNP2 motifs play an important role to nucleotide binding. These results indicate that the 3D structure of *tt*Csp1 is quite similar to those of other Csps and the CSD, suggesting that *tt*Csp1 possesses similar molecular properties including the ability to bind DNA.

Table 5-1. Data collection, refinement and model statistics

Data collection	
Beamline	BL44B2, SPring-8
Wavelength (Å)	1.00
Space group	*P*1
Unit-cell parameters	a = 28.22 Å, b = 29.86 Å, c = 38.26 Å
	$\alpha = 67.37°, \beta = 81.44°, \gamma = 79.49°$
Resolution range [a] (Å)	50.0–1.65 Å (1.71–1.65 Å)
No. of measured reflections	50,732
No. of unique reflections	12,948
Redundancy [a]	3.9 (3.7)
Completeness [a] (%)	95.2% (87.4%)
R_{merge} [a, b] (%)	3.1% (9.5%)
Average $I/\sigma(I)$ [a]	46.9 (13.9)
Refinement statistics	
Resolution range [a] (Å)	50.0–1.65 Å (1.75–1.65 Å)
R_{work} [a]	16.5% (20.0%)
R_{free} [a]	17.4% (19.6%)
Model statistics	
R.m.s. deviations from ideal values	
Bond lengths (Å)	0.028 Å
Bond angle (deg)	2.1°
Mean *B*-factor (Å^2)	16.9Å^2
Ramachandran plot (%)	
Most favored	86.4%
Additional allowed	13.6%
Generously allowed	0
Disallowed	0

[a] Values in parentheses correspond to the reflections observed in the highest resolution shell.
[b] $R_{merge} = \sum_{hkl} \sum_i | I_{hkl} - < I_{hkl} > | / \sum_{hkl} \sum_i I_{hkl}$, where I is the observed intensity and $<I>$ is the averaged intensity for multiple measurement.

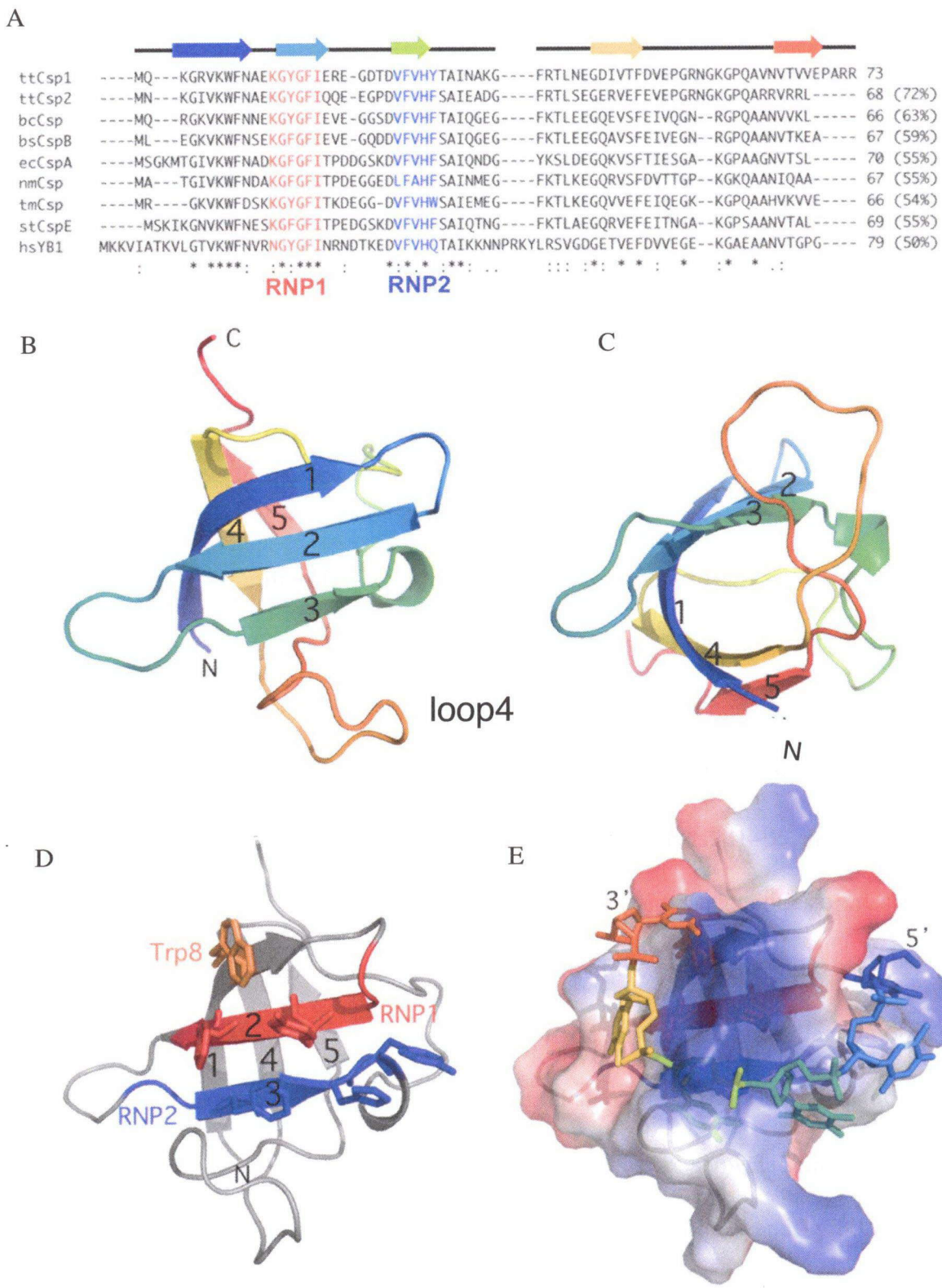
A
ttCsp1 ----MQ---KGRVKWFNAEKGYGFIERE-GDTDVFVHYTAINAKG----FRTLNEGDIVTFDVEPGRNGKGPQAVNVTVVEPARR 73
ttCsp2 ----MN---KGIVKWFNAEKGYGFIQQE-EGPDVFVHFSAIEADG----FRTLSEGERVEFEVEPGRNGKGPQARRVRRL----- 68 (72%)
bcCsp ----MQ---RGKVKWFNNEKGYGFIEVE-GGSDVFVHFTAIQGEG----FKTLEEGQEVSFEIVQGN--RGPQAANVVKL----- 66 (63%)
bsCspB ----ML---EGKVKWFNSEKGFGFIEVE-GQDDVFVHFSAIQGEG----FKTLEEGQAVSFEIVEGN--RGPQAANVTKEA---- 67 (59%)
ecCspA ----MSGKMTGIVKWFNADKGFGFITPDDGSKDVFVHFSAIQNDG----YKSLDEGQKVSFTIESGA--KGPAAGNVTSL----- 70 (55%)
nmCsp ----MA---TGIVKWFNDAKGFGFITPDEGGEDLFAHFSAINMEG----FKTLKEGQRVSFDVTTGP--KGKQAANIQAA----- 67 (55%)
tmCsp ----MR----GKVKWFDSKKGYGFITKDEGG-DVFVHWSAIEMEG----FKTLKEGQVVEFEIQEGK--KGPQAAHVKVVE---- 66 (54%)
stCspE -----MSKIKGNVKWFNESKGFGFITPEDGSKDVFVHFSAIQTNG----FKTLAEGQRVEFEITNGA--KGPSAANVTAL----- 69 (55%)
hsYB1 MKKVIATKVLGTVKWFNVRNGYGFINRNDTKEDVFVHQTAIKKNNPRKYLRSVGDGETVEFDVVEGE--KGAEAANVTGPG---- 79 (50%)
RNP1
RNP2
B
C
1
2
3
4
5
N
loop4
C
2
3
1
4
5
N
D
Trp8
RNP1
2
1
4
5
3
RNP2
N
E
3'
5'

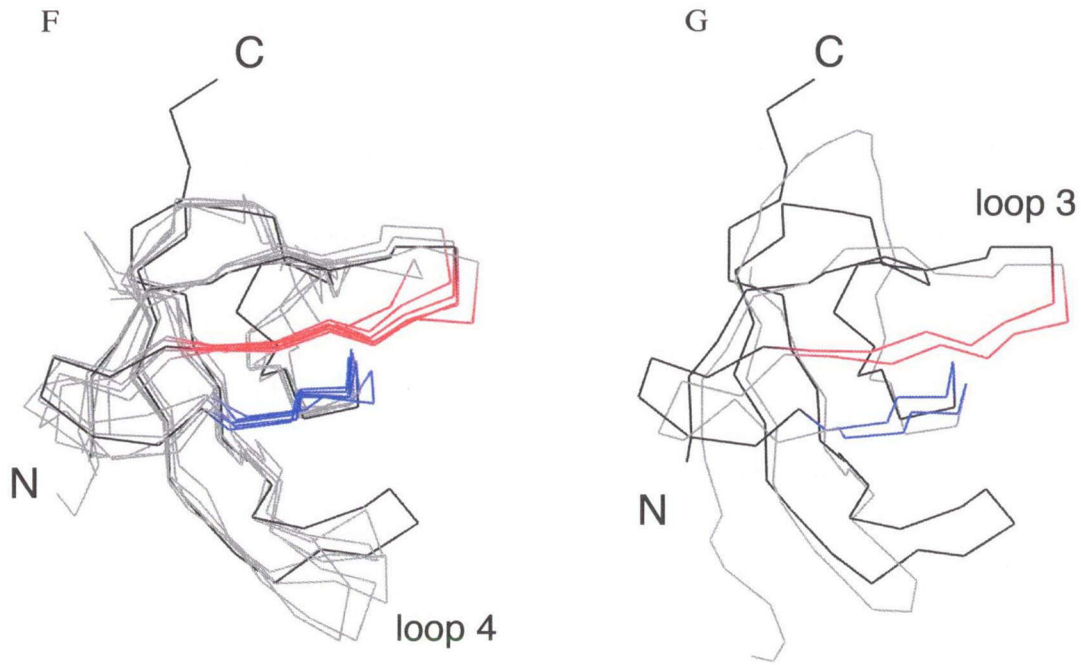

Figure 5-1. Overall structure of *tt*Csp1 and sequence alignment of Csps

(A) Sequence alignment of 8 Csps and the CSD of hsYB1 using the ClustalW2 program (EBI web server: http://www.ebi.ac.jk/tools/clustalw2). Identical and homologous residues are marked with asterisks and colons, respectively. The RNP1 and RNP2 motifs are designated by red and blue characters, respectively. The β-strands, β1–β5, are indicated by arrows. Values in parentheses correspond to the pairwise identities of *tt*Csp1 with Csps or the CSD. (B) The schematic ribbon diagram of the overall structure of *tt*Csp1. The β-strands are shown as curved arrows. (C) The schematic ribbon diagram of *tt*Csp1 seen from the bottom, which emphasizes the barrel structure. (D) The schematic ribbon diagram of the overall structure of *tt*Csp1. The β-strands are shown as curved arrows. Side chains of RNP1 (Tyr15 and Phe17, red), RNP2 (Phe27, His29 and Tyr30, blue), and Trp8 (orange) are depicted in stick form. (E) A model of the *tt*Csp1–dT6 complex. *tt*Csp1 is shown along with its electron potential map on a scale from negative

(red) to positive (blue) in the same orientation as in Figure 5-1D. (F) Cα trace of superposed *tt*Csp1 and five cold shock proteins (*bc*Csp, *bs*CspB, *tm*Csp, *ec*CspA and *mn*Csp) from the same view as in Figure 5-1B. (G) Cα trace of superposed *tt*Csp1 and *hs*YB1 from the same view as in Figure 5-1B. The structure of *tt*Csp1 and other cold shock proteins or *hs*YB1 were shown in black and gray, respectively. The RNP1 and RNP2 motifs are colored red and blue, respectively.

5-3 Comparison of surface charges of Csps

To determine the distinguishing structural features between cold-inducible (group a in Figure 5-2) and non-cold-inducible (group b) Csps, I used structure homology modeling to determine the model structures of Csps listed in Table 5-2. The surface charges of these Csps are shown in Figure 5-2. Examination of these structures reveals there are no obvious differences between the two groups of proteins. Nonetheless, it is interesting to note that in group b, four non-cold-induced Csps, including *tt*Csp1, possess a structurally conserved positively charged region. The amino acid residues in this region in *tt*Csp1, *ec*CspD, *ec*CspH, and *bb*CspD are Arg73, Lys43, Arg13, and Lys57, respectively. Hence, this region of the protein displays a similar surface charge distribution even though the amino acid sequence is not well conserved. Because this positively charged region is discrete from the nucleotide-binding site, it might be important in controlling the stabilities of complex between Csps and nucleotides or other target factors.

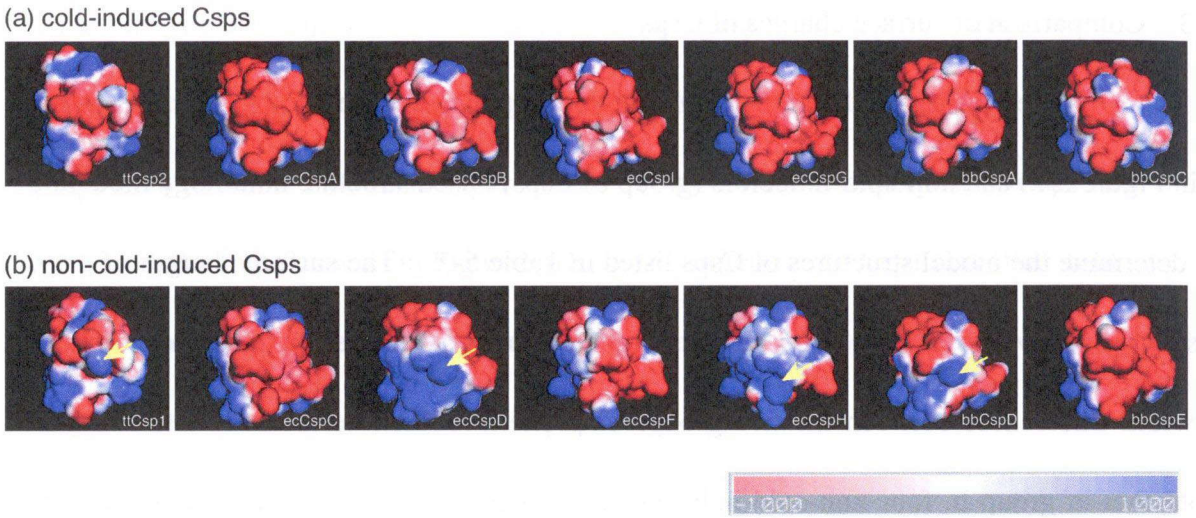

Figure 5-2. Comparison of surface charges between *tt*Csp1 and other Csps

Surface charges of (a) cold-inducible Csps and (b) non-cold-inducible Csps are shown using the APBS1.3 program. Electrostatic potential is indicated as red (negative) or blue (positive). Among the group in (b), 4 Csps (*tt*Csp1, *ec*CspD, *ec*CspH, and *bb*CspD) have a conserved positively charged region indicated by yellow arrows.

Table 5-2. Candidates for surface electrical charge comparison

(a) Cold-inducible group		PDB code
E. coli	CspA	1MJC
E. coli	CspB	model
E. coli	CspE	model
E. coli	CspG	model
E. coli	CspI	model
B. subtilis	CspB	2ES2
B. subtilis	CspC	model
B. bronchiseptica	CspA	model
B. bronchiseptica	CspB	model
B. bronchiseptica	CspC	model
T. thermophilus	Csp2	model
(b) Non-cold-inducible group		
E. coli	CspC	model
E. coli	CspD*	model
E. coli	CspF	model
E. coli	CspH*	model
B. bronchiseptica	CspD*	model
B. bronchiseptica	CspE	model
T. thermophilus	Csp1*	3A0J: this study

* These Csps have positive regions.

6 Oligonucleotide-binding and recognition of *tt*Csp1

6-1. DNA-binding activity of *tt*Csp1

In order to confirm the formation of complex with *tt*Csp1 and DNA, analytical size-exclusion chromatography was carried out using 7-mer oligo-dT (dT7) and 31-mer oligo-dT (dT31) (Figure 6-1). In the absence of DNA, *tt*Csp1 eluted at the volume corresponding to an apparent molecular weight of 7,300, judging from the calibration curve. As the calculated molecular weight of *tt*Csp1 is 8,200, *tt*Csp1 was considered to exist as a monomer in solution. In the present of dT7 (M.w. 2,100) or dT31 (M.w. 9,400), the elution peaks were shifted to elution volumes corresponding to around 15,700 and 48,000, respectively. Since oligonucleotids behave on gel-filtration column as larger molecules than globular proteins, these values roughly corresponded to the complex with one *tt*Cps1 and one dT7 molecules (calculated M.w. 9,400), and with five *tt*Csp1 and one dT31 molecules (calculated M.w. 45,900). The ratio A_{260}/A_{280} of the elution peak in the present of dT7 was 1.05, which coincides with the calculated ratio A_{260}/A_{280}, 0.97, of the 1:1 complex with *tt*Csp1 (ε_{260}, 0.82 x 10^4 $M^{-1}cm^{-1}$; ε_{280}, 1.35x10^4 $M^{-1}cm^{-1}$) and dT7 (ε_{260}, 3.42 x 10^4 $M^{-1}cm^{-1}$; ε_{280}, 2.22 x 10^4 $M^{-1}cm^{-1}$). The ratio A_{260}/A_{280} of the elution peak in the present of dT31 was 1.13, which also coincides with the calculated ratio A_{260}/A_{280}, 1.14, of the complex with the 5:1 complex with *tt*Csp1 and dT31 (ε_{260}, 16.15x10^4; ε_{280}, 10.92x10^4). These results indicate that *tt*Csp1 strongly binds to ssDNA.

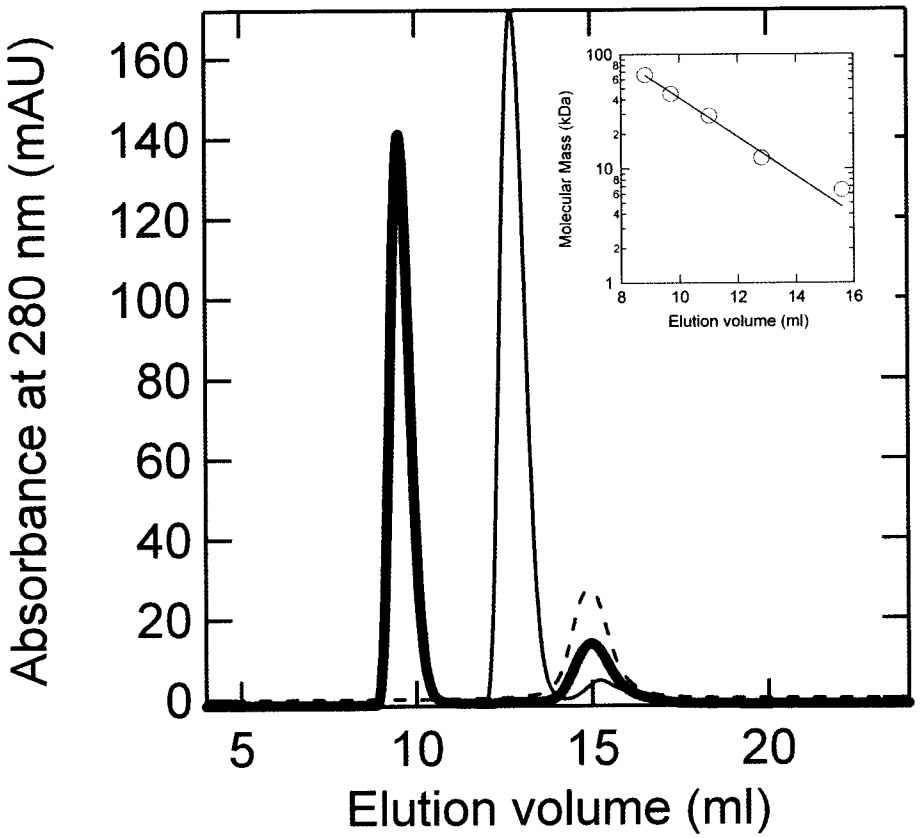

Figure 6-1. Size-exclusion chromatography of *tt*Csp1.

The dashed line, thin line and thick line represent elution profiles in the absence and the presence of dT7 and dT31, respectively. The inset shows the calibration curve. Standard proteins were used: albumin from bovine serum, 66 kDa; albumin from chicken egg, 45 kDa; carbonic anhydrase from bovine erythrocytes, 29 kDa; cytochrome c from horse heart, 12.4 kDa; aprotinin from bovine lung, 6.5 kDa.

6-2. Affinity for various oligonucleotides

As mentioned above, the structures of the β-barrel containing RNP1 and RNP2 motifs are highly conserved in cold shock proteins including *tt*Csp1. The crystal structures of *bs*CspB complexed with ssDNA (Max, K. E. *et al.*, 2006) and bcCsp complexed with ssDNA (Max, K. E. *et al.*, 2007) were reported. In these structures, not only the aromatic residues from RNP1 and RNP2 motifs, but also Trp8 near RNP1 motif form stacks with

nucleobases. This tryptophan residue is conserved in almost all cold shock proteins. *tt*Csp1 also has the Trp8, which is the only tryptophan residue in the sequence of *tt*Csp1. In the crystal structure of *tt*Csp1, Trp8 is solvent-exposed (see Figure 5-1D).

In order to analyze the binding affinity for various sequences and the secondary structures of oligonucleotides (Table 6-1, Figure 6-2), the intrinsic fluorescence from Trp8 was utilized. As shown in Figure 6-3A, the fluorescence spectrum of *tt*Csp1 had an optimum intensity around 340 nm and the fluorescence intensity was almost quenched on binding of oligonucleotide, similar to the case for *bc*Csp (Max, K. E. *et al.*, 2007). These phenomena coincide with the structural feature of Trp8. The dissociation constants K_d for oligonucleotides were calculated from the decrease of fluorescence intensity to an increase of oligonucelotides (Table 6-2). Because the K_d value for dT7 was more than ten times as small as that for dA7, *tt*Csp1 has a binding preference for polypyrimidiens over polypurines. The K_d value for dT31 was the smallest among the oligonucelotide used, indicating more than two molecules of *tt*Csp1 simultaneously can bind to dT31. From the result of analytical size exclusion chromatography, about five molecules of *tt*Csp1 could bind to dT31, suggesting the binding site of *tt*Csp1 accommodates about six nucleotides. It should be noted that The K_d value for stem3dT7 is the smallest among the olioconuleotides containg dT7 region. These result shows not only that *tt*Csp1 bind to polypyrimidiens more strongly than polypurines, but also that the binding affinity of *tt*Csp1 for oligonucletide is influenced by the secondary stracture around dT7 region. Specifically, *tt*Csp1 might preferentially bind to unconstrained nucleotides. Furthermore, stem3dT7 bound to *tt*Csp1 more tightly than stem5dT7. This suggests that the location of the stem is

important for the binding and function of *tt*Csp1.

Next, K_d values of the oligo-ribonucleotide containing the U7 region with or without secondary structure were examined (Figure 6-3D and Table 6-2). Like ssDNA, the K_d value of stem3U7 was least among the other single-stranded RNAs (ssRNAs). Furthermore, loopU7 bound to *tt*Csp1 more weakly than the other ssRNAs. It should be noted that *tt*Csp1 bound to stem3U7 more tightly than to linearU7. This suggests that U-rich sequences possessing stem structures on their upstream regions might be the targets of *tt*Csp1.

Table 6-1. The sequences of ssDNA and ssRNA ligands.

Name	Sequence	Length
dT7	TTTTTTT	7
dA7	AAAAAAA	7
loopdT7	CCgggCgCgCgCTTTTTTTgCgCgCgCCCgg	31
loopdT7dA4	AAgggCgCgCgCTTTTTTTgCgCgCgCCCAA	31
loopdT1	gggCgCgCgCTTTTTTTTTTTgCgCgCgCCC	31
stem5dT7	TTTTTTTgggCgCgCgCAAAAgCgCgCgCCC	31
stem3dT7	gggCgCgCgCAAAAgCgCgCgCCCTTTTTTT	31
dT31	TTTTTTTTTTTTTTTTTTTTTTTTTTTTTTT	31
dA31	AAAAAAAAAAAAAAAAAAAAAAAAAAAAAAA	31
U7	UUUUUUU	7
loopU7	CCgggCgCgCgCUUUUUUUgCgCgCgCCCgg	31
stem5U7	UUUUUUUgggCgCgCgCAAAAgCgCgCgCCC	31
stem3U7	gggCgCgCgCAAAAgCgCgCgCCCUUUUUUUU	31

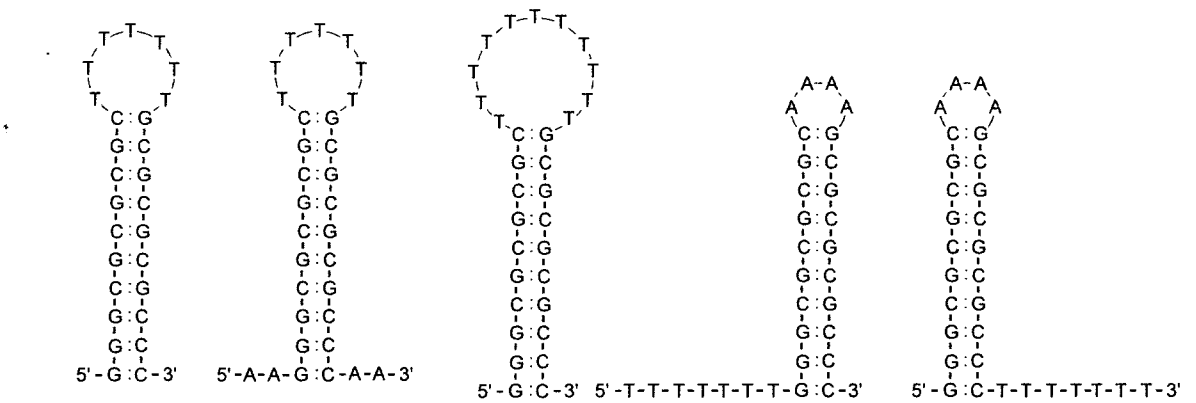

loopdT7 loopdT7dA4 loopdT11 stem5dT7 stem3dT7

Figure 6-2. The predicted secondary structures of ssDNA
The ligands of loopdT7, loopdT7dA4, loopdT11, stem5dT7 and stem3dT7 were prepared by incubating at 95°C for 2 min and 60°C for 10 min to form the secondary structures.

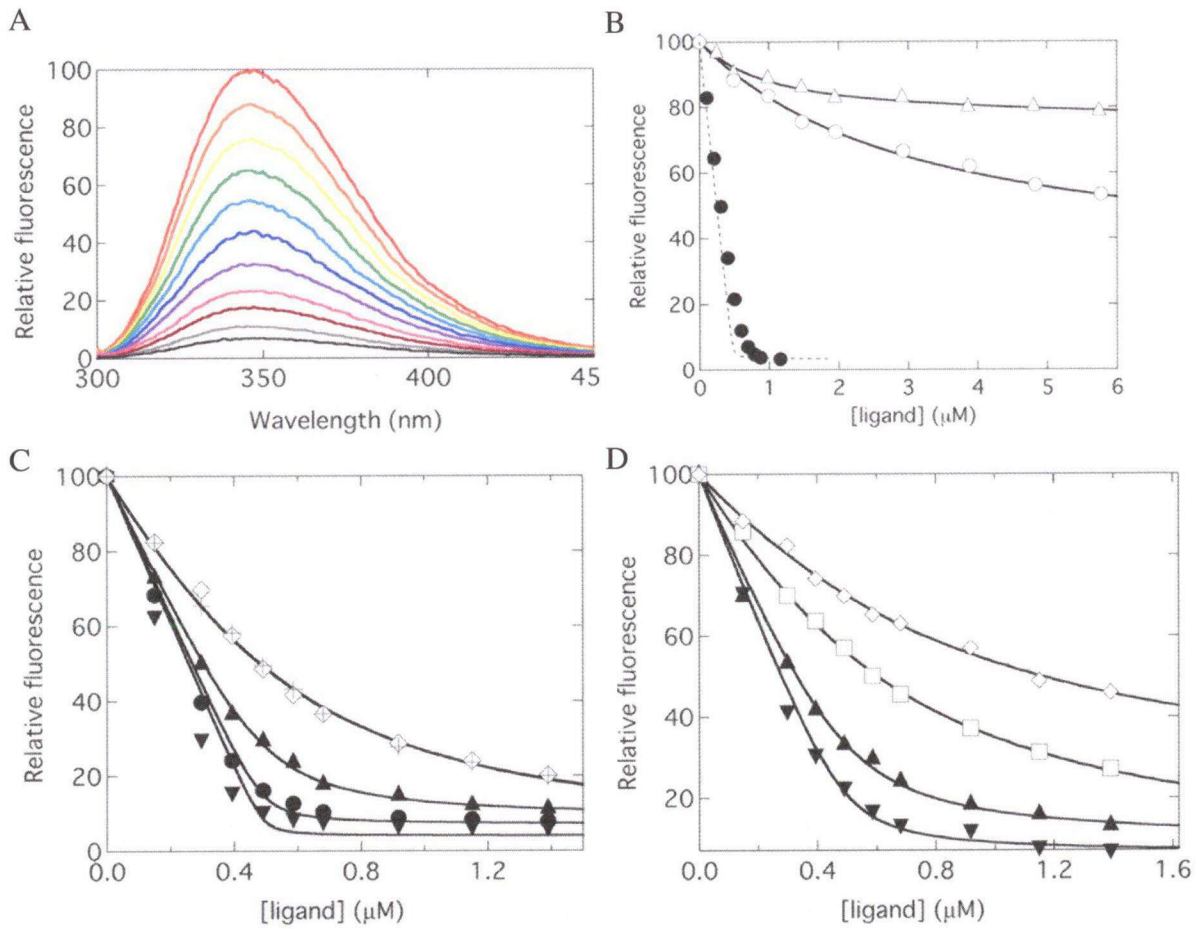

Figure 6-3 Binding of *tt*Csp1 to nucleic acids

(A) Fluorescence spectra of *tt*Csp1 in the presence of various concentrations of dT7: 0 (red), 0.1 (orange), 0.2 (yellow), 0.3 (light green), 0.4 (cyan), 0.5 (blue), 0.6 (purple), 0.7 (pink), 0.8 (brown), 0.9 (grey), and 1.0 μM (black). (B) Changes in fluorescence intensity at 350 nm: dT7 (filled circles), dA7 (open circles), and dT4 (open triangles). The dashed line was calculated from the K_d, which was determined by the competition experiment. (C) Change in fluorescence intensity at 350 nm in the presence of 10 μM dT4 as a competitor: dT7 (filled circles), loopdT7 (open diamonds), loopdT11 (crosses), stem5dT7 (filled triangles), and stem3dT7 (filled inverse triangles). (D) Change in fluorescence intensity at 350 nm in the presence of 10 μM dT4 as a competitor: U7 (open squares), loopU7 (open diamonds), stem5U7 (filled triangles), and stem3U7 (filled inverse triangles).

Table 6-2. The dissociation constants of *tt*Csp1 for ssDNA and ssRNA ligands

ligand	length	K_d (nM)	method
dT4	4	2800	direct
dA7	4	590	direct
dT7	7	0.91	competition
loopdT7	31	57	competition
loopdT11	31	55	competition
stem5dT7	31	6.9	competition
stem3dT7	31	0.27	competition
U7	7	80	competition
loopU7	31	130	competition
stem5U7	31	11	competition
stem3U7	31	3.6	competition

The description of "direct" in the method column represents the fluorescence titration of *tt*Csp1 with a ligand, and "competition" represents the titration in the presence of dT4 (see *Materials and Methods* for details).

[a] The dissociation constant for dT31 was undetectable by using this method, because of the too strong affinity above the detection limit of the fluorescence spectrophotomerter.

7. Effect of *tt*Csp1 on RNase activity

Now I know that *tt*Csp1 can work both on transcriptional and translational processes. Some of gene expressions under the cold condition might be conrtolled by changing the amounts of mRNAs. To test the hypothesis that *tt*Csp1 helps RNase degrade mRNAs, I measured exonuclease activity of a RNase in the absence and presence of *tt*Csp1 *in vitro*. The employed RNase was TTHA0252 of *T. thermophilus* HB8, which has single-strand-specific 5'-3' exonuclease activity (Ishikawa, H. *et al.*, 2006). The RNA substrate employed was 50-mer hairpin RNA (h-RNA) as shown in Figure 7-1. When TTHA0252 was reacted with h-RNA, two main products were observed on a gel (Figure 7-2). Among these two bands, the upper band (P1) was likely to correspond to the fragment degraded to the bottom of the stem, since the exonuclease activity of TTHA0252 was specific to single-stranded RNA and inhibited by the double-stranded region. The lower band (P2) was a single nucleotide, which was produced by complete digestion of the substrate by the enzyme. By the addition of *tt*Csp1, there was no change in the degradation rate of the full-length substrate (S), but the amount of P1 decreased and the amount of P2 increased (Figure 7-3). These results suggest that *tt*Csp1 did not affect the nuclease activity of RNase, but melted the stem structure of the substrate to help RNase to proceed through the stem-loop. The effect of *tt*Csp1 on RNA degradation dependent on melting of the secondary structure may be important for adaptation to stress conditions.

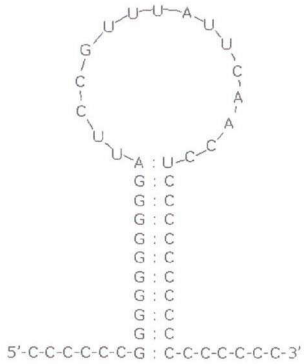

Figure 7-1. Sequence and predicted secondary structure of h-RNA.

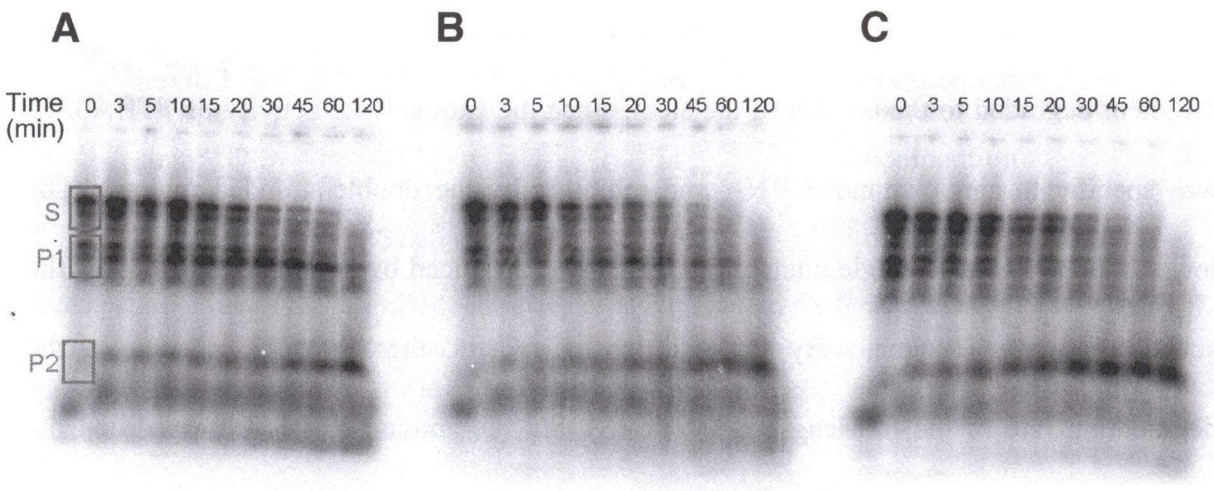

Figure 7-2. Degradation of h-RNA with 0 μM (A), 0.2 μM (B) and 23 μM (C) *tt*Csp1.

The substrate h-RNA was radiolabeled at 3'-end. The assay was performed at 37°C.

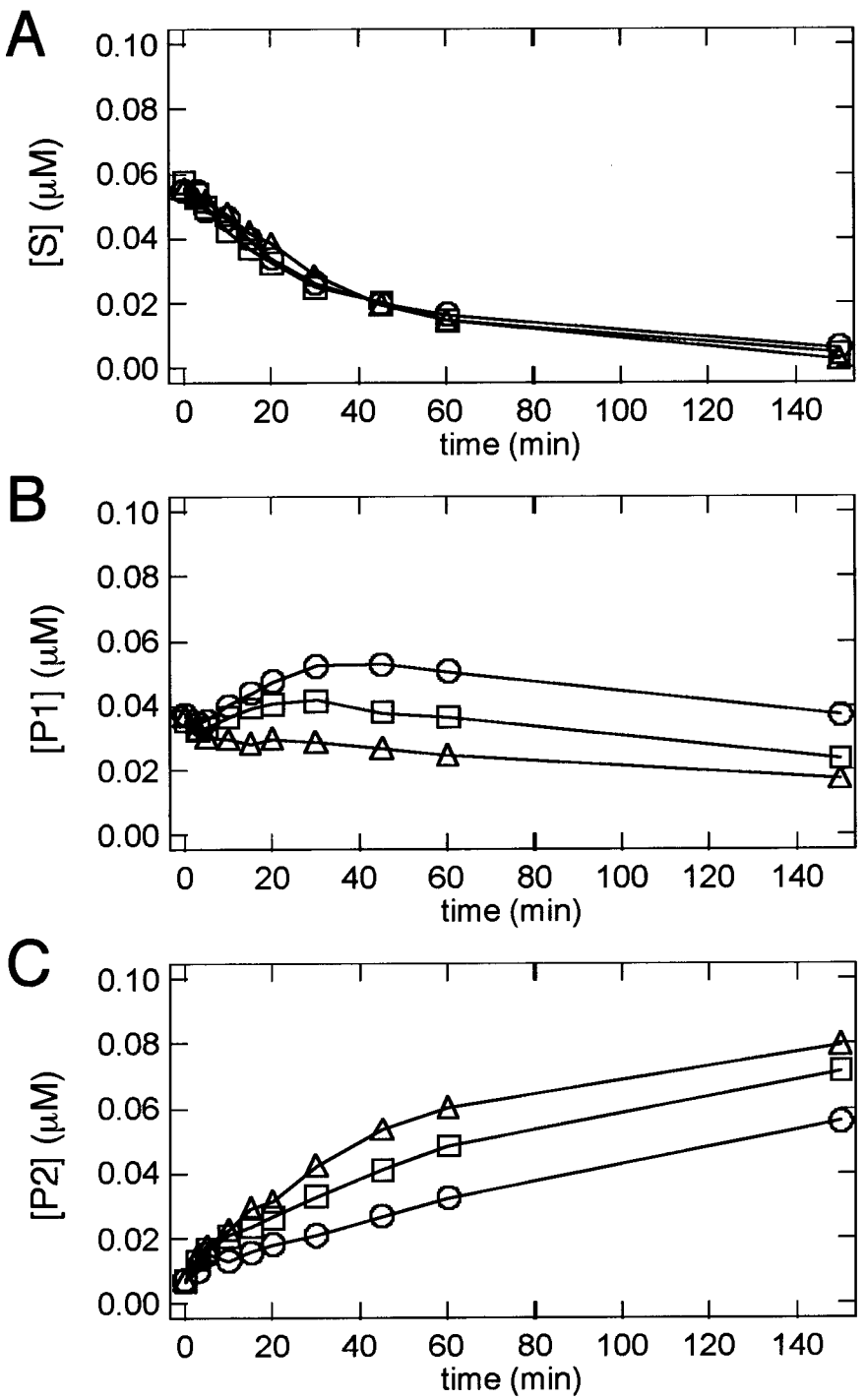

Figure 7-3. Effect of *tt*Csp1 on RNase activity to hairpin RNA.

The amounts of band S (A), P1 (B) and P2 (C) in the presence of 0 μM (circles), 0.2 μM (squares) and 23 μM (triangles) *tt*Csp1were plotted against reaction time.

8. Working mechanism of *tt*Csp1 under optimal and cold condition

Under optimal growth conditions there were no differences in the growth curves (Figure 1-1) and gene expression profiles of wild-type and Δ*ttcsp1* cells. These results indicate *tt*Csp1 does not significantly contribute to the transcriptional regulation at the physiological temperature (70°C). However, it is reported that single-gene disruptants of *ttcsp1* exhibit similar growth patterns to wild-type cells and Δ*ttcsp2* was not lethal at 45°C. Moreover, the double disruptant (*ttcsp1* and *ttcsp2*) exhibited a lower growth rate by comparison to the other three strains (wild-type and disruptants of *ttcsp1* or *ttcsp2* strains) at 45°C. These results suggest that *tt*Csp1 can compensate for the functions of *tt*Csp2 at low temperature. There was a time lag between the mRNA (30 s) and protein expression (10 min) of *tt*Csp2 after a temperature drop (Mega, R. *et al.*, 2010). In addition, the microarray data show that there were up-regulated genes at 45°C in only wild-type cells. These results suggest that *tt*Csp1 regulates gene expression by acting as a transcriptional anti-terminator until *tt*Csp2 is expressed at low temperature. Indeed, constitutively expressed Csps, *ec*CspC and *ec*CspE, have been shown to operate as transcriptional anti-terminators in *E. coli* (Bae, W. *et al.*, 2000, Phadtare, S. *et al.*, 2007). It is, *tt*Csp1 can work also as a transcriptional regulator under the cold condition. The influences of *tt*Csp1 on RNase activities support the existence of the transcriptional regulation system which *tt*Csp1 is involved in.

From the comparison of results from microarray and proteome, about more than half of influenced proteins by *ttcsp1* deletion, significant changes of gene expression were

detected only in translational level (see chapter 4 groupB). In addition, without *tt*Csp1, any changes of transcriptional levels were not detected under the optimal growth condition although the amount of some proteins (translational level) were increased or decreaced. *In vitro* experiments revealed that *tt*Csp1 binds to single-stranded oligonucleotides with low specificity to bases and secondary structures of oligonucleotides, although these results were based on limited variation of nucleotides. Nevertheless, it is possible to suppose that the states of nucleotide affect binding to *tt*Csp1. From the obtained results, I focused on the working mechanism of *tt*Csp1 in translational level under the optimal condition in this section. I propose the following models.

8-1 Translation of some proteins are inhibitted by *tt*Csp1.

As shown in Figure 8-1A, where translation is inhibited by *tt*Csp1, the mRNA has a U-rich region and the 5' region is predicted to form a secondary structure. *tt*Csp1 binds to the U-rich region and a large stem and loop are formed (Figure 8-1B). Furthermore, *tt*Csp1 interacts with the sugar-phosphate backbone of the stem, stabilizing the complex (Figure 8-1C). This stable complex inhibits translation from the mRNA. In the absence of *tt*Csp1, no large stem and loop are formed, although, two small stems and loops that do not inhibit the translation of the mRNA are generated (Figure 8-1D).

8-2 *tt*Csp1 stimulates the translation of some proteins.

Where translation is stimulated by *tt*Csp1, the mRNA has a U-rich region that is predicted to form a secondary structure (Figure 8-2A). *tt*Csp1 binds to the U-rich region

and prevents it from forming a secondary structure (Figure 8-2B). In the absence of *tt*Csp1, a large stem and loop are formed where translation arrest readily occurs (Figure 8-2C). This is a very sophisticated control system because mRNA conformations are in flux and easily altered by intracellular and/or extracellular environmental conditions; thus, *tt*Csp1 can function as both an enhancer and inhibitor of translation.

In conclusion, through a combination of transcriptome and proteome analyses, I have demonstrated that the control systems of transcription and translation are even more complex than originally thought, even in prokaryotes. I suggest that non-cold-inducible Csps are candidates for translational controllers. Some, but not all, non-cold-inducible Csps may play a role in monitoring stress and fine tuning cellular processes in order to adapt to changing environmental conditions. In addition to temperature, the structure of mRNA can be influenced by pH, osmotic pressure and salt concentrations. Thus, I conclude that Csp family proteins may respond to different stress factors by alterations to their nucleotide binding affinities according to the structures of the target nucleotides. Moreover, the electric potential of Csps around the RNP motifs may be an important factor in determining their distinct functions. Consequently, the control mechanism for Csps is extremely flexible. The flexibility of the function is important for the fine tuning against subtle cahnges of conditions.

A

781 -

CCCCAGGAGTTCGCCCTCAAGGTCCAGGTGGAGGGGGAGGCCCTCAGGGAGGCGGTGCGC

CGGGTGAGCGTCCTCTCCGACCGGCAGAACCACCGGGTGGACCTCCTTTTGGAGGAAGGC

CGGATCCTCCTCTCCGCCGAGGGGGACTACGGCAAGGGGCAGGAGGAGGTGCCCGCCCAG

- 960

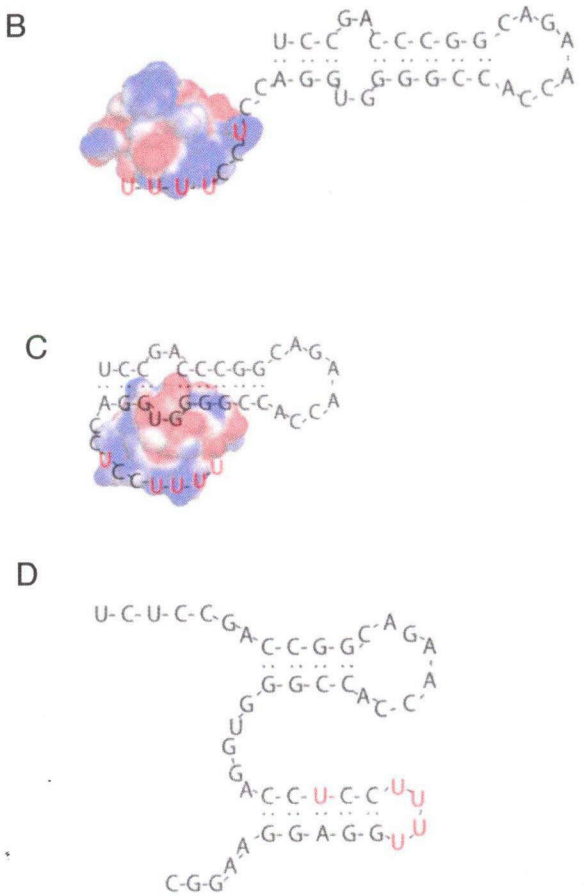

Figure 8-1. The gene down-regulated in Δ*ttcsp1*, TTHA0001

(A) Nucleotide sequence of TTHA0001. The dT(U)-rich region is indicated by a box. Underline indicates the region predicted to form the secondary structure. The secondary structure of the dT(U)-rich box was predicted using vsfold5 (Dawson, W. *et al.*, 2007) (B) Binding of *tt*Csp1 to the dT-rich region and formation of a large stem and loop. (C) Stabilization of the *tt*Csp1 complex with the target region. (D) Formation of 2 small stems and loops that do not inhibit the translation of the mRNA in the absence of *tt*Csp1.

A

421 –

GAGGAGCTCCGCCAGCGCTACGCCGAGCTCGTCCCCGTGGAGCGGGAGGCCCAGGAAAAG

GACCACCTCTTCGTCCGCACCGAGGAGGGGGCGGAGTTCCCCATTGACCTCGCTAAAGCC

CTTCCCCACGTGCGGGAGGCCCTCCTCGGCAAGAAGGCGGGGGACGTGGTCATGGTCCCC

- 600

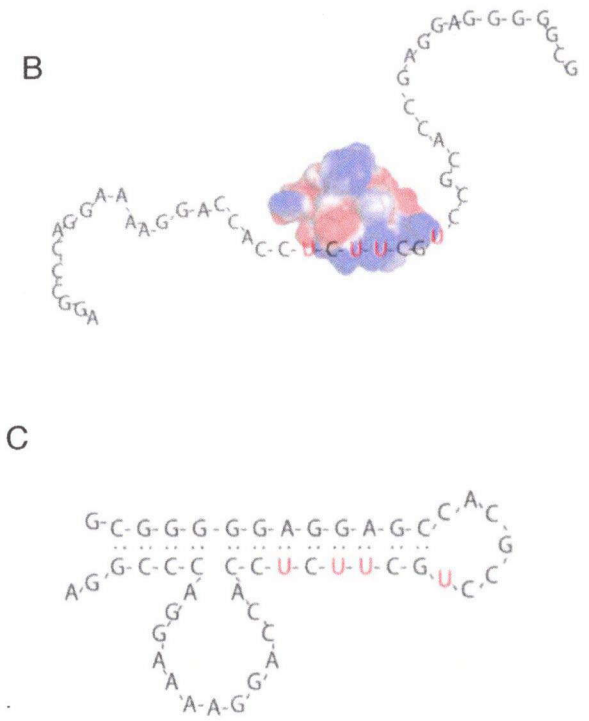

Figure 8-2. The gene up-regulated in Δ*ttcsp1*, TTHA0614

(A) Nucleotide sequence of TTHA0614. The dT(U)-rich region is indicated by a box. Underline indicates the region predicted to form the secondary structure. (B) Binding of *tt*Csp1 to the dT(U)-rich region. (C) Formation of a large stem and loop in the absence of *tt*Csp1.

REFERENCES

Adachi, S., Oguchi, T., Tanida, H., Park, S. Y., Shimizu, H., Miyatake, H., Kamiya, N., Shiro, Y., Inoue, Y., Ueki, T., and Iizuka, T. (2001) The RIKEN structural biology beamline II (BL44B2) at the SPring-8. *Nucl. Instrum. Meth.* **A467**, 711-714.

Bae, W., Xia, B., Inouye, M., and Severinov, K. (2000) *Escherichia coli* CspA-family RNA chaperones are transcription antiterminators. *Proc. Natl. Acad. Sci. USA* **97**, 7784-7789.

Brandi, A., Pietroni, P., Gualerzi, C. O., and Pon, C. L. (1996) Post-transcriptional regulation of CspA expression in *Escherichia coli*. *Mol. Microbiol.* **19**, 231-240.

Bruenger, A. T., Adams, P. D., Clore, G. M., DeLano, W. L., Gros, P., Grosse-Kunstleve, R. W., Jiang, J. S., Kuszewski, J., Nilges, M., Pannu, N. S., Read, R. J., Rice, L. M., Simonson, T., and Warren, G. L. (1998) Crystallography & NMR system: A new software suite for macromolecular structure determination. *Acta Cryst.* **D54**, 905-921.

Budde, I., Steil, L., Scharf, C., Voelker, U., and Bremer, E. (2006) Adaptation of *Bacillus subtilis* to growth at low temperature: a combined transcriptomic and proteomic appraisal. *Microbiology* **152**, 831-853.

Burd, C. G., and Dreyfuss, G. (1994) Conserved structures and diversity of functions of RNA-binding proteins. *Science* **265**, 615-621.

Candiano, G., Bruschi, M., Musante, L., Santucci, L., Ghiggeri, G. M., Carnemolla, B., Orecchia, P., Zardi, L., and Righetti, P. G. (2004) Blue silver: A very sensitive colloidal Coomassie G-250 staining for proteome analysis. *Electrophoresis* **25**, 1327-1333.

Collaborative Computational Project N. (1994) The CCP4 suite: programs for protein crystallography. *Acta Cryst.* **D50**, 760-763.

Dawson, W., Fujiwara, K., Kawai, G., Futamura, Y., and Yamamoto, K. (2007) A method for finding optimal RNA secondary structures using a new entropy model (vsfold). *Nucleosides Nucleotides Nucleic Acids* **25**, 171-189.

DeLano, W. L. (2002) Unraveling hot spots in binding interfaces: progress and challenges. *Curr. Opin. Struct. Biol.* **12**, 14-20.

Delbruck, H., Mueller, U., Perl, D., Schmid, F. X., and Heinemann, U. (2001) Crystal structures of mutant forms of the *Bacillus caldolyticus* cold shock protein differing in thermal stability. *J. Mol. Biol.* **313**, 359-369.

Eftink, M. R. (1997) Fluorescence methods for studying equilibrium macromolecule-ligand interactions. *Methods Enzymol.* **278**, 221-257.

El-Sharoud, W. M., and Graumann, P. L. (2007) Cold shock proteins aid coupling of transcription and translation in bacteria. *Sci. Prog.* **90**, 15-27.

Ermolenko, D. N., and Makhatadze, G. I. (2002) Bacterial cold-shock proteins. *Cell. Mol. Life Sci.* **59**, 1902-1913.

Feng, Y., Huang, H. Liao, J., and Cohen, S. N. (2001) *Escherichia coli* Poly(A)-binding Proteins That Interact with Components of Degradosomes or Impede RNA Decay Mediated by Polynucleotide Phosphorylase and RNase E. *J. Biol. Chem.* 276, 31651-31656.

Feng, W., Tejero, R., Zimmerman, D. E., Inouye, M., and Montelione, G. T. (1998) Solution NMR structure and backbone dynamics of the major cold-shock protein (CspA) from *Escherichia coli*: evidence for conformational dynamics in the single-stranded RNA-binding site. *Biochemistry* **37**, 10881-10896.

Fersht, A. R. (1999) *Structure and mechanism in protein science: a guide to enzyme catalysis and protein folding.* Chapter 6 (p.191-215), W. H. Freeman and Company, New York

Goldenberg, D., Azar, I., and Oppenheim, A. B. (1996) Differential mRNA stability of the *cspA* gene in the cold-shock response of *Escherichia coli*. *Mol. Microbiol.* **19**, 241-248.

Goldstein, J., Pollitt, N. S., and Inouye, M. (1990) Major cold shock protein of *Escherichia coli*. *Proc. Natl. Acad. Sci. USA* **87**, 283-287.

Gualerzi, C. O., Giuliodori, A. M., and Pon, C. L. (2003) Transcriptional and post-transcriptional control of cold-shock genes. *J. Mol. Biol.* **331**, 527-539.

Hashimoto, Y., Yano, T., Kuramitsu, S., and Kagamiyama, H. (2001) Disruption of *Thermus thermophilus* genes by homologous recombination using a thermostable kanamycin-resistant marker. *FEBS Lett.* **503**, 231-234.

Horn, G., Hofweber, R., Kremer, W., and Kalbitzer, H. R. (2008) Structure and function of bacterial cold shock proteins. *Cell. Mol. Life Sci.* **64**, 1457-1470.

Hoseki, J., Yano, T., Koyama, Y., Kuramitsu, S., and Kagamiyama, H. (1999) Directed evolution of thermostable kanamycin-resistance gene: a convenient selection marker for *Thermus thermophilus*. *J. Biochem.* **126**, 951-956.

Ishikawa, H., Nakagawa, N., Kuramitsu, S., and Masui, R. (2006) Crystal structure of TTHA0252 from Thermus thermophilus HB8, a RNA degradation protein of the metallo-beta-lactamase superfamily. *J. Biochem.* **140**, 535-542.

Johnston, D., Tavano, C., Wicker, S., and Trun, N. (2006) Specificity of DNA binding and dimerization by CspE from *Escherichia coli*. *J. Biol. Chem.* **281**, 40208-40215.

Jones, P. G., VanBogelen, R. A., and Neidhardt, F. C. (1987) Induction of proteins in response to low temperature in *Escherichia coli*. *J. Bacteriol.* **169**, 2092-2095.

Kaan, T., Homuth, G., Maeder, U., Bandow, J., and Schweder, T. (2002) Genome-wide transcriptional profiling of the *Bacillus subtilis* cold-shock response. *Microbiology* **148**, 3441-3455.

Kabasch, W. (1976) A solution for the best rotation to relate two sets of vectors. *Acta Cryst.* **A32**, 922-923.

Kloks, C. P., Spronk, C. A., Lasonder, E., Hoffmann, A., Vuister, G. W., Grzesiek, S., and Hilbers, C. W. (2002) The solution structure and DNA-binding properties of the cold-shock domain of the human Y-box protein YB-1. *J. Mol. Biol.* **316**, 317-326.

Kremer, W., Schuler, B., Harrieder, S., Geyer, M., Gronwald, W., Welker, C., Jaenicke, R., and Kalbitzer, H. R. (2001) Solution NMR structure of the cold-shock protein from the hyperthermophilic bacterium *Thermotoga maritima*. *Eur. J. Biochem.* **268**, 2527-2539.

Kuramitsu, S., Hiromi, K., Hayashi, H., Morino, Y., and Kagamiyama, H. (1990) Pre-steady-state kinetics of *Escherichia coli* aspartate aminotransferase catalyzed reactions and thermodynamic aspects of its substrate specificity. *Biochemistry* **29**, 5469-5476.

Ladomery, M. (1997) Multifunctional proteins suggest connections between transcriptional and post-translational processes. *BioEssays* **19**, 903-909.

Laskowski, R. A., MacArthur, M. W., Moss, D. S., and Thornton, J. M. (1993) PROCHECK: A program to check the stereochemical quality of protein structures. *J. Appl. Cryst.* **26**, 283-291.

Lee, S. J., Xie, A., Jiang, W., Etchegaray, J. P., Jones, P. G., and Inouye, M. (1994) Family of the major cold-shock protein, CspA (CS7.4), of *Escherichia coli*, whose members show a high sequence similarity with the eukaryotic Y-box binding proteins. *Mol. Microbiol.* **11**, 833-839.

Looman, A. C., Bodlaender, J., Comstock, L. J., Eaton, D., Jhurani, P., de Boer, H. A., and van Knippenberg, P. H. (1987) Influence of the codon following the AUG initiation codon on the expression of a modified *lacZ* gene in *Escherichia coli*. *EMBO J.* **6**, 2489-2492.

Max, K. E. A., Zeeb, M., Bienert, R., Balbach, J., and Heinemann, U. (2006) T-rich DNA

single strands bind to a preformed site on the bacterial cold shock protein Bs-CspB. *J. Mol. Biol.* **360**, 702-714.

Max, K. E. A., Zeeb, M., Bienert, R., Balbach, J., and Heinemann, U. (2007) Common mode of DNA binding to cold shock domains. Crystal structure of hexathymidine bound to the domain-swapped form of a major cold shock protein from *Bacillus caldolyticus*. *FEBS J.* **274**, 1265-1279.

McRee, D. E. (1999) XtalView /Xfit–A versatile program for manipulating atomic coordinates and electron density. *J. Struct. Biol.* **125**, 156-165.

Mega, R., Manzoku, M., Shinkai, A., Nakagawa, N., Kuramitsu, S., and Masui, R. (2010) Very rapid induction of a cold shock protein by temperature downshift in *Thermus thermophilus*. *Biochem. Biophs. Res. Commun.* **399**, 336-340.

Morgan, H. P., Wear, M. A., McNae, I., Gallagher, M. P., and Walkinshaw, M. D. (2009) Crystallization and X-ray structure of cold-shock protein E from *Salmonella typhimurium*. *Acta Cryst.* ***F*65**, 1240-1245.

Mueller, U., Perl, D., Schmid, F. X., and Heinemann, U. (2000) Thermal stability and atomic-resolution crystal structure of the *Bacillus caldolyticus* cold shock protein. *J. Mol. Biol.* **297**, 975-988.

Murzin, A. Z. (1993) OB(oligonucleotide/oligosaccharide binding)-fold: common structural and functional solution for non-homologous sequences. *EMBO J.* **12**, 861-867.

Nakashima, K., Kanamaru, K., Mizuno, T., and Horikoshi, K. (1996) A novel member of the cspA family of genes that is induced by cold shock in *Escherichia coli*. *J. Bacteriol.* **178**, 2994-2997.

Newkirk, K., Feng, W., Jiang, W., Tejero, R., Emerson, S. D., Inouye, M., and Montelione, G. T. (1994) Solution NMR structure of the major cold shock protein (CspA) from *Escherichia coli*: identification of a binding epitope for DNA. *Proc. Natl. Acad. Sci. USA* **91**,

5114-5118.

Otwinowski, Z., and Minor, W. (1997) Processing of X-ray diffraction data collected in oscillation mode. *Methods Enzymol.* **276**, 307-326.

Perrakis, A., Morris, R., and Lamzin, V. S. (1999) Automated protein model building combined with iterative structure refinement. *Nat. Struct. Biol.* **6**, 458-463.

Perrakis, A., Harkiolaki, M., Wilson, K.S., and Lamzin, V.S. (2001) ARP/wARP andmolecular replacement. *Acta Cryst.* **D57**, 1445-1450.

Phadtare, S. (2004) Recent developments in bacterial cold-shock response. *Curr. Issues Mol. Biol.* **6**, 125-136.

Phadtare, S., and Inouye, M. (1999) Sequence-selective interactions with RNA by CspB, CspC and CspE, members of the CspA family of *Escherichia coli*. *Mol. Microbiol.* **33**, 1004-1014.

Phadtare, S., Kazakov, T., Bubunenko, M., Court, D. L., Pestova, T., and Severinov, K. (2007) Transcription antitermination by translation initiation factor IF1. *J. Bacteriol.* **189**, 4087-4093.

Phadtare, S., Tyagi, S., Inouye, M., and Severinov, K. (2002) Three amino acids in *Escherichia coli* CspE surface-exposed aromatic patch are critical for nucleic acid melting activity leading to transcription antitermination and cold acclimation of cells. *J. Biol. Chem.* **277**, 46706-46711.

Qiu, Y., Kathariou, S., and Lubman., D. M. (2006) Proteomic analysis of cold adaptation in a Siberian permafrost bacterium -- *Exiguobacterium sibiricum* 255-15 by two-dimensional liquid separation coupled with mass spectrometry. *Proteomics* **6**, 5221-5233.

Ren, J., Nettleship, J. E., Sainsbury, S., Saunders, N. J., and Owens, R. J. (2008) Structure

of the cold-shock domain protein from *Neisseria meningitidis* reveals a strand-exchange dimer. *Acta Cryst.* **F64**, 247-251.

Schindelin, H., Jiang, W., Inouye, M., and Heinemann, U. (1994) Crystal structure of CspA, the major cold shock protein of *Escherichia coli*. *Proc. Natl. Acad. Sci. USA* **91**, 5119-5123.

Schindelin, H., Marahiel, M. A., and Heinemann, U. (1993) Universal nucleic acid-binding domain revealed by crystal structure of the *B. subtilis* major cold-shock protein. *Nature* **364**, 164-168.

Shinkai, A., Kira, S., Nakagawa, N., Kashiharam, A., Kuramitsu, S., and Yokoyama, S. (2007) Transcription Activation Mediated by a Cyclic AMP Receptor Protein from *Thermus thermophilus* HB8. *J. Bacteriol.* **189**, 3891-3901.

Uppal, S., Akkipeddi, V. S., and Jawali, N. (2007) Posttrascriptional regulation of *cspE* in *Escherichia coli*: involvement of the short 5'-untranslated region. *FEMS Microbiol. Lett.* **279**, 83-91.

Vagin, A., and Teplyakov, A. (1997) MOLREP: an automated program for molecular replacement. *J. Appl. Cryst.* **30**, 1022-1025.

Wang, N., Yamanaka, K., and Inouye, M. (1999) CspI, the ninth member of the CspA family of *Escherichia coli*, is induced upon cold shock. *J. Bacteriol.* **181**, 1603-1609.

Yamanaka, K., and Inouye, M. (1997) Growth-phase-dependent expression of cspD, encoding a member of the CspA family in *Escherichia coli*. *J. Bacteriol.* **179**, 5126-5130.

Yamanaka, K., Mitani, T., Ogura, T., Niki, H., and Hiraga, S. (1994) Cloning, sequencing, and characterization of multicopy suppressors of a mukB mutation in *Escherichia coli*. *Mol. Microbiol.* **13**, 301-312.

Zhang, C., and Kim, S. H. (2000) A comprehensive analysis of the Greek key motifs in

protein b-barrels and b-sandwiches. *Proteins* **40**, 409-419.

Publication list

Tanaka, T., Mega, R., Kim, K., Shinkai, A., Masui, R., Kuramitsu, S. and Nakagawa, N.
A non-cold-inducible cold shock protein homolog mainly contributes to translational control under optimal growth conditions
FEBS J. (2012)

Miyazaki, T., Bressan, DA., Shinohara, M., Haber, JE., and Shinohara, A.
In vivo assembly and disassembly of Rad51 and Rad52 complexes during double-strand break repair.
EMBO J. (2004) **23**(4), 939-949.

Hayase, A., Takagi, M., Miyazaki, T., Oshiumi, H., Shinohara, M., and Shinohara, A.
A protein complex containing Mei5 and Sae3 promotes the assembly of the meiosis-specific RecA homolog Dmc1.
Cell (2004) **119**(7), 927-940.

Tsukamoto, M., Yamashita, K., Miyazaki, T., Shinohara, M., and Shinohara, A.
The N-terminal DNA-binding domain of Rad52 promotes RAD51-independent recombination in *Saccharomyces cerevisiae.*
Genetics (2003) **165**(4), 1703-1715.